GROUND COLLISION AVOIDANCE USING A VARIABLE INCIDENCE ALTITUDE MEASUREMENT SYSTEM FOR THE A-7 AIRCRAFT

THESIS

Thomas A. Hartung
Captain, USAF

AFIT/GAE/ENY/91D-15

REPORT DOCUMENTATION PAGE

Form Approved
OMB No. 0704-0188

1. AGENCY USE ONLY (Leave blank)	2. REPORT DATE	3. REPORT TYPE AND DATES COVERED
	December 1991	Master's Thesis

4. TITLE AND SUBTITLE
Ground Collision Avoidance Using a Variable Incidence Altitude Measurement System for the A-7 Aircraft

5. FUNDING NUMBERS

6. AUTHOR(S)

Thomas A. Hartung, Captain, USAF

7. PERFORMING ORGANIZATION NAME(S) AND ADDRESS(ES)

Air Force Institute of Technology, WPAFB OH 45433-6583

8. PERFORMING ORGANIZATION REPORT NUMBER

AFIT/GAE/ENY/91D-15

9. SPONSORING/MONITORING AGENCY NAME(S) AND ADDRESS(ES)

10. SPONSORING/MONITORING AGENCY REPORT NUMBER

11. SUPPLEMENTARY NOTES

12a. DISTRIBUTION/AVAILABILITY STATEMENT

Approved for public release; distribution unlimited

12b. DISTRIBUTION CODE

13. ABSTRACT (Maximum 200 words)

This study examines the use of a forward looking sensor in the implementation of an automatic terrain following system. The effect of the incidence angle is studied as well as methodologies to include dynamic motion in the pointing of the sensor beam. The methods examined include fixed angle with respect to the aircraft, dynamics driven by a simple gain, and dynamics directed to gather the terrain information a fixed time interval ahead of the aircraft. Incidence angles of 25, 50, 75, and 90 are examined. The terrain obstacles include a single parabolic hill, a step change in terrain, and a double parabolic hill. Compensator design was accomplished using MATLAB™ software using Linear Quadratic Gaussian techniques. State space system realization of the closed loop dynamics were used by a FORTRAN program to run the simulations. Performance was judged by qualitative assessment of flight path, quantitative score of summed distances away from commanded 300 ft AGL altitude,and amount of control power required. The best performance was achieved by the 50 degree incidence angle. Dynamic motion of the sensor beam improved performance but required more control deflection. The best dynamic pointing method was the constant time interval technique.

14. SUBJECT TERMS	15. NUMBER OF PAGES
Terrain Following, Terrain Avoidance, Look-ahead Distance, A-7, Ground Collision Avoidance, Radar Altimeter, Forward Sensor	113
	16. PRICE CODE

17. SECURITY CLASSIFICATION OF REPORT	18. SECURITY CLASSIFICATION OF THIS PAGE	19. SECURITY CLASSIFICATION OF ABSTRACT	20. LIMITATION OF ABSTRACT
Unclassified	Unclassified	Unclassified	UL

GENERAL INSTRUCTIONS FOR COMPLETING SF 298

The Report Documentation Page (RDP) is used in announcing and cataloging reports. It is important that this information be consistent with the rest of the report, particularly the cover and title page. Instructions for filling in each block of the form follow. It is important to **stay within the lines to meet optical scanning requirements.**

Block 1. Agency Use Only (Leave Blank)

Block 2. Report Date. Full publication date including day, month, and year, if available (e.g. 1 Jan 88). Must cite at least the year.

Block 3. Type of Report and Dates Covered. State whether report is interim, final, etc. If applicable, enter inclusive report dates (e.g. 10 Jun 87 - 30 Jun 88).

Block 4. Title and Subtitle. A title is taken from the part of the report that provides the most meaningful and complete information. When a report is prepared in more than one volume, repeat the primary title, add volume number, and include subtitle for the specific volume. On classified documents enter the title classification in parentheses.

Block 5. Funding Numbers. To include contract and grant numbers; may include program element number(s), project number(s), task number(s), and work unit number(s). Use the following labels:

C	- Contract	**PR**	- Project
G	- Grant	**TA**	- Task
PE	- Program Element	**WU**	- Work Unit Accession No.

Block 6. Author(s). Name(s) of person(s) responsible for writing the report, performing the research, or credited with the content of the report. If editor or compiler, this should follow the name(s).

Block 7. Performing Organization Name(s) and Address(es). Self-explanatory.

Block 8. Performing Organization Report Number. Enter the unique alphanumeric report number(s) assigned by the organization performing the report.

Block 9. Sponsoring/Monitoring Agency Names(s) and Address(es). Self-explanatory.

Block 10. Sponsoring/Monitoring Agency. Report Number. (If known)

Block 11. Supplementary Notes. Enter information not included elsewhere such as: Prepared in cooperation with...; Trans. of ..., To be published in .... When a report is revised, include a statement whether the new report supersedes or supplements the older report.

Block 12a. Distribution/Availablity Statement. Denote public availability or limitation. Cite any availability to the public. Enter additional limitations or special markings in all capitals (e.g. NOFORN, REL, ITAR)

DOD - See DoDD 5230.24, "Distribution Statements on Technical Documents."
DOE - See authorities
NASA - See Handbook NHB 2200.2.
NTIS - Leave blank.

Block 12b. Distribution Code.

DOD - DOD - Leave blank
DOE - DOE - Enter DOE distribution categories from the Standard Distribution for Unclassified Scientific and Technical Reports
NASA - NASA - Leave blank
NTIS - NTIS - Leave blank.

Block 13. Abstract. Include a brief (Maximum 200 words) factual summary of the most significant information contained in the report.

Block 14. Subject Terms. Keywords or phrases identifying major subjects in the report.

Block 15. Number of Pages. Enter the total number of pages.

Block 16. Price Code. Enter appropriate price code (NTIS only).

Blocks 17. - 19. Security Classifications. Self-explanatory. Enter U.S. Security Classification in accordance with U.S. Security Regulations (i.e., UNCLASSIFIED). If form contains classified information, stamp classification on the top and bottom of the page.

Block 20. Limitation of Abstract. This block must be completed to assign a limitation to the abstract. Enter either UL (unlimited) or SAR (same as report). An entry in this block is necessary if the abstract is to be limited. If blank, the abstract is assumed to be unlimited.

AFIT/GAE/ENY/91D-15

GROUND COLLISION AVOIDANCE USING A VARIABLE INCIDENCE ALTITUDE MEASUREMENT SYSTEM FOR THE A-7 AIRCRAFT

THESIS

Presented to the Faculty of the School of Engineering

of the Air Force Institute of Technology

Air University

In Partial Fulfillment of the

Requirements for the Degree of

Master of Science in Aeronautical Engineering

Thomas A. Hartung, B.S.

Captain, USAF

November 1991

Preface

The purpose of this study was to investigate different ways to implement a forward looking sensor system to be used in an automated terrain following (ATF) system. I chose this project because it brought together many of the concepts studied during the classwork and it seemed to have application to the real world. The A-7 was used as an example, because the flight characteristics were readily available and it represents a good classic aircraft. No, I don't expect anyone will be running right out to put an ATF system on the A-7, but I hope the investigation I have done will be helpful to someone in designing some other system.

I owe a great debt of thanks to my advisor, Maj Curt Mracek, and the rest of the controls faculty, who taught these concepts and methods. I also want to thank my fellow controls/optimization classmates for all the help throughout the 'AFIT Experience'. It's always helpful to see things from a different perspective to gain a little insight yourself.

Finally, I give my greatest appreciation to my wife, Tricia, who has supported me through all the late nights and busy finals weeks. She has been as busy as I have; chasing the kids, leading new activities, and maintaining some sort of controlled chaos around the house so I could work. She has been a source of support, understanding, and stability that I can always rely on. Thank you all. Lord, Guard and Guide...

Tom Hartung

Table of Contents

List of Figures

List of Tables

Abstract

This study examines the use of a forward looking sensor in the implementation of an automatic terrain following system. The effect of the incidence angle is studied as well as methodologies to include dynamic motion in the pointing of the sensor beam. The methods examined include fixed angle with respect to the aircraft, dynamics driven by a simple gain, and dynamics directed to gather the terrain information a fixed time interval ahead of the aircraft. Incidence angles of 25, 50, 75, and 90 are examined. The terrain obstacles include a single parabolic hill, a step change in terrain, and a double parabolic hill. Compensator design was accomplished using MATLAB™ software using Linear Quadratic Gaussian techniques. State space system realization of the closed loop dynamics were used by a FORTRAN program to run the simulations. Performance was judged by qualitative assessment of flight path, quantitative score of summed distances away from commanded 300 ft AGL altitude,and amount of control power required. The best performance was achieved by the 50 degree incidence angle. Dynamic motion of the sensor beam improved performance but required more control deflection. The best dynamic pointing method was the constant time interval technique.

GROUND COLLISION AVOIDANCE USING A VARIABLE INCIDENCE ALTITUDE MEASUREMENT SYSTEM FOR THE A-7 AIRCRAFT

I. Introduction

Background

As modern aircraft become more complex, the pilot workload continues to increase dramatically. In addition to maintaining a basic flight attitude, a pilot must constantly be aware of location, weapons status, gauge readings, formation position, radar contacts, and a myriad of other distractions. As a result, the Air Force has experienced an increasing number of aircraft mishaps due to what is termed 'controlled flight into terrain', or CFIT. These are accidents in which well-maintained aircraft, flown by capable pilots, crash into the terrain due to pilot incapacitation, disorientation, or distraction. This danger is especially great during low level terrain following missions where the low altitude provides only a very small margin for error.

The goal of a terrain following system is to maintain a preset altitude above ground level (AGL) by conforming the flight path as nearly as possible to the varying terrain. To effectively perform a low altitude terrain following mission, the aircraft control system must be warned of a change in the terrain with enough time to change the aircraft attitude to match it. Unfortunately, most aircraft are only able to measure the distance to the ground directly below them. A system based on this input would only be effective in terrain where the rate of change would be slower than the maneuvering rates of the aircraft. To provide advance warning to the control system it is necessary to gather information about terrain a given distance ahead of the current location. Several methods under development would provide this capability.

Current Initiatives. One method being researched to eliminate the sensor problem involves storing the mapped terrain information in a digital database which the onboard computer can view to detect terrain obstacles and the most efficient path around them. The aircraft confirms its current position through updates from the inertial navigation system (INS), global positioning system (GPS), and/or comparing the current radar returns to the stored terrain database. This methodology has the advantage of not requiring a forward-looking sensor and having knowledge of the terrain 360° around the aircraft. This system does have the disadvantage of having to have mapped, digitized and stored the terrain prior to the

mission. An excellent source for more information regarding look ahead distances on a digital database is Capt Greg Bice's Master's Thesis [1].

A reliable forward looking radar methodology would allow the aircraft to enter previously unmapped terrain or deviate from the planned course and still perform a terrain following mission without excessive risk of ground collision. One problem to overcome concerns the omnidirectional nature of a radar wave. Because the wave propagates in all directions at the same speed, it will read the nearest object it strikes, even if the major power of the beam was not in that direction. This object is almost always the ground directly beneath the aircraft. This is why most radar altimeters are pointed downward; the power might as well be directed where the return is most likely to come from anyway.

New systems, such as the low altitude navigation and targeting infra-red for night (LANTIRN) system use infra-red scanning and a laser range finder for navigation and target information. This allows the pilot to see obstacles even at night and to determine the exact distance of an object which is not directly below the aircraft. It is a system like this which will allow a guidance computer to gather terrain information ahead of the current position without the data being cluttered by returns from terrain it is already crossing safely. One of the major remaining variables is how far ahead the sensor should be aimed. Additionally, should the aiming angle be fixed to the aircraft, constant to a local horizon, varied so as to

maintain a constant time interval ahead of the current position, or positioned based on some other set of variables?

In researching this problem, a literature review was conducted to ascertain whether look ahead distances had been the subject of any previous studies. Although several studies of terrain following have been made, none seem to specifically address the subject of look ahead distance other than Capt Bice's thesis. This study will concentrate on radar techniques which could be used in areas for which no digital map may exist, or for aircraft which do not have the computational power to store and utilize such a technique.

The aircraft model used in this study was the A-7D Corsair II. This is representative of a small lightweight fighter/attack type aircraft. It is a high-wing, single engine aircraft known for its capabilities in the ground attack role. The variables of interest in this investigation are:

Pitch Angle	θ	measured (deg) from local horizon to body X axis
Radar Incidence Angle	Σ	measured (deg) from body X axis to radar beam
Radar Range	R	measured (ft) along Σ from aircraft to the ground
Elevator Deflection	δ_e	measured (deg) positive as trailing edge down

Figure 1-1 is provided to illustrate the radar and aircraft geometry.

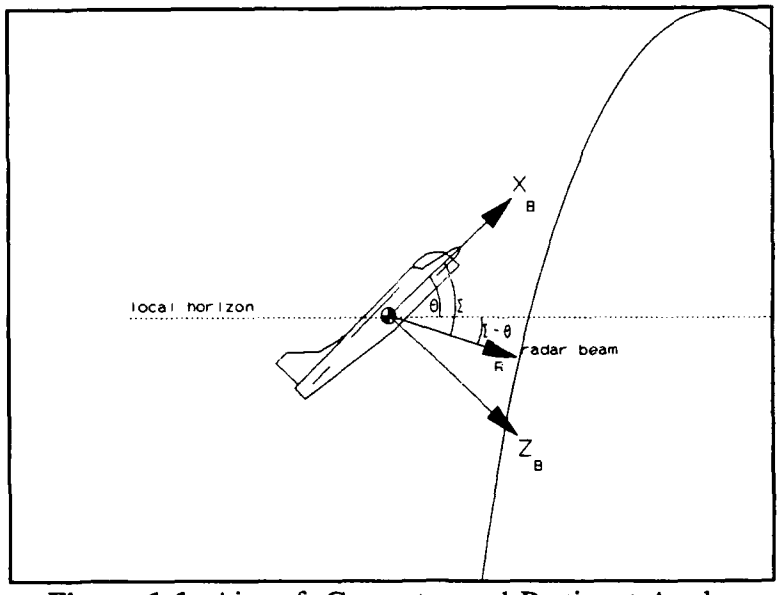

Figure 1-1: Aircraft Geometry and Pertinent Angles

Problem Statement

This report will present an evaluation of using a look-ahead approach in the sensor input to a ground collision avoidance algorithm. It examines the ability of the control system of the aircraft to maintain a pre-determined altitude AGL while maneuvering over a terrain obstacle. For this study, the primary obstacle will be a hill described mathematically by

$$H = -\frac{(X-6000)^2}{4000} + 1000 \qquad (1\text{-}1)$$

where

H = elevation of the terrain

X = downrange distance from starting point

When the hill equation has a negative value the elevation is set to zero. A plot of this obstacle would look like Figure 1-2.

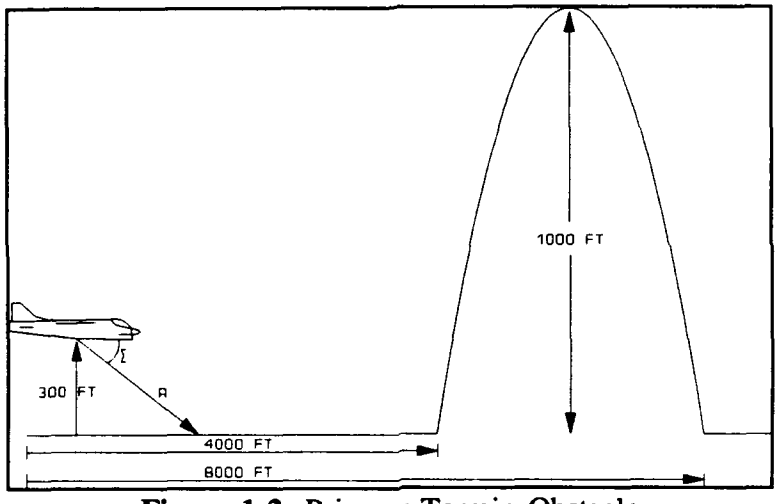

Figure 1-2: Primary Terrain Obstacle

The study will examine variations in the pointing angle of the sensor, both as a fixed installation and dynamic pointing centering around a variable nominal value. The dynamic pointing will be studied using a selectable constant gain and attempting to maintain a constant look-ahead time interval.

The goal of this study is to determine the best method to implement a ground collision avoidance system utilizing a forward looking sensor. The determination of the 'best' methodology is based upon multiple criteria: 1) successfully avoiding the terrain obstacle, 2) approximating an optimal solution which maintains a constant altitude AGL while precisely following the terrain features, and 3) returning the aircraft to its original attitude once the recovery maneuver is complete. Another important factor

requires that any increase in the complexity of the system results in a substantial gain in performance. Recommendations will be made for the best implementation of a look ahead system.

II. State Space Model Development

Matrix Developement

The first step in modern control design of an automatic control system for the A-7 requires the definition of a state space model for the aircraft. A design point of M = 0.6 at sea level altitude was chosen to represent a typical terrain following mission profile. A search of previous studies failed to provide a suitable model; therefore, one had to be generated using the longitudinal transfer function factors for a clean aircraft. The longitudinal transfer functions as presented in USAF-TPS-CUR-86-02 [4] are

Characteristic Eqn: $(s^2 + 3.2249s + 17.7241)(s^2 + .0140s + .0049)$ (2-1)

Pitch Rate Numerator: $-30.6s^3 - 55.1473s^2 - 0.6682s$ (2-2)

X Velocity Numerator: $8.3s^3 + 1040.2s^2 + 1787.7s + 1733.6$ (2-3)

Z Velocity Numerator: $-165s^3 - 20792s^2 - 209s - 9.17$ (2-4)

Pitch Angle Numerator: $-30.6s^2 - 55.1473s - .6682$ (2-5)

This study will assume the terrain avoidance maneuver is a wings level symmetric pull-up, and therefore only the longitudinal dynamics will be affected. The transfer function to state space transformation was accomplished using PRO-MATLAB™. The final four-state longitudinal model of the A-7 at this flight condition is shown in equation 2-6.

$$\dot{X} = [A]\{X\} + [B]\{U\} \tag{2-6}$$

where

$$X = \{ q\ u\ w\ \Theta \}^T \qquad U = \{\delta_e\}$$

$$A = \begin{bmatrix} -1.3145 & 0.0014 & -0.0226 & 0.0009 \\ -33.4156 & -0.0123 & 0.0557 & -31.6013 \\ 672.3107 & -0.0025 & -1.9120 & -1.6113 \\ 1.0000 & 0.0000 & 0.0000 & 0.0000 \end{bmatrix} \qquad B = \begin{bmatrix} -30.60 \\ 8.34 \\ -165.00 \\ 0.00 \end{bmatrix}$$

where

q = pitch rate (rad/sec)

u = incremental forward velocity (ft/sec)

w = incremental vertical velocity (ft/sec)

Θ = pitch angle (rad)

Now that the state space representation of the basic aircraft has been established, it was necessary to model the servo time lags and include them in the model. The servo was modeled as a simple first order time lag with a time constant of 0.1 sec. Additional states were also added to account for other variables of interest, namely the altitude, since this is not a variable in the four state model, but is needed for terrain following. With the internal states identified, the control inputs and measured outputs must be established. The primary control input for the longitudinal mode of the A-7 is the elevator, and therefore it is the only input variable to the

aircraft system model. The outputs which the terrain following system will need to measure and feed back to the aircraft plant are pitch rate, angle of attack, and load factor. This establishes the open loop aircraft dynamic model of the A-7 basic aircraft. Graphically, this is shown in Figure 2-1.

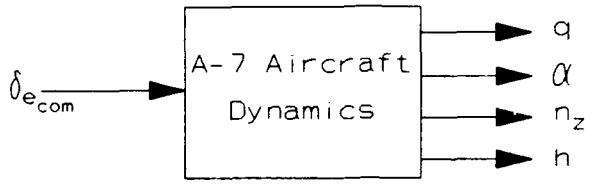

Figure 2-1: A-7 Open Loop Block Diagram

Radar Dynamics. There is one more variable which must be taken into account. To accurately measure the terrain ahead of the aircraft, the radar beam must be directed ahead at some incidence angle. One of the goals of this study is to determine the best angle at which this beam should be pointed. Additionally, we will investigate the advantages of using a fixed installation angle with respect to the aircraft body axis system, or whether the direction of the beam should be changed as the attitude of the aircraft changes. If the installation angle is to be fixed to the body, the system model created up to this point is sufficient. However, to investigate the aspects of dynamic radar pointing, we must include an additional state to track the motion of the radar. This state will also take into account a simple time lag in the servo which would point the beam

where it was commanded. This also adds a second command input and another measured output to the system model.

This study will examine three radar pointing scenarios. The first will assume the radar beam is projected at a fixed angle with respect to the aircraft body. The second case will use a simple gain on the delta range information from the radar to control the incidence angle. The delta range is a comparision of the range value at the initial conditions (straight, level flight, flat terrain) to the value of the radar range given the current aircraft attitude and terrain profile. The system tries to maintain the initial range value while following the changes in the terrain. A negative delta range value indicates the aircraft is too close to the terrain, and therefore should pull up. In the same way, using the simple gain radar dynamics, a negative delta range reading would result in the beam being pointed farther ahead; i.e., decreasing the angle between the aircraft X body axis and the radar beam.

The third case attempts to maintain a constant look ahead time interval. This means that, in theory, the radar beam would always strike the terrain at the point where current attitude would predict it would be above in a preset time interval. This interval is a function of the initial values of altitude, velocity, pitch angle, and nominal radar angle setting. This method continually calculates the forward horizontal velocity and points the radar at the predicted future location. The time intervals used

in this study were calculated from the same starting point as the other cases to allow for more accurate comparision between techniques.

Open Loop System Model. It is now possible to model the dynamics of the aircraft. The aircraft states used in the complete A-7 longitudinal model are

$$X = \{ q \; u \; w \; \Theta \; \delta_e \; h \; \Sigma \}^T$$

where

q = pitch rate (rad/sec)

u = incremental forward velocity (ft/sec)

w = incremental vertical velocity (ft/sec)

Θ = pitch angle (rad)

δ_e = elevator deflection (rad)

h = altitude above mean sea level (ft)

Σ = radar incidence angle (rad)

For the linearized system $\dot{h}$ can be equated to aircraft vertical velocity, which is $U_o(\theta-\alpha)$. The two other additional states simply show the time lag of the servos with a time constant of 0.1 sec. The control inputs for the model are

$$U = \{ \delta_{e_{com}} \; \Sigma_{com} \}^T$$

where

$\delta_{e_{com}}$ = commanded elevator deflection

Σ_{com} = commanded radar incidence angle

The measurements which the model will use as feedback variables are

$$Y = \{ q \ \alpha \ n_z \ h \ \Sigma \}^T$$

where

q = pitch rate (rad/sec)

α = angle of attack (rad)

n_z = normal load factor (g)

h = altitude above mean sea level (ft)

Σ = radar incidene angle (rad)

The angle of attack, in our linearized model, can be approximated by the vertical velocity divided by the freestream velocity of the aircraft at the stated condition of 0.6M at sea level. By differentiating the vertical velocity equation, $\dot{h}$, we obtain an output expression for the normal load factor of the aircraft, shown in equation 2-7.

$$n_z = \dot{w} - qU_o \tag{2-7}$$

where

n_z = Z body axis acceleration (ft/sec^2)

$\dot{w}$ = body axis vertical acceleration (ft/sec^2)

q = pitch rate (rad/sec)

U_o = steady-state velocity on X body axis (ft/sec)

Both of these equations are used in the output matrix to calculate the measurands; the other three measurands (q, h, and Σ) are simply outputs of the value of that particular state.

The longitudinal state space system matrix model for the open loop system is

$$\dot{X} = [A]\{X\} + [B]\{U\}$$
$$Y = [C]\{X\} + [D]\{U\} \qquad (2\text{-}8)$$

where

$$X = \{ q\ u\ w\ \Theta\ \delta_e\ h\ \Sigma \}^T \quad U = \{ \delta_{e_{com}}\ \Sigma_{com} \}^T \quad Y = \{ q\ \alpha\ n_z\ h\ \Sigma \}^T$$

$$A = \begin{bmatrix} -1.3145 & 0.0014 & -0.0226 & 0.0009 & -30.6000 & 0.0000 & 0.0000 \\ -33.4156 & -0.0123 & 0.0557 & -31.6013 & 8.3400 & 0.0000 & 0.0000 \\ 672.3107 & -0.0025 & -1.9120 & -1.6113 & -165.0000 & 0.0000 & 0.0000 \\ 1.0000 & 0.0000 & 0.0000 & 0.0000 & 0.0000 & 0.0000 & 0.0000 \\ 0.0000 & 0.0000 & 0.0000 & 0.0000 & -10.0000 & 0.0000 & 0.0000 \\ 0.0000 & 0.0000 & 1.0000 & -669.8400 & 0.0000 & 0.0000 & 0.0000 \\ 0.0000 & 0.0000 & 0.0000 & 0.0000 & 0.0000 & 0.0000 & -20.0000 \end{bmatrix}$$

$$B = \begin{bmatrix} 0.0 & 0.0 \\ 0.0 & 0.0 \\ 0.0 & 0.0 \\ 0.0 & 0.0 \\ 10.0 & 0.0 \\ 0.0 & 0.0 \\ 0.0 & 20.0 \end{bmatrix} \qquad D = \begin{bmatrix} 0.0 & 0.0 \\ 0.0 & 0.0 \\ 0.0 & 0.0 \\ 0.0 & 0.0 \\ 0.0 & 0.0 \end{bmatrix}$$

$$C = \begin{bmatrix} 1.0000 & 0.0000 & 0.0000 & 0.0000 & 0.0000 & 0.0000 & 0.0000 \\ 0.0000 & 0.0000 & 0.0015 & 0.0000 & 0.0000 & 0.0000 & 0.0000 \\ 2.4707 & -0.0025 & -1.9120 & -1.6113 & 165.0000 & 0.0000 & 0.0000 \\ 0.0000 & 0.0000 & 0.0000 & 0.0000 & 0.0000 & 1.0000 & 0.0000 \\ 0.0000 & 0.0000 & 0.0000 & 0.0000 & 0.0000 & 0.0000 & 1.0000 \end{bmatrix}$$

In transfer function form, we can also represent this system as

$$Y(s) = C(sI - A)^{-1}B\{U\} \qquad (2\text{-}9)$$

This particular representation allows us to see that the poles of the system are the determinant of (sI - A). The eigenvalues, or poles, of the

completed open loop longitudinal system and representative modes are listed in Table 2.1. Note that the A-7 exhibits the standard aircraft longitudinal mode characteristics. The phugoid mode is lightly damped with a long cyclic period; the short period mode has the high frequency oscillations we would expect, and is significantly more damped than the phugoid. However, the frequency of the short period is not extremely fast

Table 2-1: Characteristic Modes of the A-7 Aircraft

Mode	Eigenvalue	Damping Ratio	Frequency
Phugoid	$-.007 \pm .0695i$	.100	.0698
Short Period	$-1.6124 \pm 3.889i$	.383	4.21
Radar Servo	-20.0	1.0	20.0
Elevator Servo	-10.0	1.0	10.0

and therefore the maneuvering of the aircraft may not be very quick. The task now is to create a controller which feeds back the measurands to improve the overall performance.

Controller Design Methodology

Graphically, the open loop system can be represented by Figure 2-2. The system has two control inputs and five measured outputs. Because the goal of a terrain following system is to maintain a preset altitude AGL, the

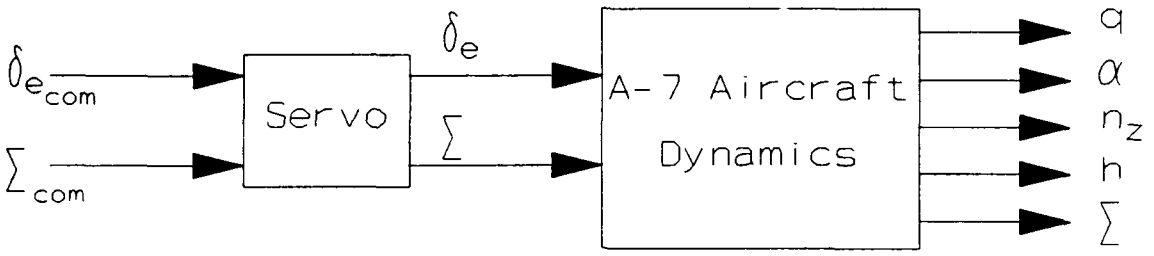

Figure 2-2: Block Diagram of A-7 Model with Servos

controller which will best fill the need is an altitude command following system. In the cases where dynamic control of the radar incidence angle is important, the system will also be required to follow this command input. At the same time, other outputs should be regulated to zero as much as possible.

Linear Quadratic Gaussian Control Design. The Linear Quadratic Gaussian (LQG) controller is a combination of the Linear Quadratic Regulator (LQR) and the Linear Quadratic Estimator (LQE) or Kalman Filter. The regulator design will create a static gain matrix. The control law which will optimize a quadratic performance index is then the product of this gain matrix and the state vector. The filter provides the regulator with estimates of the states which are corrupted by process noise or sensor noise or cannot be measured directly by some sensor on the aircraft. By combining these two components into a single system, we create the best control inputs allowed by the inaccuracies of the estimates.

The solution to the LQG problem is prescribed by the **separation principle**, which states that the optimal result is achieved by adopting the following procedure. First, obtain an optimal estimate $\hat{x}$ of the state x (optimal in the sense that $E\{(x - \hat{x})^T(x - \hat{x})\}$ is minimized), and then use this estimate as if it were an exact measurement of the state to solve the problem. The point of this procedure is that it reduces the problem to two sub-problems, the solutions to which are known [2:223]. The state estimates are found through Kalman filter theory, and we then use these estimates in the LQR design to minimize the standard LQR quadratic cost function

$$\int_0^\infty (x^T Q_c x + u^T R_c u) dt \tag{2-10}$$

The solution to the regulator problem is to let the control signal u be a linear function of the state:

$$u = -K_c \hat{x} \tag{2-11}$$

where K_c is the optimal state-feedback matrix given by

$$K_c = R_c^{-1} B^T P_c \tag{2-12}$$

where P_c satisfies the algebraic Riccati equation with $R_c = R_c^T > 0$ and $Q_c = Q_c^T \geq 0$:

$$A^T P_c + P_c A - P_c B R_c^{-1} B^T P_c + Q_c = 0 \quad \text{and } P_c = P_c^T \geq 0. \tag{2-13}$$

The Kalman-filter gain matrix K_f is given by

$$K_f = P_f C^T R_f^{-1} \tag{2-14}$$

where P_f satisfies another algebraic Riccatti equation (dual to LQR) with $R_c = R_c^T > 0$ and $Q_c = Q_c^T \geq 0$:

$$P_f A^T + A P_f - P_f C^T R_f^{-1} C P_f + Q_f = 0 \quad \text{and} \quad P_f = P_f \geq 0 \quad (2\text{-}15)$$

The compensator [3:6-11] which results from this design can be represented in the Laplace domain by

$$K_c(sI - A + BK_c + K_f C)^{-1} K_f \quad (2\text{-}16)$$

This is then placed in series ahead of the inputs to the servo actuators. As shown in Figure 2-3, the outputs of the plant are returned to the compensator through unity negative feedback and the two outputs which represent the active controls (h, Σ) are compared to any external control signal which may be present before being sent into the compensator inputs.

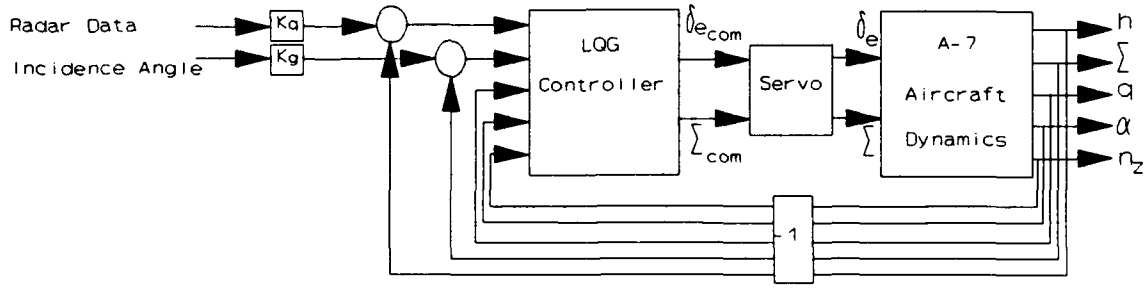

Fig 2-3: Closed Loop System Block Diagram

The primary task of the control system designer is to choose the weighting matrices in such a manner as to optimize the dynamic response of the system. Each variation of the weighting matrices will cause changes

in the resulting closed loop system, because it equates to placing more (or less) emphasis on a particular state or input in the overall performance index. A good starting point to make a first cut at a design is to set the weighting matrices equal to the identity matrix of a compatible size. Another common choice is to 'square' one of the system matrices (i.e. C^TC). The weighting matrices chosen in this analysis are as follows:

$$R_c = \begin{bmatrix} 1 & 0 \\ 0 & 1 \end{bmatrix} \quad Q_c = \begin{bmatrix} 7.1044 & -0.0062 & -4.7240 & -3.9811 & -407.6700 & 0 & 0 \\ -0.0062 & 6.3e\text{-}6 & 0.0048 & 0.0041 & 0.4148 & 0 & 0 \\ -4.7240 & 0.0048 & 3.6557 & 3.0808 & 315.4800 & 0 & 0 \\ -3.9811 & 0.0041 & 3.0808 & 2.5963 & 265.8700 & 0 & 0 \\ -407.6700 & 0.4148 & 315.4800 & 265.8700 & 27225.00 & 0 & 0 \\ 0 & 0 & 0 & 0 & 0 & 1 & 0 \\ 0 & 0 & 0 & 0 & 0 & 0 & 4 \end{bmatrix}$$

$$R_f = \begin{bmatrix} 0.1 & 0 & 0 & 0 & 0 \\ 0 & 0.1 & 0 & 0 & 0 \\ 0 & 0 & 0.1 & 0 & 0 \\ 0 & 0 & 0 & 0.1 & 0 \\ 0 & 0 & 0 & 0 & 1e\text{-}5 \end{bmatrix} \quad Q_f = \begin{bmatrix} 0 & 0 & 0 & 0 & 0 & 0 & 0 \\ 0 & 0 & 0 & 0 & 0 & 0 & 0 \\ 0 & 0 & 0 & 0 & 0 & 0 & 0 \\ 0 & 0 & 0 & 0 & 0 & 0 & 0 \\ 0 & 0 & 0 & 0 & 0 & 0 & 0 \\ 0 & 0 & 0 & 0 & 0 & 1 & 0 \\ 0 & 0 & 0 & 0 & 0 & 0 & 6 \end{bmatrix}$$

The Q_c matrix is C^TC, while the Q_f matrix concentrates only on the two states which are being fed back as command inputs. The relative magnitudes indicate an attempt to estimate the radar state with extra precision as a result of higher process noise. Although, in this design, changes in R_c appeared to have no significant effect on the system performance, changes in R_f did affect the speed of response. This corresponds to varying levels of confidence in these estimates due to sensor

noise. By setting the weighting values less than one, the closed loop response time decreased. Physically, this would mean that the sensor noises are not very large and the measurements have a high degree of reliability. The step response characteristics of the system resulting from the weighting matrices shown was responsive and well behaved, and therefore was chosen as the final compensator design.

Compensator Modeling. All of the aircraft modeling and compensator design work was done on the Air Force Institute of Technology (AFIT) VAX/VMS cluster using PRO-MATLAB™. The MATLAB software allows complete automation of this entire design process. By connecting the compensator in series upline from the plant, we can now combine the two into a single integrated system. Note, however, that this system is still open loop and does not provide feedback of any of the measured quantities. Therefore, the next step is to create the feedback loops to return the measured values from the plant back to the compensator. Closing this loop results in a system which has five outputs and five inputs, only two of which use data from the external environment. The standard state space system matrices for the closed loop are shown on the following pages. The system now has a total of nineteen states. However, five additional states were added by MATLAB during the matrix feedback manipulations. Although these five states contain no information, we will continue to carry them in the model because they provide variables

names where other information may be tracked during the simulation runs. This information will include calculations based upon the nonlinear terrain inputs and the control law for the constant time case studies.

$$A_{cl} = \begin{bmatrix}
-1.3145 & 0.0014 & -0.0226 & 0.0009 & -30.6000 & 0 & 0 & 0 & 0 & 0 & 0 & 0 & 0 & 0 & 0 & 0 & 0 & 0 & 0 \\
-33.4160 & -0.0123 & 0.0557 & -31.601 & 8.3400 & 0 & 0 & 0 & 0 & 0 & 0 & 0 & 0 & 0 & 0 & 0 & 0 & 0 & 0 \\
672.31 & -0.0025 & -1.9120 & -1.6113 & -165 & 0 & 0 & 0 & 0 & 0 & 0 & 0 & 0 & 0 & 0 & 0 & 0 & 0 & 0 \\
1 & 0 & 0 & 0 & 0 & 0 & 0 & 0 & 0 & 0 & 0 & 0 & 0 & 0 & 0 & 0 & 0 & 0 & 0 \\
1517.2000 & 0.1739 & 0.4058 & 10445 & -1678 & -10 & 0 & 0 & 0 & 0 & 0 & 0 & 0 & 0 & 0 & 0 & 0 & 0 & 0 \\
0 & 0 & 1 & -669.84 & 0 & -3.1623 & 0 & 0 & 0 & 0 & 0 & 0 & -3.1623 & 0 & 0 & 0 & 0 & 0 & 0 \\
0 & 0 & 0 & 0 & 0 & 0 & -799.5800 & 0 & 0 & 0 & 0 & 0 & 0 & -754.8500 & 0 & 0 & 0 & 0 & 0 \\
0 & 0 & 0 & 0 & 0 & 0 & 0 & -1.3145 & -0.0014 & -0.0226 & -0.0009 & -30.6000 & 0 & 0 & 0 & 0 & 0 & 0 & 0 \\
0 & 0 & 0 & 0 & 0 & 0 & 0 & -33.4160 & -0.0123 & 0.0557 & -31.6010 & 8.3400 & 0 & 0 & 0 & 0 & 0 & 0 & 0 \\
0 & 0 & 0 & 0 & 0 & 0 & 0 & 672.3100 & -0.0025 & -1.9120 & -1.6113 & -165 & 0 & 0 & 0 & 0 & 0 & 0 & 0 \\
0 & 0 & 0 & 0 & 0 & 0 & 0 & 1 & 0 & 0 & 0 & 0 & 0 & 0 & 0 & 0 & 0 & 0 & 0 \\
-1517.2000 & -0.1739 & -0.4058 & -10445 & 1668 & 10 & 0 & 0 & 0 & 0 & 0 & 0 & -10 & 0 & 0 & 0 & 0 & 0 & 0 \\
0 & 0 & 0 & 0 & 0 & 0 & 0 & 0 & 0 & 1 & -669.8400 & 0 & 0 & 0 & 0 & 0 & 0 & 0 & 0 \\
0 & 0 & 0 & 0 & 0 & 0\ 24.7210 & 0 & 0 & 0 & 0 & 0 & 0 & -20 & 0 & 0 & 0 & 0 & 0 & 0 \\
0 & 0 & 0 & 0 & 0 & 0 & 0 & 0 & 0 & 0 & 0 & 0 & 0 & 0 & 0 & 0 & 0 & 0 & 0 \\
0 & 0 & 0 & 0 & 0 & 0 & 0 & 0 & 0 & 0 & 0 & 0 & 0 & 0 & 0 & 0 & 0 & 0 & 0 \\
0 & 0 & 0 & 0 & 0 & 0 & 0 & 0 & 0 & 0 & 0 & 0 & 0 & 0 & 0 & 0 & 0 & 0 & 0 \\
0 & 0 & 0 & 0 & 0 & 0 & 0 & 0 & 0 & 0 & 0 & 0 & 0 & 0 & 0 & 0 & 0 & 0 & 0 \\
0 & 0 & 0 & 0 & 0 & 0 & 0 & 0 & 0 & 0 & 0 & 0 & 0 & 0 & 0 & 0 & 0 & 0 & 0
\end{bmatrix}$$

$$B_{cl} = \begin{bmatrix} 0 & 0 & 0 & 0 & 0 \\ 0 & 0 & 0 & 0 & 0 \\ 0 & 0 & 0 & 0 & 0 \\ 0 & 0 & 0 & 0 & 0 \\ 0 & 0 & 0 & 0 & 0 \\ 0 & 0 & 0 & 3.1623 & 0 \\ 0 & 0 & 0 & 0 & 754.8548 \\ 0 & 0 & 0 & 0 & 0 \\ 0 & 0 & 0 & 0 & 0 \\ 0 & 0 & 0 & 0 & 0 \\ 0 & 0 & 0 & 0 & 0 \\ 0 & 0 & 0 & 0 & 0 \\ 0 & 0 & 0 & 0 & 0 \\ 0 & 0 & 0 & 0 & 0 \\ 0 & 0 & 0 & 0 & 0 \\ 0 & 0 & 0 & 0 & 0 \\ 0 & 0 & 0 & 0 & 0 \\ 0 & 0 & 0 & 0 & 0 \end{bmatrix}$$

$$C_{cl} = \begin{bmatrix} 0 & 0 & 0 & 0 & 0 & 0 & 0 & 1 & 0 & 0 & 0 & 0 & 0 & 0 & 0 & 0 & 0 & 0 & 0 \\ 0 & 0 & 0 & 0 & 0 & 0 & 0 & 0 & 0 & 0.0015 & 0 & 0 & 0 & 0 & 0 & 0 & 0 & 0 & 0 \\ 0 & 0 & 0 & 0 & 0 & 0 & 0 & 2.4707 & -0.0025 & -1.9120 & -1.6113 & -165 & 0 & 0 & 0 & 0 & 0 & 0 & 0 \\ 0 & 0 & 0 & 0 & 0 & 0 & 0 & 0 & 0 & 0 & 0 & 0 & 1 & 0 & 0 & 0 & 0 & 0 & 0 \\ 0 & 0 & 0 & 0 & 0 & 0 & 0 & 0 & 0 & 0 & 0 & 0 & 0 & 1 & 0 & 0 & 0 & 0 & 0 \end{bmatrix}$$

$$D_{cl} = \begin{bmatrix} 0 & 0 & 0 & 0 & 0 \\ 0 & 0 & 0 & 0 & 0 \\ 0 & 0 & 0 & 0 & 0 \\ 0 & 0 & 0 & 0 & 0 \\ 0 & 0 & 0 & 0 & 0 \end{bmatrix}$$

III. Terrain Following Simulation

Simulation Program

To fully examine the effect of the radar incidence angle, a predictor-corrector nonlinear simulation program, written in FORTRAN, was used. The aircraft system model is entered as a data input file along with timing parameters, gain values and initial conditions. A sample input file and a listing of the source code are presented in the Appendix. The program is designed to simulate the motion of the aircraft and also model the changing terrain. The primary input to our model is the range value given by the radar return, just as it would be on the aircraft. The capability of the program to handle nonlinearities is especially important here due to the nature of the terrain inputs. Because the radar range measurement is a function of the airacraft attitude as well as the geographic contour, this input is quite nonlinear and the value cannot be predicted in advance. The program compares the measured range value with the initial range it calculated before encountering the terrain obstacle. The magnitude of the elevator commands are then based upon the magnitude of the range difference between measured and initial. This difference is amplified by a gain and then sent into the system as $\delta_{e_{com}}$.

The radar dynamics are commanded by different methods depending upon which modeling method is being used. For fixed installation, the radar pointing command is set to zero. The incidence angle then remains at the

value set by the input file. For radar pointing with simple gain dynamics, Σ_{com} is derived similarly to $\delta_{e_{com}}$. The angular command is the product of the range difference and a gain established in the input file. If the difference is negative, the incidence angle is decreased and the radar energy is directed farther in front of the aircraft. A positive difference will increase the incidence angle so that the beam is directed more toward the z body axis. The third scenario attempts to maintain a constant look ahead time on the ground track. To accomplish this, the horizontal velocity is calculated to determine how far downrange the aircraft will travel in the given time interval. The incidence angle to that point is calculated and the beam is directed there for the next measurement.

To provide a quantitative comparison of each simulation run, a score is developed for each. This score is the sum of the square of the differences between how high above the terrain the aircraft actually was and the initial value the model was trying to maintain. Since this is a measurement of the total error of the simulation, a low score is desirable. An output file captured the time, x-distance, altitude, terrain height, delta range, radar angle (if applicable), and elevator deflection at each iteration step. This allows for a graphical comparison of the position of the aircraft and the shape of the terrain or the time history of the control surfaces. The 'goodness' of a run was determined by the quantitative score, qualitative look at the position trace of

the aircraft, and a check of the control power used to determine if the angles and rates of the elevator were reasonable.

Radar Models

Case 1: Fixed Radar Angle. The first set of runs examined used a fixed radar angle. Different incidence angles of 25, 50, 75, and 90 degrees were analyzed. One of the first tasks in running the simulation was to determine the gain ranges which could be used at each incidence angle. Minimum gain was defined as the lowest gain value with which the aircraft could successfully maneuver over the terrain. Although the minimum level often included extremely close approaches to the hill (i.e. the landing gear had better be retracted or you weren't going to make it), any success was acceptable as the starting point for the gain range. Maximum gain was defined as the highest gain value which could be used without causing a ground collision due to excessively high magnitude maneuvers. These maximum runs usually involved elevator deflections and rates which were beyond any physical reality. Interestingly enough, at extremely high gains, many simulations would crash at one gain, but survive at a higher one. The determining factors were the aircraft attitude and the point in the oscillation cycle as the radar measurements were taken. As expected, higher gains produce better scores as the model was able to respond very quickly to any changes in the terrain.

Figure 3-1 shows the improvement in score as the gains were increased for each angle. All four curves show the same trend of a rapid improvement

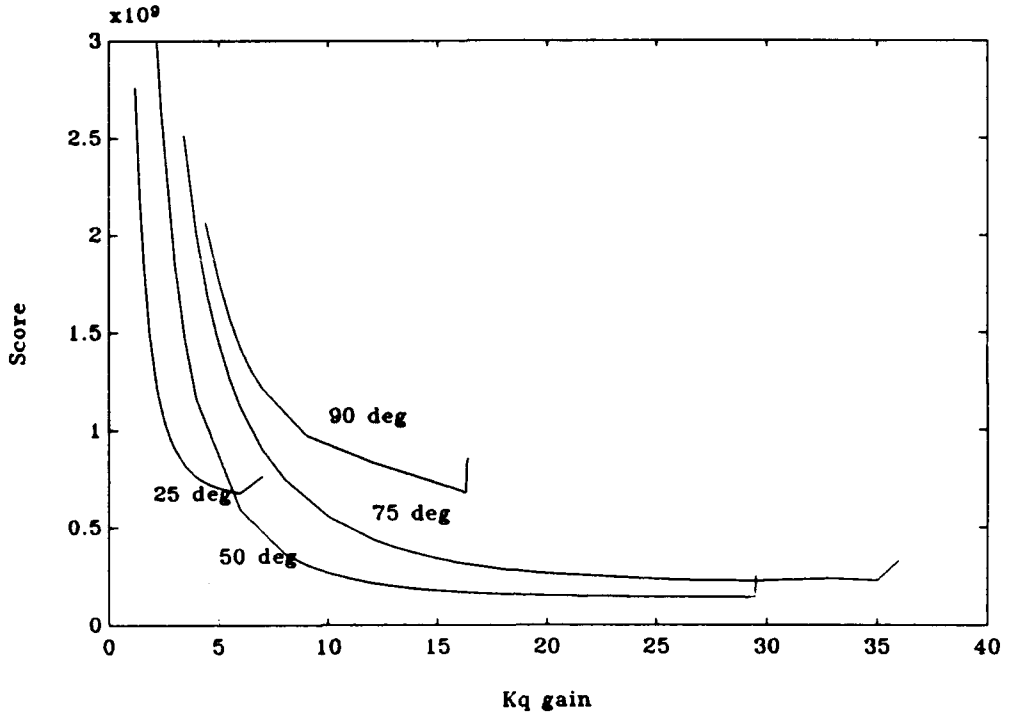

Figure 3-1: Quantitative Score as a function of Gain

from minimum gain over a comparatively small increase in gain and then leveling off so that the rate of change in score was much less at high gain. This trend can be used as an advantage by choosing the 'best' gain as one of the midrange gains near the elbow of the curve. This way the system receives the benefits of the smaller score while not using the extreme amounts of control power which are required at high gain. Table 3-1 lists the gain value chosen for each angle analyzed.

Table 3-1: Gain Ranges for Fixed Angle

Angle (deg)	Minimum Gain	Best Gain	Gain for Min Score	Maximum Gain
25	1.2	3.0	5.92	7.0
50	2.2	8.0	29.13	29.5
75	3.4	12.0	29.29	36.0
90	4.4	8.0	16.23	16.4

90 Degree Incidence Angle. The first angle examined in this study was directing the beam along the z body axis of the aircraft. This forms a good basis to which we can compare all subsequent runs. This trial also demonstrates the shortcomings of using a radar system without look ahead capability to attempt terrain following. The minimum gain value for 90 deg is higher than any other angle and the control power required to avoid the terrain is substantial even at low gain. Graphically, the flight path for a 90 degree incidence angle is erratic and would be unacceptable to the pilot as an automated system. The position traces for each significant run are shown in Figure 3-2. As a sidenote, it should be pointed out that these position graphs are scaled to present the most magnified view possible. Mathematically, the hill is four times as wide as it is tall and therefore the incline is not nearly as steep as the magnified plots would appear to make it.

Figure 3-3 shows the elevator deflections for each run as the aircraft maneuvered over the terrain. It is clearly seen that the control power required

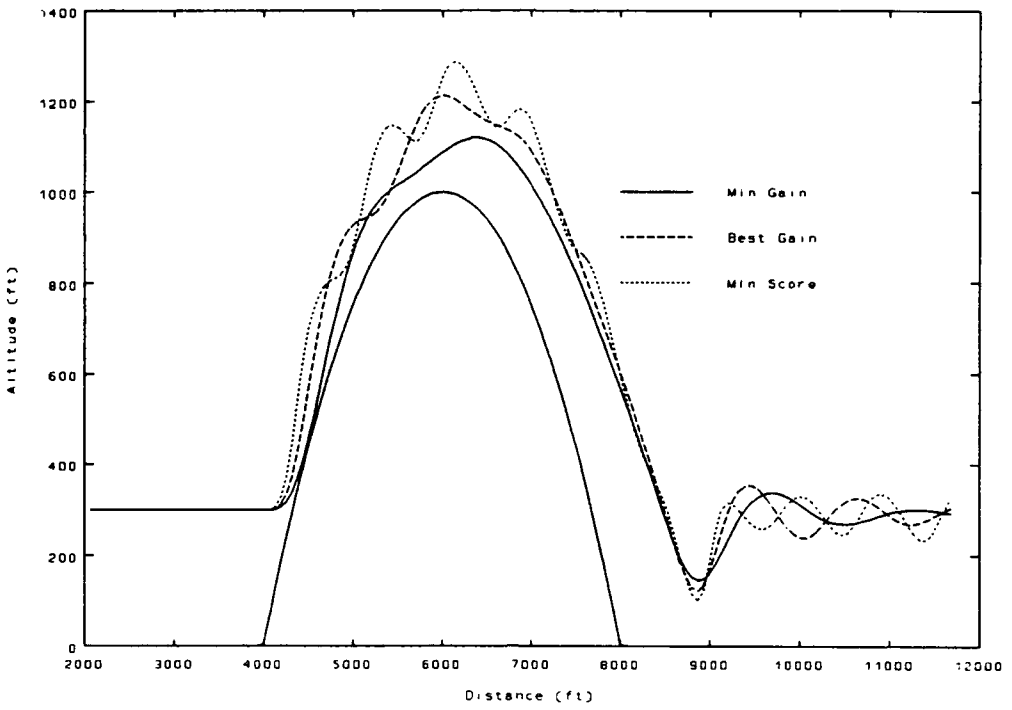

Figure 3-2: Position Trace for Σ = 90 deg

to maintain the 300 ft AGL condition for the min score is far to excessive to even consider this particular design. Even at the medium gain level, the flight is not smooth and requires 25 degrees of elevator, which is the mechanical limit on most modern aircraft. In order to have a reasonable control power usage, it is necessary to use minimum gain. Based upon the poor performance in the pull-up, this is not a reasonable option either. Therefore, it is clear that to successfully maintain a safe height above a terrain obstacle, the control system requires some advance warning in order to maneuver.

75 Degree Incidence Angle. The first look-ahead angle examined was 75 degrees down from the nose. This will allow a slight

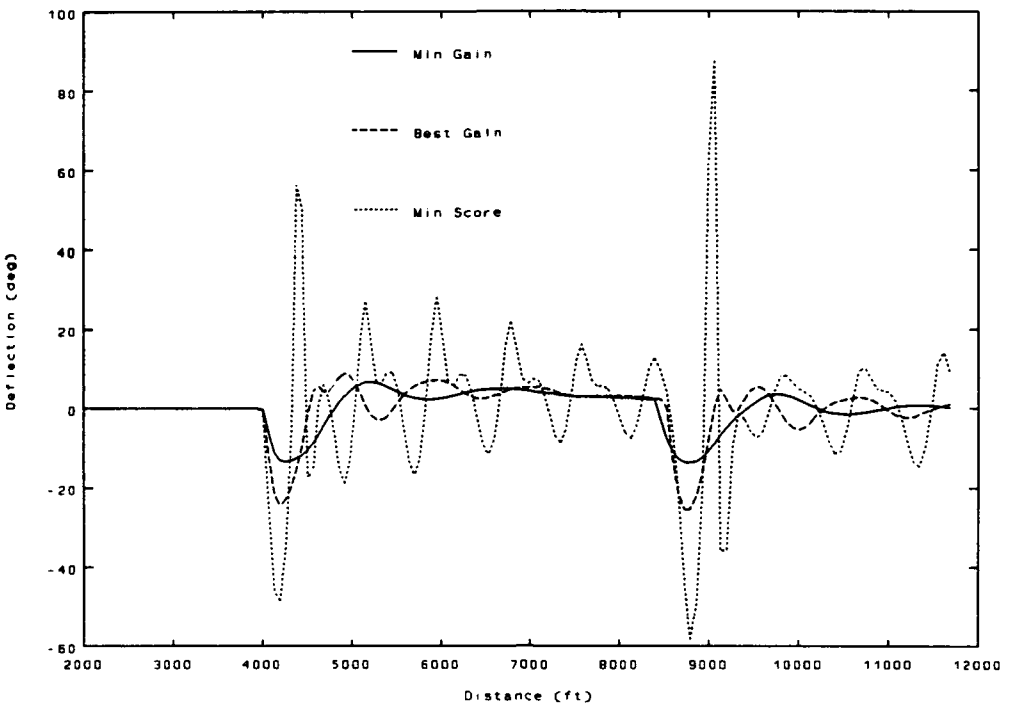

Figure 3-3: Control Power for Σ = 90 deg

advance warning, and yet we do not run the risk of looking so far ahead that the aircraft is reacting to distant problems when the near ones are much more urgent. As shown previously, this incidence angle allows the highest gains before it becomes uncontrollable. However, to maintain reasonable control usage, the medium gain chosen is less than a third of the best score performer. These gain values result in the position traces shown in Figure 3-4. We now see that the pull-up begins just before the start of the slope, which indicates that the radar is gathering range data ahead of the aircraft. The pull-up appears to still be quite abrupt, although the oscillations are not as evident as they were in the previous case. Even at high gain, the oscillations appear to

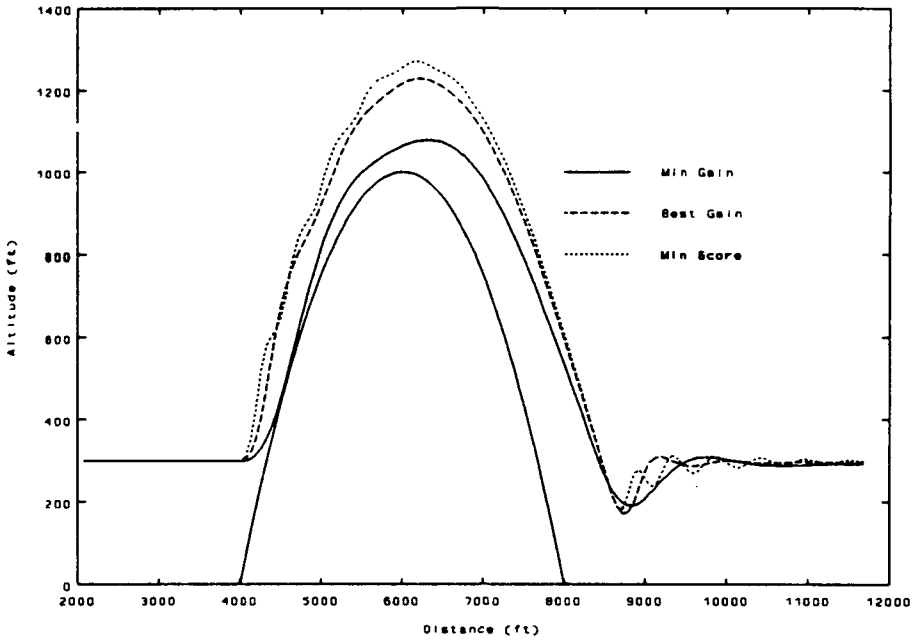

Figure 3-4: Position Trace for $\Sigma = 75$ deg

be of relatively small magnitude. The recovery at the end of the hill seems to be the worst control point.

To see how well these oscillations are being controlled, we must look at the control usage shown in Figure 3-5. Due to the extremely high gain, we now see deflections in excess of 150 degrees. To maintain control, the model then reverses the deflection. The result is a total change of over 250 degrees in slightly more than 0.1 sec. Therefore, even if the deflection were not physically impossible, the rate of change required would be unrealizable. The medium gain run also includes deflections close to 30 degrees, and therefore exceeds the standard mechanical limit. However, even though this gain is a substantial drop from the max gain, it is still quite high and there may be

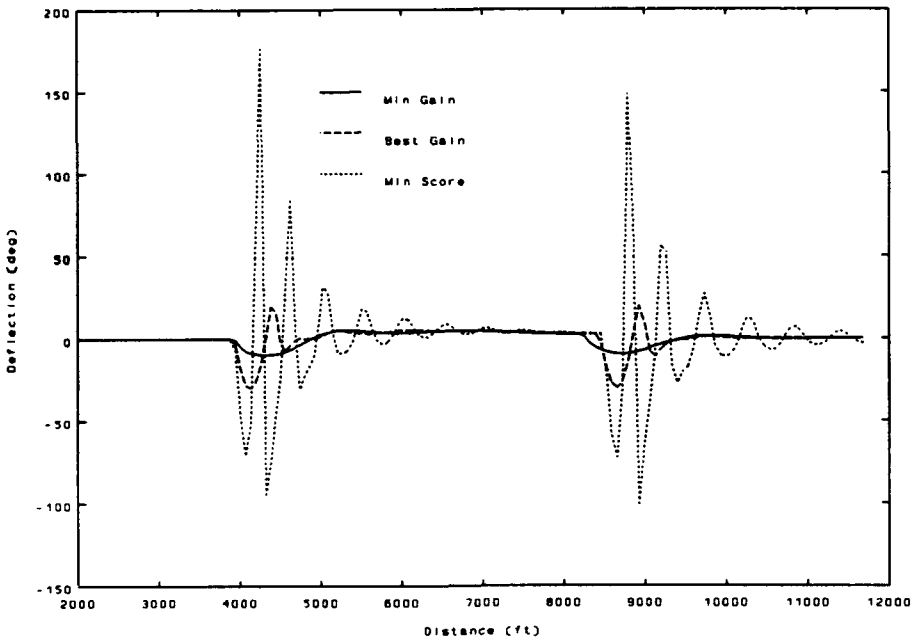

Figure 3-5: Control Power for Σ = 75 deg

room for further reduction without affecting the performance too severely. If, for some reason, there were a physical limitation on the incidence angle, it appears it would be possible to make it work by looking forward only fifteen degrees. However, we will see that pointing farther ahead is a significant improvement.

50 Degree Incidence Angle. As was shown in Figure 3-1, a 50 degree incidence angle provides the best score of any angle that was tested. Even after reducing the gain to limit the control power required, the score is as good as the 75 degree minimum score. The position traces, as shown in Figure 3-6, are also beginning to look a lot smoother. However, we are still seeing the high frequency oscillations at large gain, although the magnitude

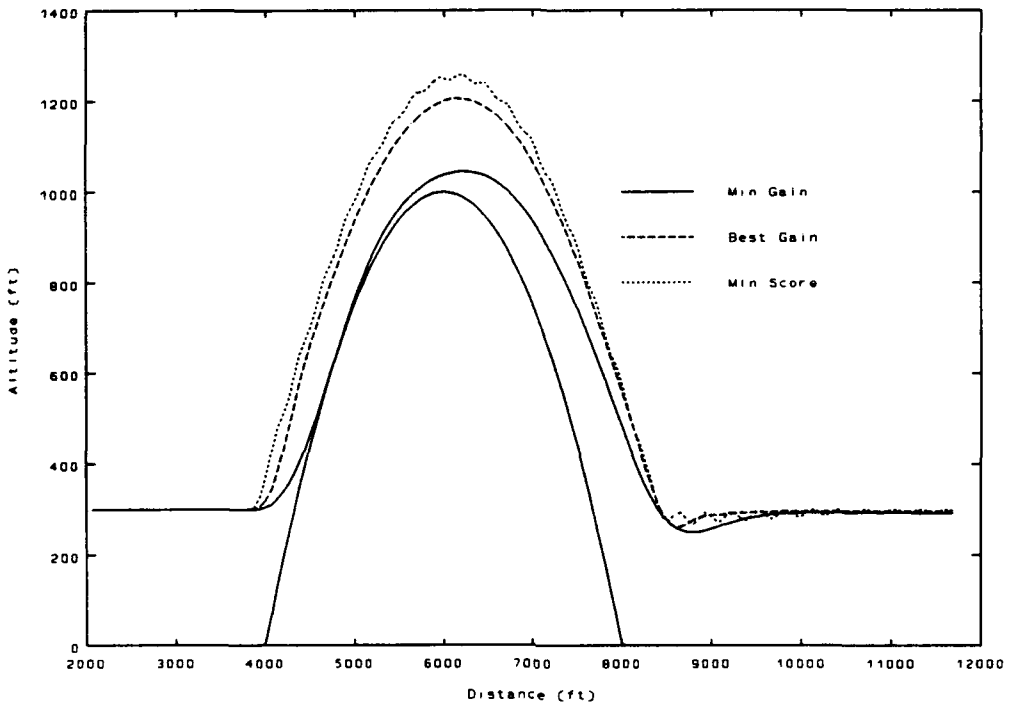

Figure 3-6: *Position Trace for* $\Sigma = 50$ deg

continues to decrease. The midrange gain run is now looking extremely smooth and, with the exception of one overshoot at the back side of the hill, appears completely free of oscillations.

In looking at the elevator deflection plot in Figure 3-7, we immediately see why the min score position plot shows so many shallow, but frequent, oscillations. The control power being used here has the elevator moving around so drastically that if these magnitudes and rates were physically possible, the actuators would need to be replaced due to fatigue after every flight. In contrast, the midrange gain shows excellent performance in both magnitude and rate. We now see a run which accomplishes the task and uses

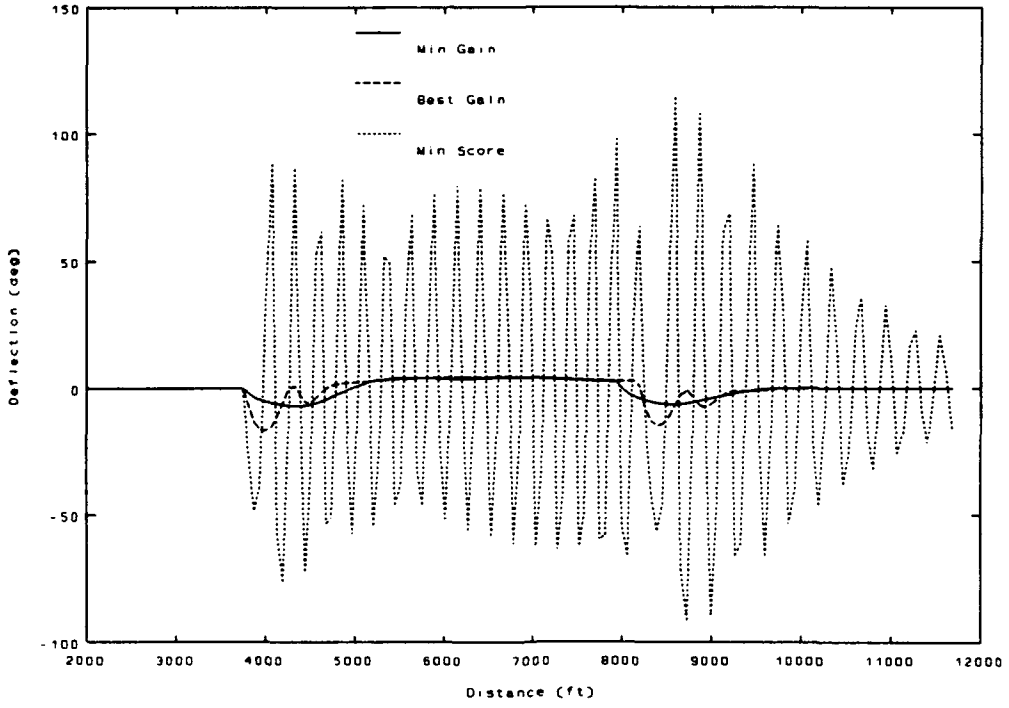

Figure 3-7: Control Power for Σ = 50 deg

a reasonable amount of control to do so. It is this run which will form the basis for the investigation of the advantages of adding dynamics to the radar.

25 Degree Incidence Angle. The last of the fixed angle investigations will gather range information far out ahead of the aircraft. By using an installation angle 25 degrees down from the nose, we will be looking at a point on the ground more than twice as far away as the current altitude. The great advantage of this scenario is that the control system receives enough advance warning that the maneuver can be performed without using much gain on the input or control power in the pull-up. Figure 3-8 supports the prediction that the curve would be extremely smooth, even at the abrupt

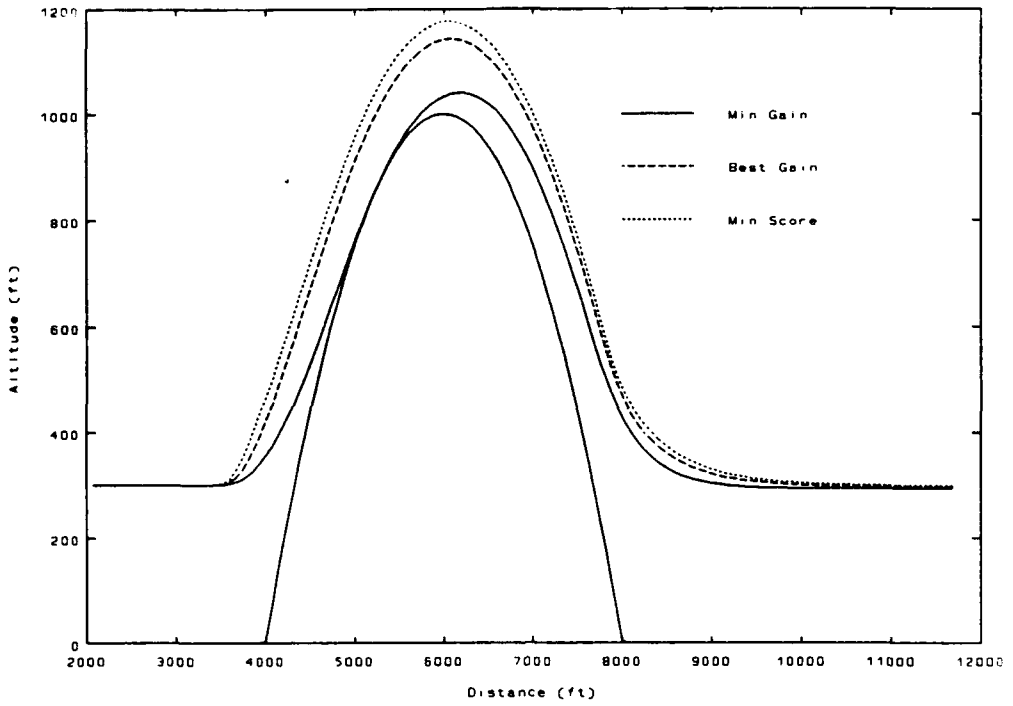

Figure 3-8: Position Trace for Σ = 25 deg

changes where the hill starts and stops, due to the early detection. The main problem with this case, even though the flights are smooth, is that the score value indicates that it is not maintaining the desired altitude buffer. Increasing the gain raises the track but the score never reaches the 50 deg value.

One explanation of poor score may be that the gains are so low that the aircraft is slow to respond. The low gains allow the aircraft to be very conservative with its control power usage. As shown in Figure 3-9, the magnitude of the deflections are now less than 10 degrees and the rates for the low and medium gains are very smooth and attainable. The high gain response is typical with the other angles, in that it results in high frequency

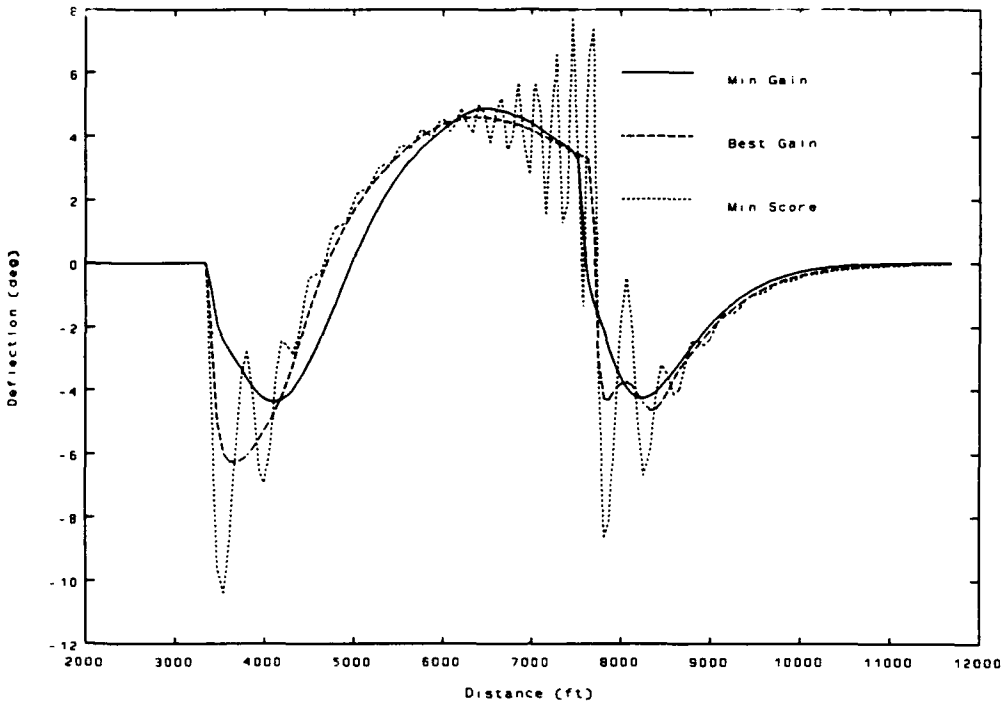

Figure 3-9: Control Power for Σ = 25 deg

oscillations of the elevator. However, in contrast to the other angles, these oscillations occur just past the crest of the hill rather than near the abrupt change at the bottom. Of course, by looking at such a small squint angle, this model is seeing the base of the hill as it is coming down the back side long before any previous run has.

Fixed Angle Summary. The investigation into the responses of a system using a fixed incidence angle has proven that such a system could be implemented successfully. The biggest driving factor appears to be the gain which the radar delta range passes through to become the elevator input. High gain causes high frequency movement of the control surface and high

magnitude deflections. Each of these pushes the control system beyond its physical capability. Despite the oscillations, higher gains do score better in maintaining the preset buffer altitude. Especially in the case of the smaller angles, the high frequency movement is so much faster than the response of the aircraft attitude that there is very little resulting disturbance in the flight path, and the aircraft stays on track.

The minimum gain simulations were included to define the possible regions in which other solutions lie. None of the minimum gain runs would seriously be considered as a final design; however, they do point to trends which could be explored at other gain levels. It also defines the minimum control power required to be successful.

The midrange gains are where the most promise is evident in developing an automated terrain following system. The gains are low enough that the control usage is not excessive and high enough to provide good scores in tracking the buffer altitude. Figure 3-10 provides a comparison between the midrange gain runs at each angle. We see clearly how much smoother the two smaller angles make the response. Even though they share the same gain value, there is a large difference in the response of the 90 degree case versus the 50 degree case. Being able to see the changes in time to correct for them in advance is a big advantage. We can also see this advantage in the control power usage in Figure 3-11. The need for large scale adjustments to the control surfaces is unnecessary, because the control system has begun the

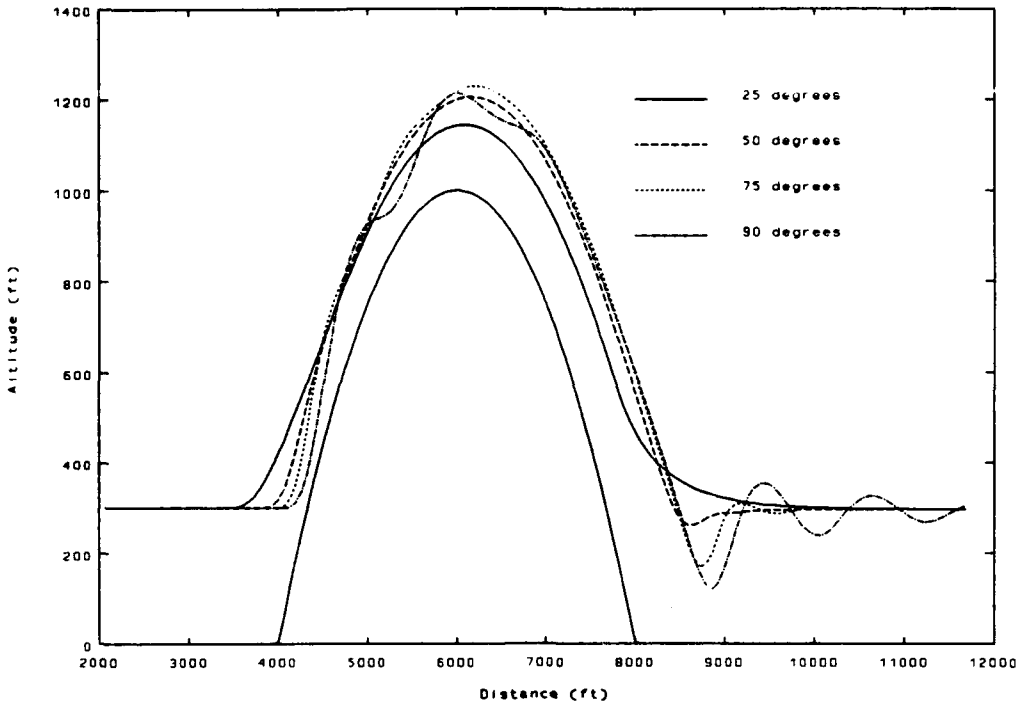

Figure 3-10: Comparison of Position Traces (Fixed Angle)

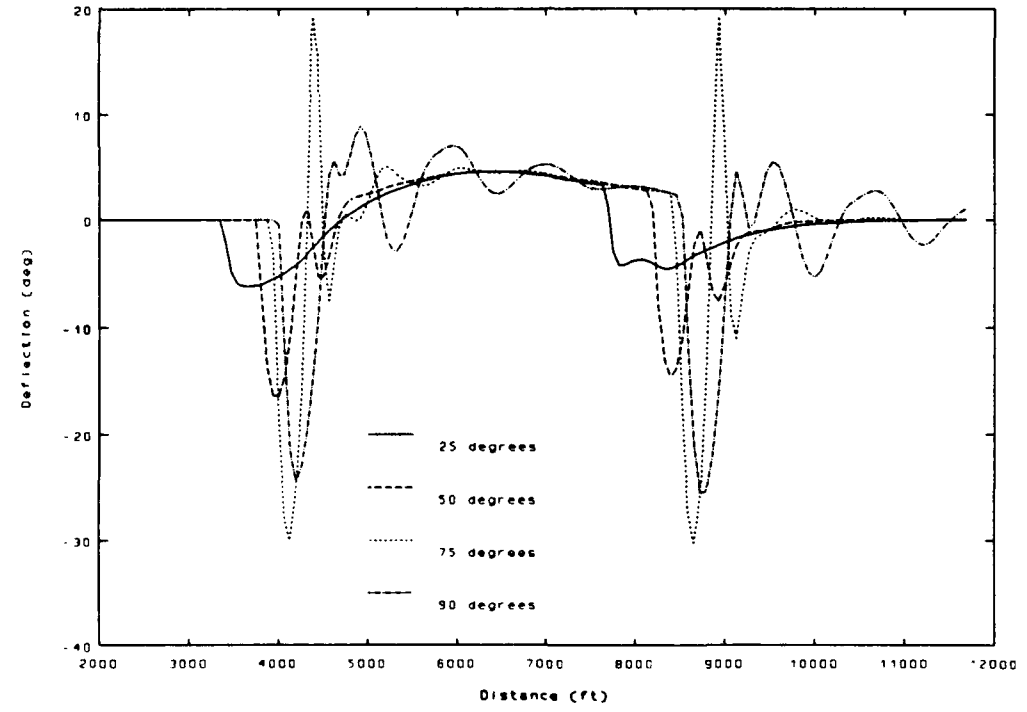

Figure 3-11: Comparison of Control Power Usage (Fixed Angle)

maneuver far enough in advance that drastic changes are not required. However, we also see that looking too far ahead can cause trouble. The radar must look ahead, but not at such a small angle that the beam overlooks an obstacle whenever the pitch angle of the aircraft raises too high. We will now examine other possible advantages which may arise from adding dynamic motion to the incidence angle of the radar beam.

Case 2: Simple Gain Radar Dynamics The first methodology studied to move the radar incidence angle was a simple gain which modified the range difference and passed the signal to the controller as the Σ_{com} input

$$\Sigma_{com} = K_{radar}(\Delta R) \tag{3-1}$$

The baseline chosen for each of these runs was the midrange elevator gain runs from the fixed angle cases. To determine the best radar gain to use, the elevator gain was fixed and the scores as the radar gain varied were noted. The 90 degree case did not work at all, as the beam would eventually travel behind the aircraft and the aircraft would then crash into oncoming terrain. Both the 75 and 50 degree cases worked well, and showed improvement in the scores recorded for those runs. The implementation of the system worked for the 25 degree case, but the scores did not improve. As can be seen in Figure 3-12, the score stayed above the fixed angle score at all gain values. Due to the lack of any advantage of using this method, this angle was not considered further.

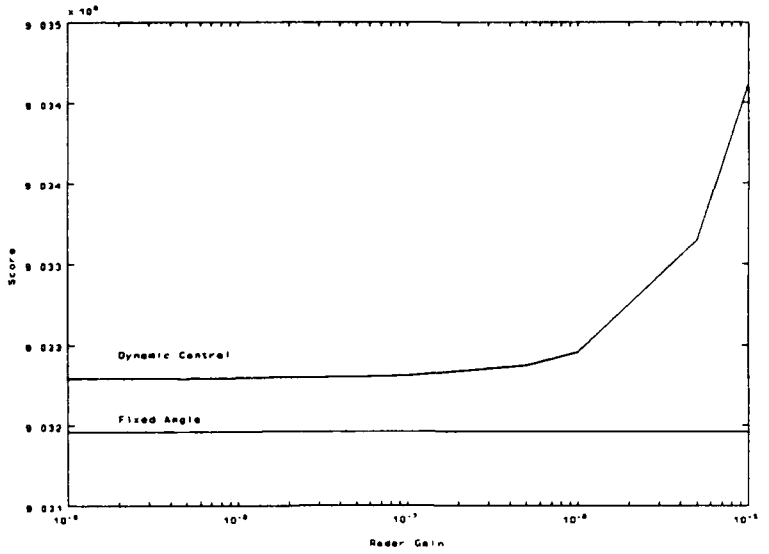

Figure 3-12: Score Variation for Simple Gain Dynamic Radar

50 Degree Incidence Angle. At this angle, the method worked extremely well. Using the dynamic radar pointing resulted in 10% improvement in quantitative score. Figure 3-13 shows the improved scores as a function of radar gain. The large spike indicates a gain value which caused the model to crash. The crashes occur when the large gain forces the radar to point beyond or above the hill. This causes an extremely large delta range which is sent through the elevator gain and into the elevator input. This causes an abrupt pitch down which crashes the simulation. Although the minimum point is at a slightly higher gain, I chose a gain of 0.0023 to run the simulation. This slightly off-optimum gain will attain a good score while hopefully avoiding the conditions which caused the crash at higher gains.

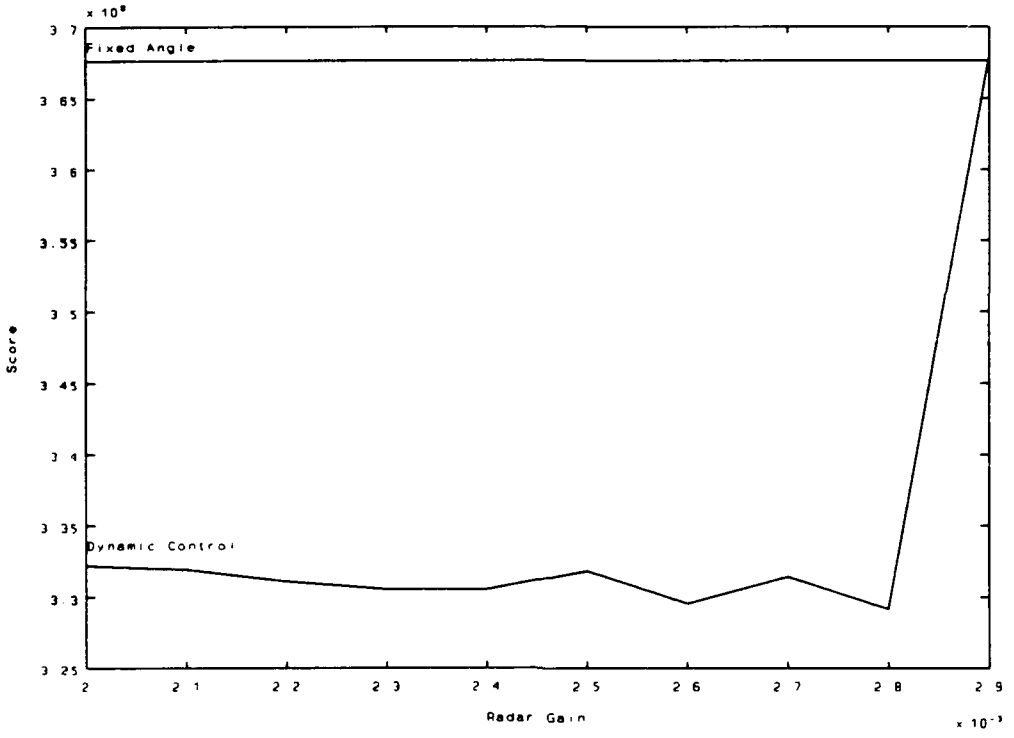

Figure 3-13: Score Comparison for $\Sigma = 50$ deg with Simple Gain Dynamics

The position trace, shown in Figure 3-14, shows excellent flight path performance with a smooth pull-up and very few oscillations. The back side of the hill requires only one small overshoot to return to the previous flight condition. Considering the improvement in the score and the visual improvement in the flight path, this seems to be a very effective method.

We may wish to know exactly how the radar incidence angle is being changed as the model completes the simulation run. This will give us a possible explanation for the score improvement. Figure 3-15 shows the change in incidence angle away from the 50 degree nominal value. As

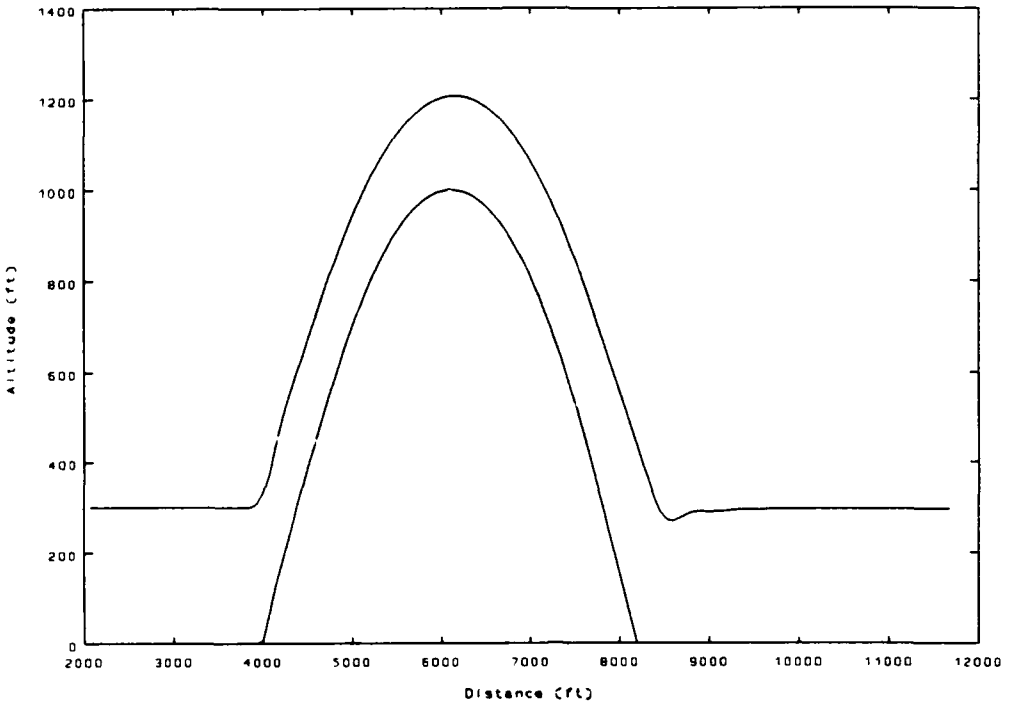

Figure 3-14: Position Trace for Σ = 50 deg; Kq = 8; Kg = .0023

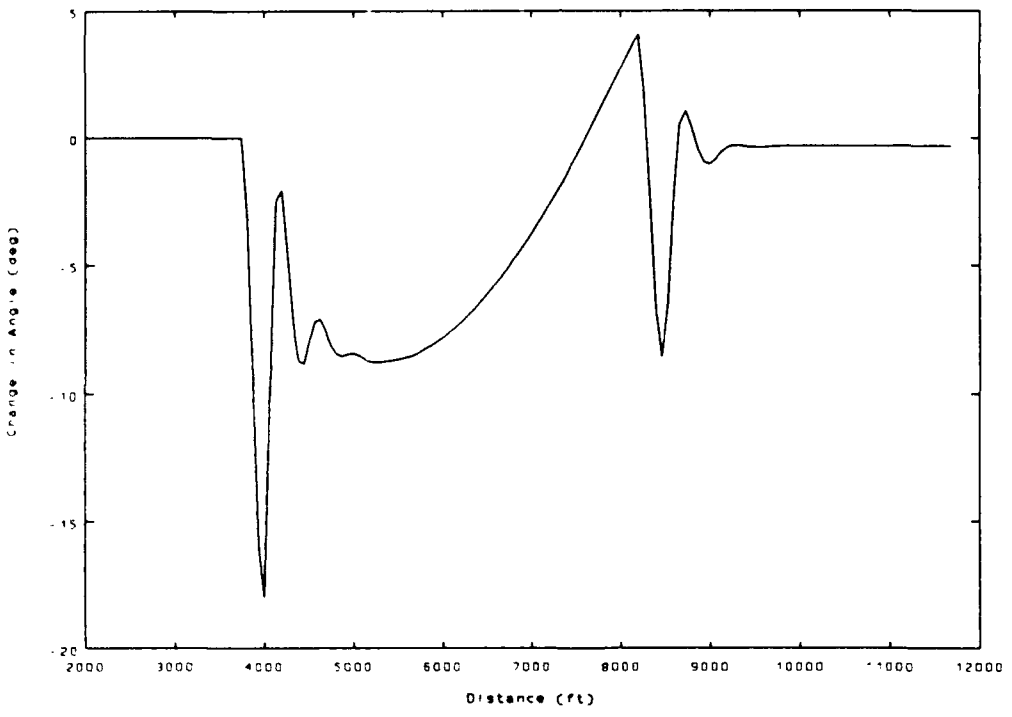

Figure 3-15: Change in Incidence Angle; Σ = 50 deg nominal

expected, the radar angle decreases when the hill is first detected. This shows that the system is working correctly; as the range decreases, the controller tries to look farther down track. Additionally, there would not be the same type of mechanical limitations on the deflection, as long as it didn't exceed a total angle of less than 0 or more than 90 degrees. The servo has also been modelled with a faster time constant, so greater angular rates would be allowed.

The final check is whether the model requires excessive control power to perform this maneuver. The control usage for this run as it avoids the hill is shown in Figure 3-16. Unfortunately, this shows that the required elevator

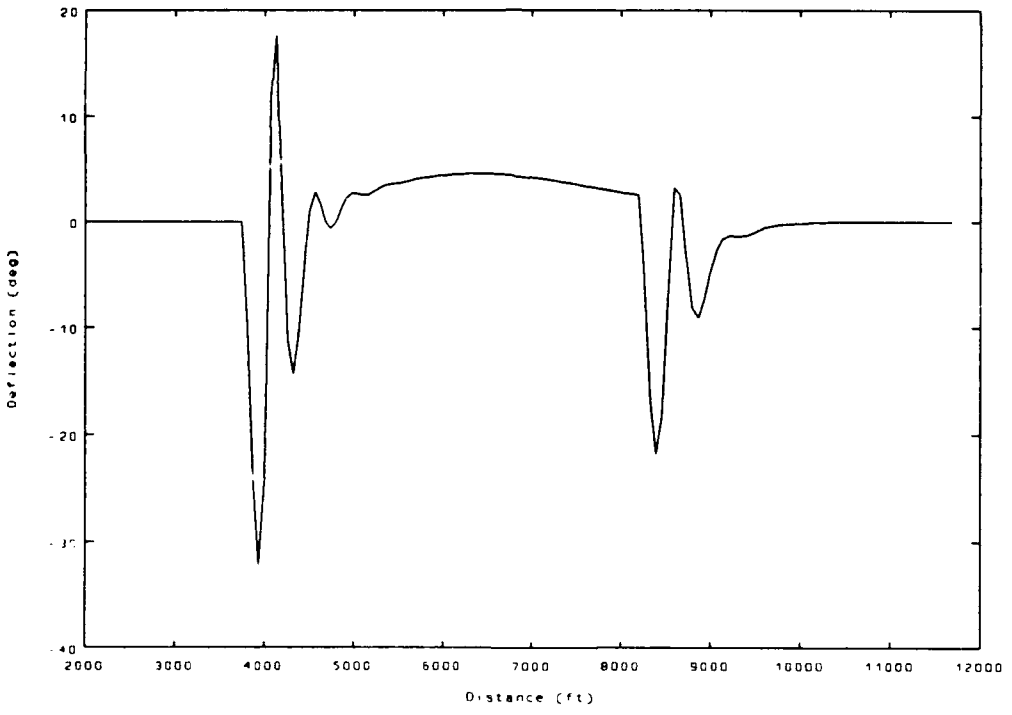

Figure 3-16: Control Power for Σ = 50 deg; Kq = 8; Kg = .0023

deflection exceeds the standard mechanical limits of $\pm$25 degrees, although the

angular rates look extremely good. Since the run with a fixed angle used much less deflection than this, it would be logical to conclude that there exists a tradeoff between the advantages of moving the radar beam about and the need for control power. This indicates that the elevator gain could be lowered and the dynamic radar pointing would allow the model to make up for the loss of responsiveness. However, because of a desire to compare the radar dynamics with the equivalent gain for fixed angle, this investigation will be left for future study.

75 Degree Incidence Angle. As the nominal angle is increased to 75 degrees, Figure 3-17 shows that the incidence of crash increases as the

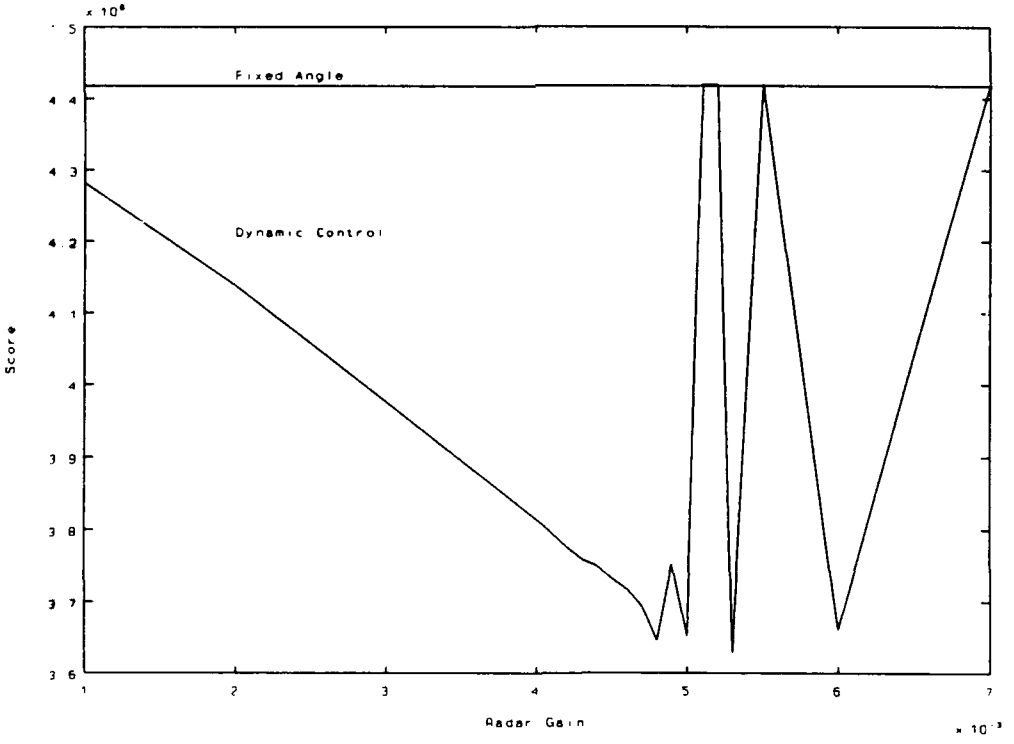

Figure 3-17: Score Improvements as Radar Gain Varies; Σ = 75 deg

radar gain is varied. Most interesting is the fact that successful runs are interspersed with the crash runs, and several times when a run is successful the score continues to drop. This makes picking an optimum gain value much more complicated. I chose a gain of 0.0048 because it was a local minimum and was still several values away from a gain value which crashed.

The position trace for this condition is shown in Figure 3-18. Once

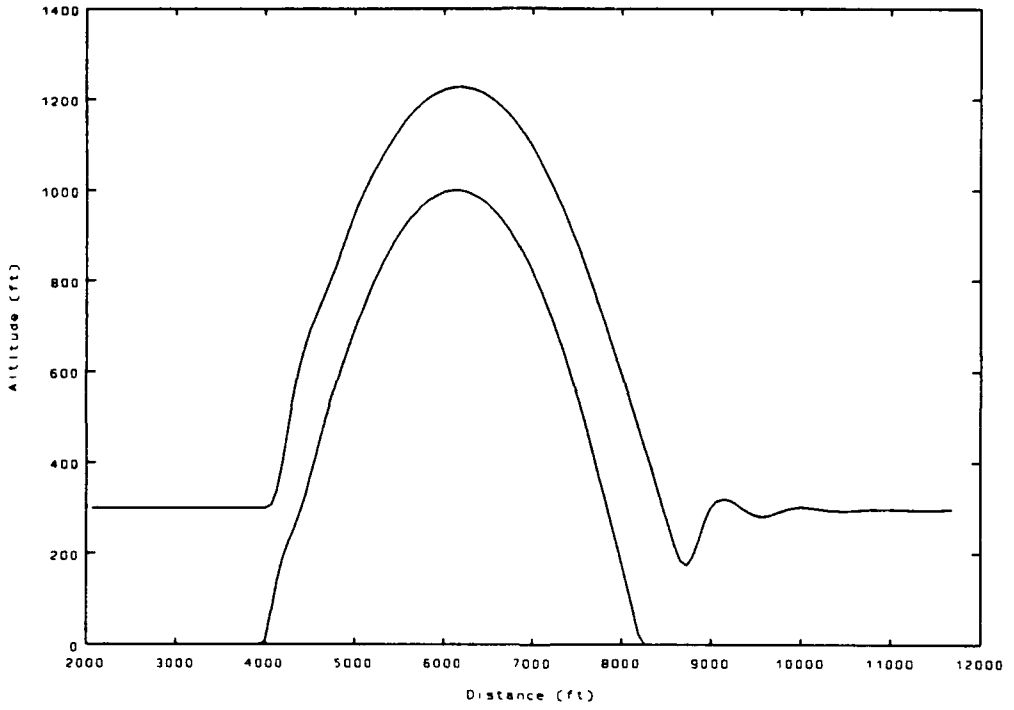

Figure 3-18: Position Trace for Σ = 75 deg; Kq = 12; Kg = .0048

again there is a strong improvement in the smoothness of the flight path due to the radar dynamics. The oscillations at the back of the hill damp out very quickly and the overall flight is much less abrupt and shaky. The vastly improved score indicates that the model does a much better job of maintaining the desired altitude buffer. Unfortunately, the initial pull-up is still quite

abrupt because of the steep slant angle and the fact that the radar dynamics don't engage until a change is detected in the range reading.

The radar dynamics shown in Figure 3-19 show us just how the radar

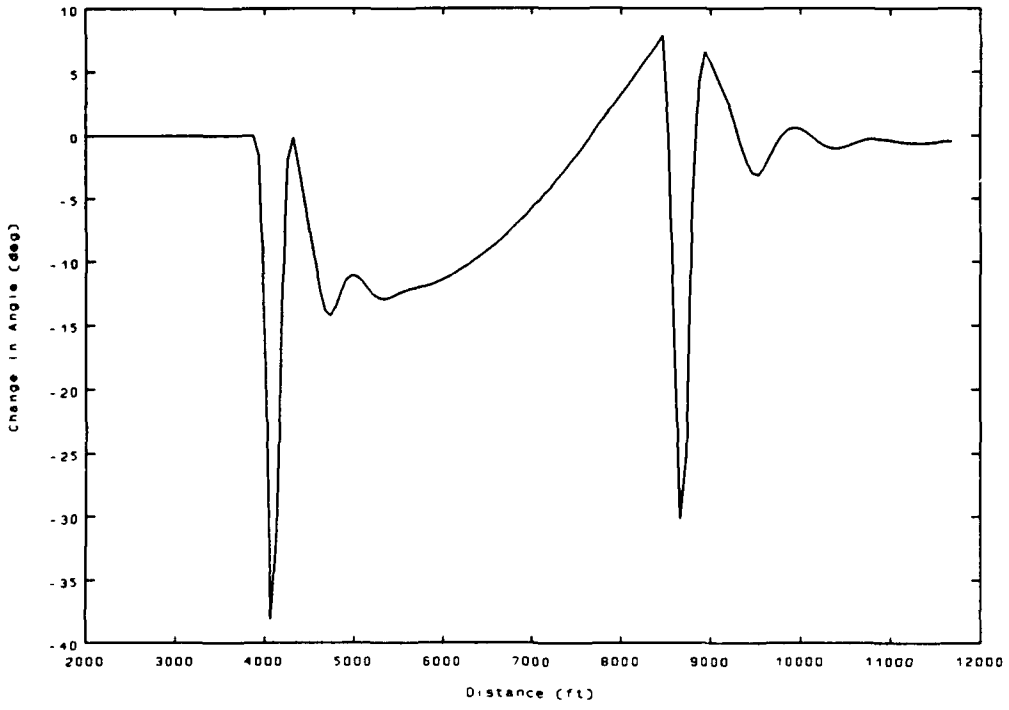

Figure 3-19: Change in Radar Angle; Σ = 75 deg; Kq = 12; Kg = .0048

is moving to get these results. The initial spike abruptly reduced the angle because of the proximity of the hill. The radar attempts to return the range measurement to the initial value by pointing farther out ahead. In this case, the first movement is a forty degree decrease. Once again, this is acceptable because of the way the radar would be mounted and pointed. The maximum deflection in the positive direction does not exceed the vertical body axis and the rates of change are very reasonable. The primary problem appears to be that for different nominal angles, a different radar gain is required. This

would also point toward a requirement for a different gain at different flight conditions. The problem would be how to derive and store all the gains needed at all of the different conditions.

As seen in Figure 3-20, the elevator response for this run is again

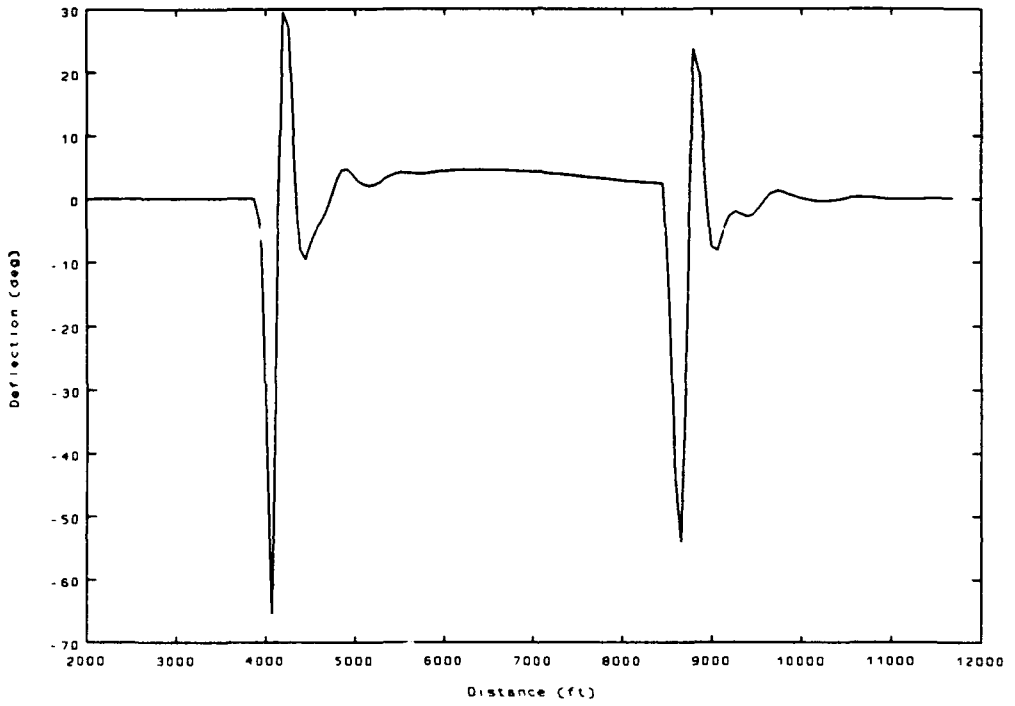

Figure 3-20: Control Power for Σ = 75 deg; Kq = 12; Kg = .0048

higher than would be physically possible. However, it also explains why the oscillations are no longer as noticeable. The graph shows only one big spike at the beginning of the hill and another smaller one at the end of the hill. Each of these take another cycle or two to damp out, but there are literally no other control inputs to cause the porpoise-like motion we have seen on other runs. Once again, it is probable that by using this dynamic radar motion, the elevator gain can be turned down. This will buy the performance without

overworking the control surfaces. However, we still see that 75 degrees is not far enough to look ahead; it really doesn't provide adequate warning.

Simple Gain Dynamics Summary. Overall, we see that adding a simple gain to control the dynamics of where to point the radar is a very effective method of smoothing out the bumps in the flight path introduced by high gains on the elevator inputs. Figure 3-21 provides a comparison of the

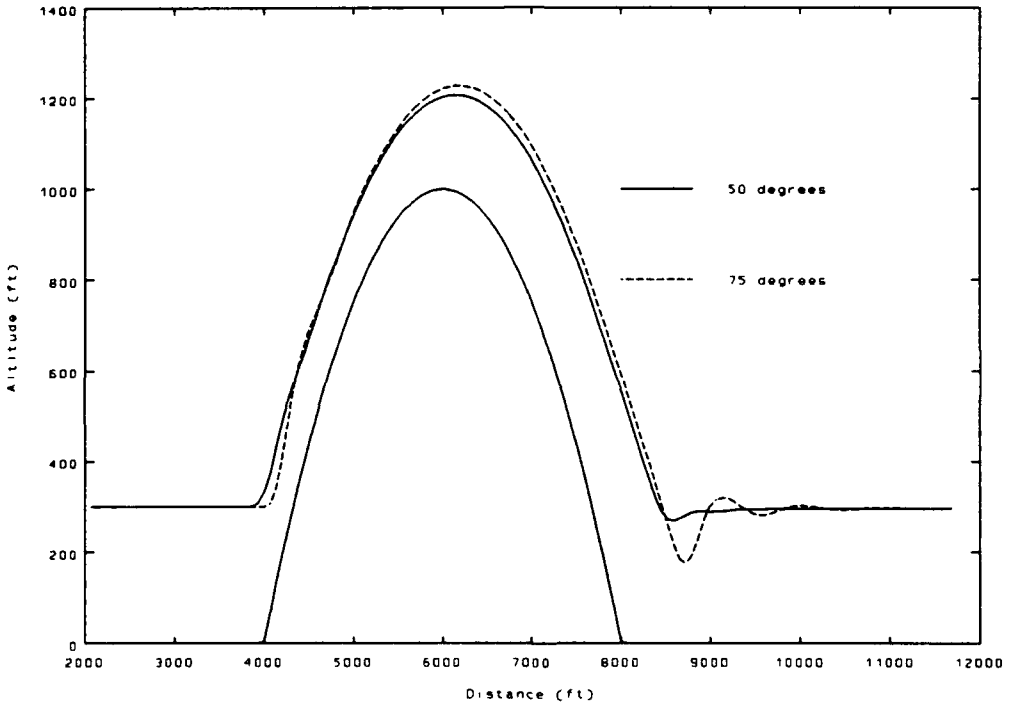

Figure 3-21: Position Trace for Simple Gain Radar Dynamics

two angles which could effectively benefit from using the gain-driven pointing methodology. We see that because of the higher gains, the 75 degree run attains a higher altitude over the crest of the hill. This may also be explained by the 50 degree run being able to see the hill fall away on the backside earlier than the other run and doing a pushover well in advance of reaching the

commanded buffer altitude. As shown before, the smaller incidence angle makes for smoother transitions from the flat ground to the hill and back to flat ground again. The effect this has on the flight path is especially evident at the backside of the hill. The 75 degree case is forced to dip way into the buffer zone before making its pullout, while the 50 degree run only needs to make a slight correction, with only one overshoot to stabilize back to straight and level flight.

The trace of the radar movement emphasizes this difference even more clearly. Figure 3-22 shows that because the 75 degree run drives in much

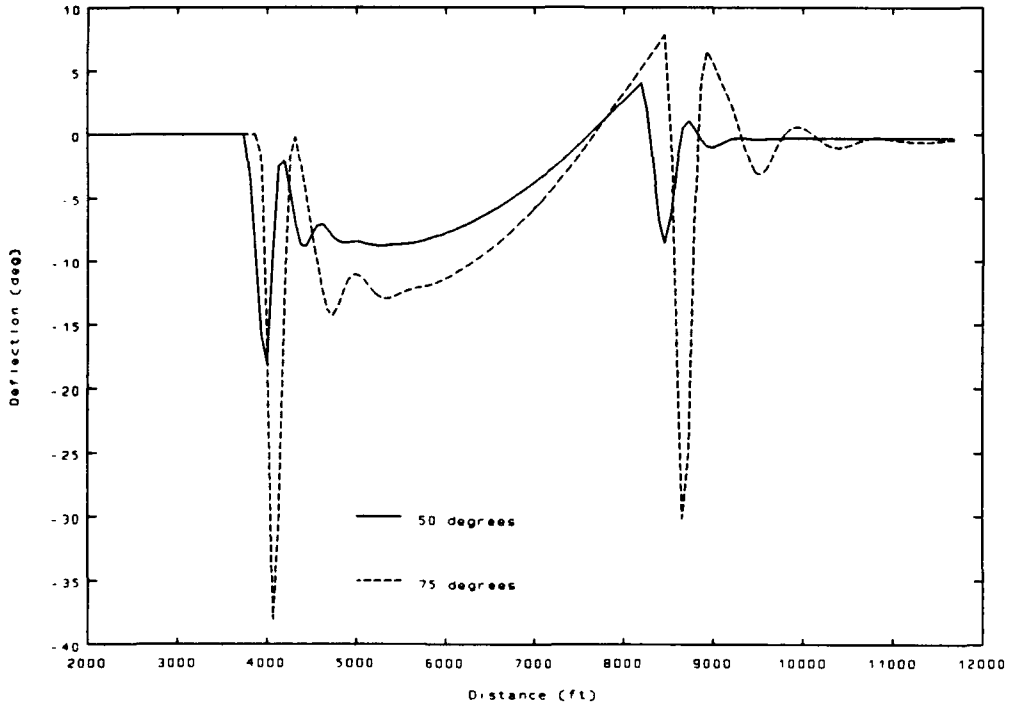

Figure 3-22: Change in Radar Angle (Simple Gain)

closer to the upcoming terrain, it requires much more drastic measures once an obstacle is detected. It is interesting to note that both cases seem to roughly

agree on the optimum angle to be looking at the beginning of the hill. The 50 degree case decreases the incidence angle by approximately 18 degrees, which points the radar at an angle of 32 degrees. The 75 degree case decreases its angle by 38 degrees, which points the radar at 37 degrees. Thus, we see that from starting out 25 degrees apart, the dynamics reduce that difference to only 5 degrees. On the backside of the hill, the convergence is even closer. The 50 degree case is reduced to 42 and the 75 degree case reduces to 45.

As noted in the individual cases, adding dynamics to the radar tends to increase the control power required to complete the maneuver. We see in Figure 3-23 that the deflection angles for both cases are increased over their

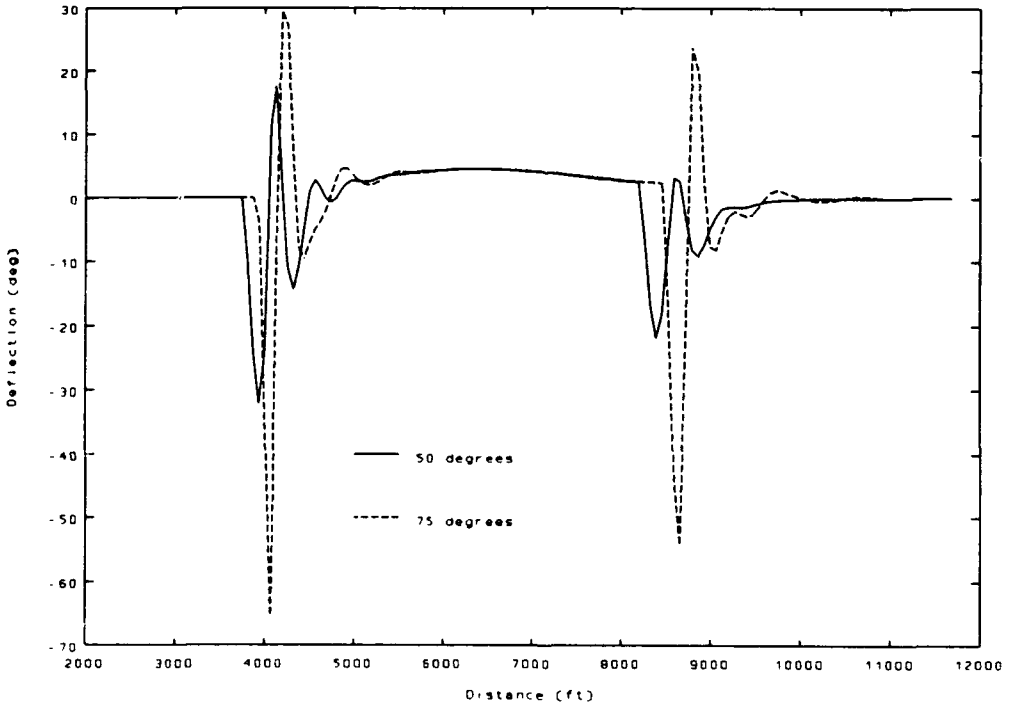

Figure 3-23: Control Power for Simple Gains

fixed angle equivalents. Although the 50 degree run is almost within the mechanical limits of the aircraft, both runs show excessive control usage.

In summary, we find that the simple gain pointing method is very effective for providing increased look ahead distance during critical phases of the flight. It gains a smoother ride, but sacrifices control usage. By implementing this system, it should be possible to match the ride quality of the fixed angle cases while using smaller gains on the control surfaces.

<u>Case 3: Constant Time Radar Dynamics.</u> The third methodology investigated involves predicting what spot on the ground the aircraft will be over after a given time interval and directing the radar energy at that point to determine the range. This range is compared with the initial range, and this difference is used to drive the elevators as in the other cases. The radar pointing command calculation, shown in equation 3-2, involves determining the instantaneous horizontal velocity and the measured range. These are used to direct the beam to the ground location which the aircraft would overfly in a preset amount of time.

$$\Sigma_{com} = \theta + \cos^{-1}\left(\frac{V_H * t_c}{R}\right) \qquad (3\text{-}2)$$

where

Σ_{com} = commanded perturbation in incidence angle (rad)

θ = pitch angle (rad)

V_H = horizontal velocity (ft/sec)

t_c = time constant (sec)

R = measured radar range (ft)

As with the previous method, only two of the incidence angles could successfully implement this technique. The 90 degree case was not run, because the concept of look ahead time is meaningless when the beam is pointing straight down. Also, the 75 degree case could not obtain a successful run due to a tendency to move the beam behind the aircraft, and therefore gather useless data.

25 Degree Incidence Angle. The time constant which was calculated for a nominal angle of 25 degrees was 1.0595 sec. As in the other methods, the 25 degree case does an excellent job of maintaining a smooth and steady flight path. As seen in Figure 3-24, the attitude changes are gradual and it performs the tracking well. The return to steady level flight is exceptionally good. Once again we see that the maximum altitude is much less than the commanded 1300 ft, but as previously proposed this is a result of a combination of weak response due to small gain, and an early pushover due to the long look ahead distance.

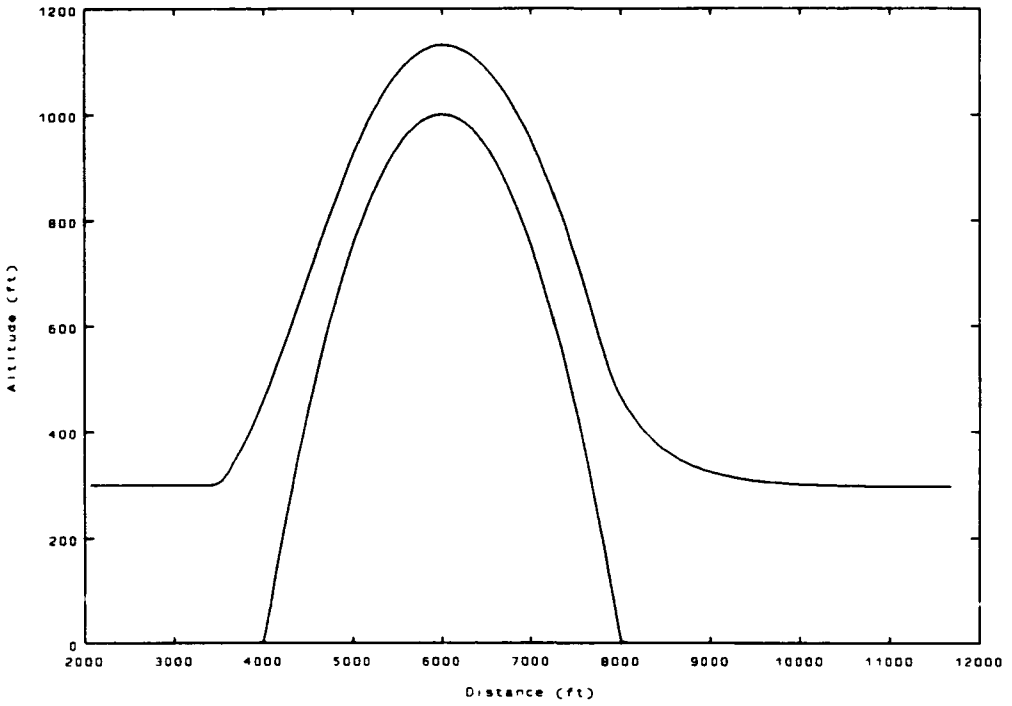

Figure 3-24: Position Trace: $\Sigma = 25$; tc = 1.0595

The trace of the radar position is very well controlled. It changes no more than 7 degrees, and the rates of change are reasonable. The maximum deflection results in a minimum incidence angle of 18 degrees. The plot of the incidence angle is shown in Figure 3-25.

The elevator deflections for this run are equally well-behaved. Considering the smoothness of the position trace, we would not expect any drastic oscillations of the control surfaces, and the trace of the elevator deflection in Figure 3-26 proves this true. The maximum deflection the model uses in the simulation is less than 18 degrees. The angular rates seem reasonable and the overall response is good.

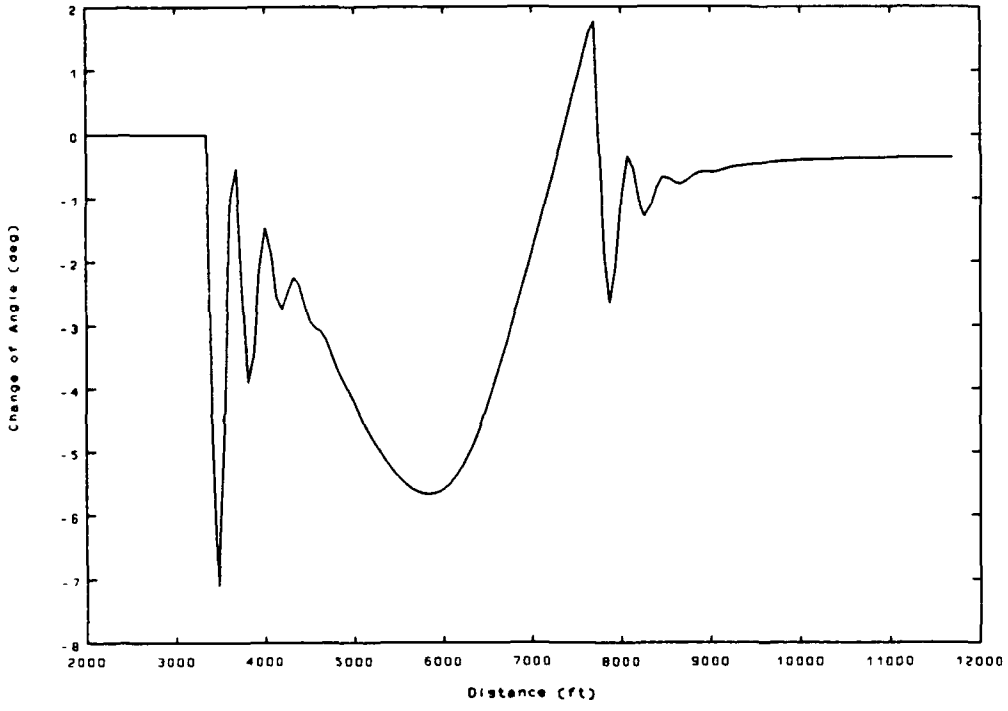

Figure 3-25: Change in Radar Angle: $\Sigma = 25$, tc = 1.0595

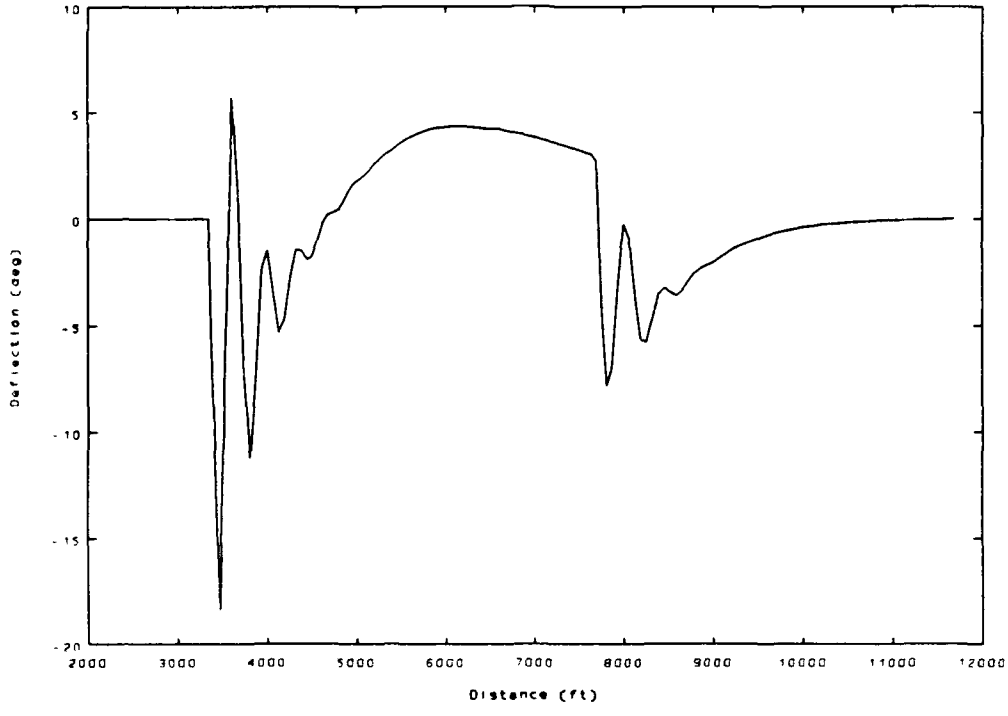

Figure 3-26: Control Power: $\Sigma = 25$, tc = 1.0595

50 Degree Incidence Angle. The time constant calculated for an incidence angle of 50 degrees was 0.58451. The flight path of this run shown in Figure 3-27 looks extremely good. Although the maximum altitude

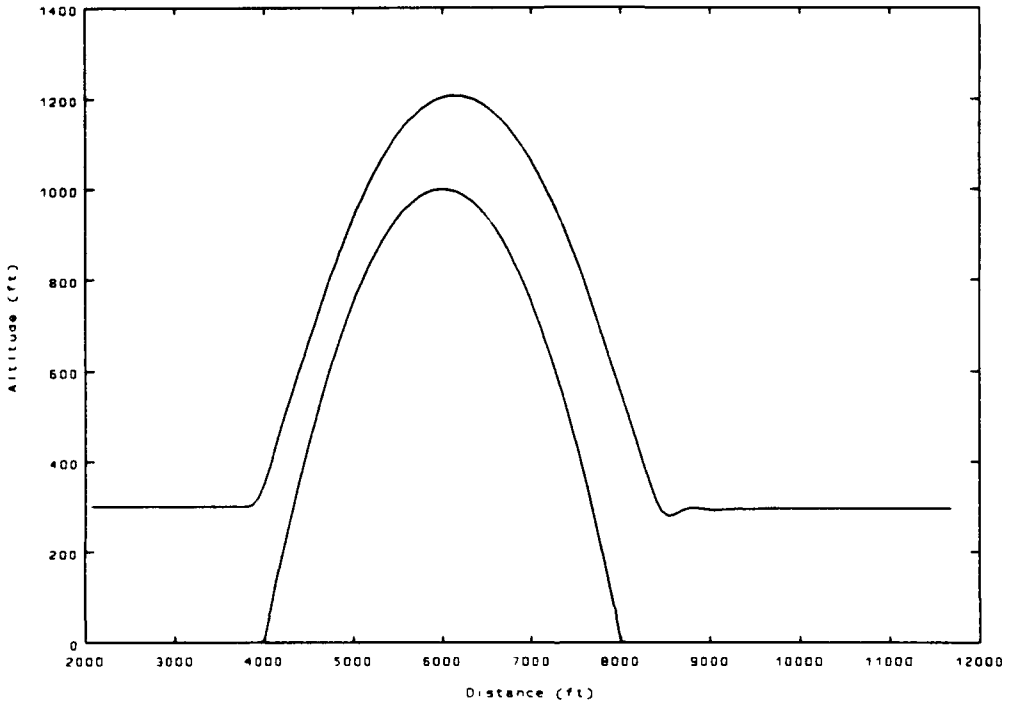

Figure 3-27: Position Trace: Σ = 50; tc = .58451

does not reach 1300, it does at least get above 1200. The initial pullup maintains excellent ground clearance and the recovery on the back side requires only one overshoot.

The radar dynamics from a nominal angle of 50 degrees are shown in Figure 3-28. Comparing the 50 degree runs to the 25 degree runs, the figure shows that the model requires more than twice as much movement on the

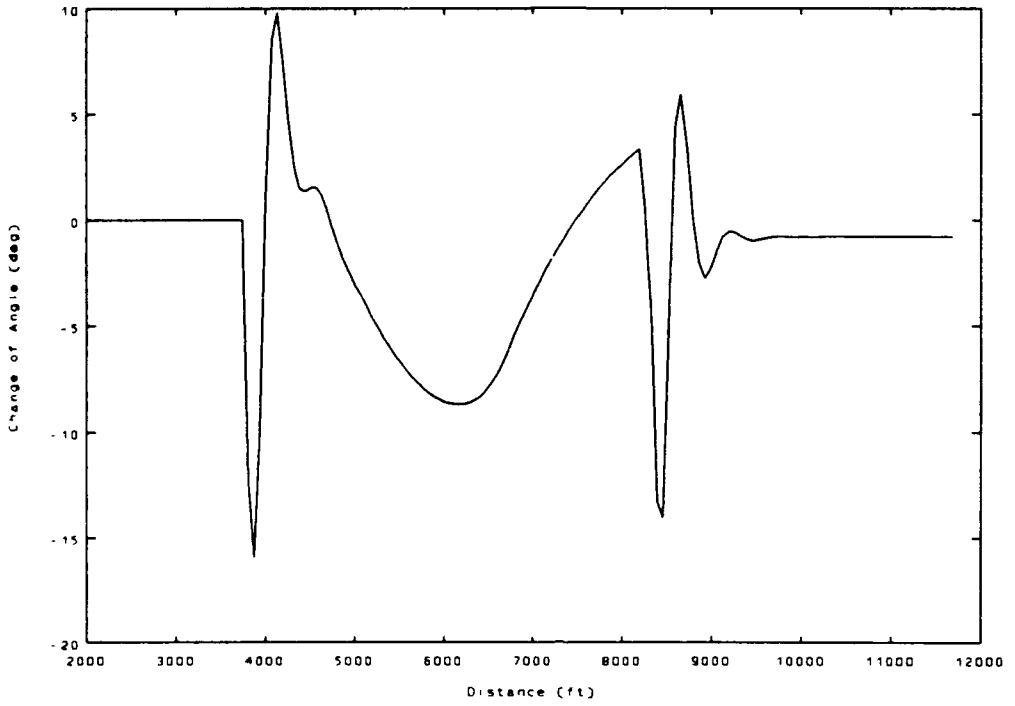

Figure 3-28: Change in Radar Angle; Σ = 50; tc = .58451

initial pullup, but overall moves around a lot less. The total range of deflection varies from 34 to 60 degrees. The rates of change are very reasonable and the overall motion is very good.

The control power used for the 50 degree simulation is slightly less than twice the amount needed for the 25 degree run. The maximum deflection is 33 degrees and occurs at the initial pullup. The response of the elevator, shown in Figure 3-29, is well damped, using only two overshoots to return to a nominal value. Although the magnitude of the deflection is greater than the mechanical limits of the aircraft, it is close and the gain on the elevator command could most likely be reduced without significantly affecting the

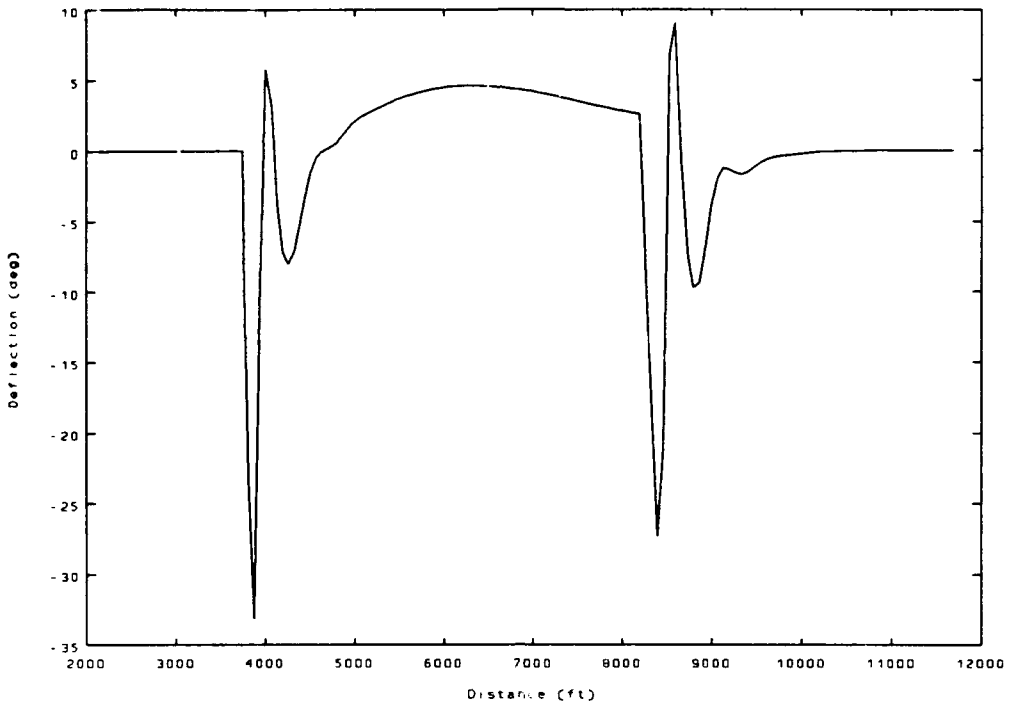

Figure 3-29: Control Power: Σ = 50, tc = .58451

terrain following performance.

<u>Time Constant Radar Dynamics Summary.</u> This method seems to hold a lot of merit. The calculations required can be done real-time. This avoids the need for having to have a large database of information compiled beforehand and then gain scheduling from point to point within the flight envelope. As we can see from Figure 3-30, both angles handle the obstacle very well. As previously discussed, the 25 degree case does not attain the desired clearance over the crest of the hill, but does have exceptional ingress/egress performance. The 50 degree case shows much better response

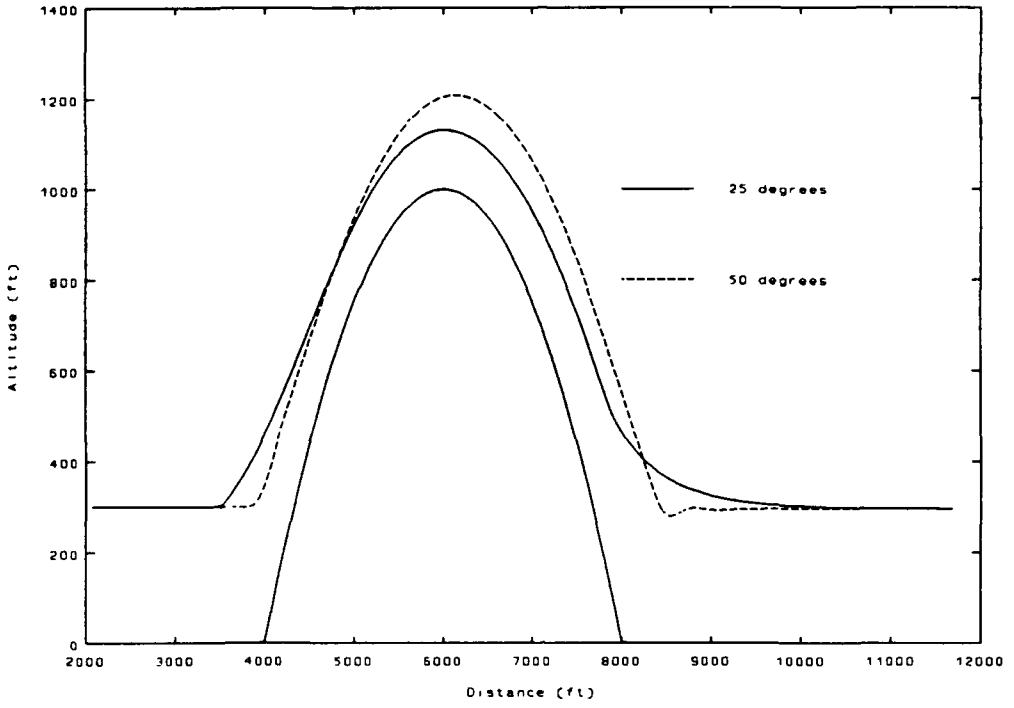

Figure 3-30: Position Trace Summary (Fixed Time Constant)

on top of the hill, but is more abrupt at the beginning and end of the obstacle.

The radar pointing response for the angles is remarkably different. Figure 3-31 shows us that the 25 degree simulation never commands a positive change in the angle with the exception of a very short time just before the end of the hill. The 50 degree simulation commands positive and negative changes during both the start and end of the hill. The dissimilarities arise because the pointing angle in this method is so much more reliant on the current aircraft attitude and position relative to the terrain beneath it. Because the 50 degree case approaches much closer to the hill before initiating the pullup, and must

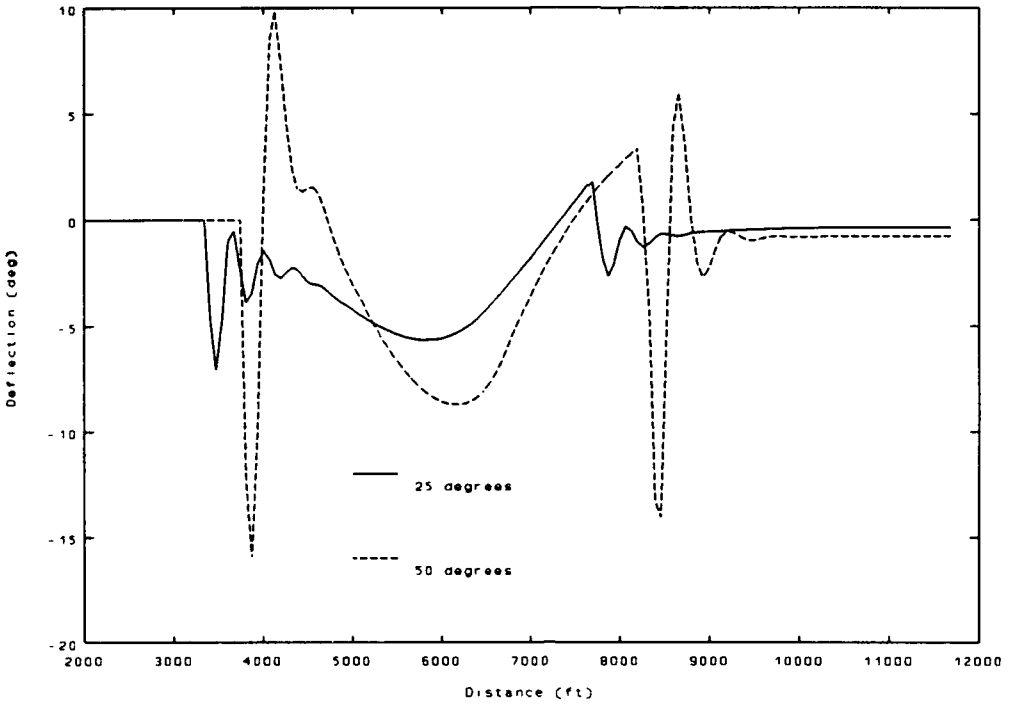

Figure 3-31: Change in Radar Angle Summary (Fixed Time Constant)

pull harder when it finally starts, the aircraft position parameters (i.e. velocity, pitch angle, and height AGL) are entirely different from the low angle case. Since these are the parameters being used to direct the incidence angle, it is logical that there would be little correlation to the 25 degree case.

Comparing the control power, shown in Figure 3-32, we see a much stronger correlation between the two cases. Although the magnitudes are different due to the higher control gain used for the higher angle, the general shape of the curves are similar. The plots are also time shifted because the low angle case detects the hill and reacts to it much sooner. The 50 degree

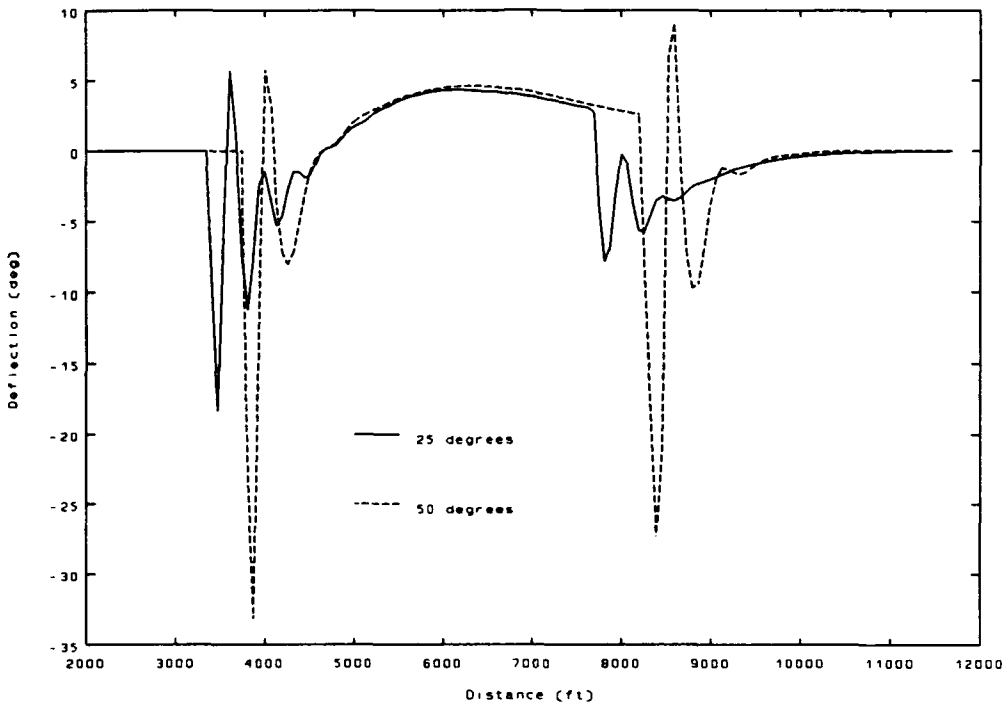

Figure 3-32: Control Power Summary: (Fixed Time Constant)

case is actually more heavily damped than the 25 degree case, as it requires one less spike to settle into a smooth command line. As noticed earlier, the magnitude of the deflection exceeds the mechanical limits, but it is believed that it would be possible to reduce the gain without sacrificing a great deal of performance.

Method Comparison

Now that we have seen how changing the nominal angle affects the results for each method, we will now look at comparing the different methods

for each nominal angle. The first angle investigated is 75 degrees. Figure 3-33 shows the flight paths resulting from each method run at this angle. The

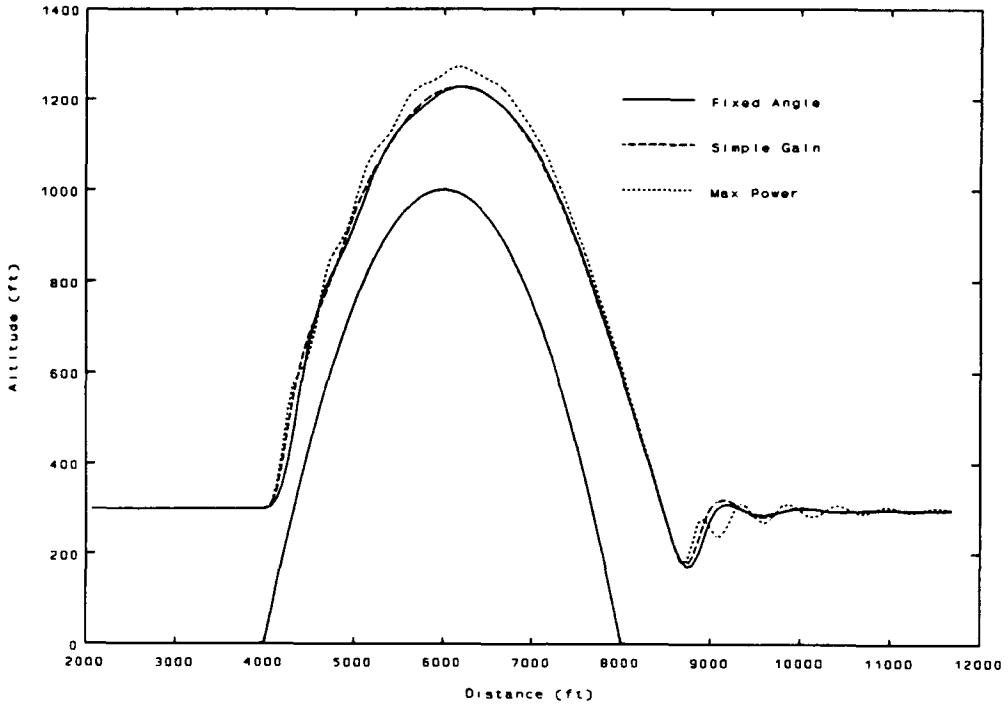

Figure 3-33: Position Trace for Σ = 75 deg

difference between the fixed and dynamic radar is especially apparent on the ascent up the hill and, to a lesser degree, at the recovery at the bottom of the hill. The max power simulation is included to show how close the other methods come to the minimum score. Other than a slight improvement in pullup, the dynamics of the radar do not seem to gain much of an advantage at this angle.

The differences in the two methods truly become apparent when we look at the control power required for each run. We see in Figure 3-34 that

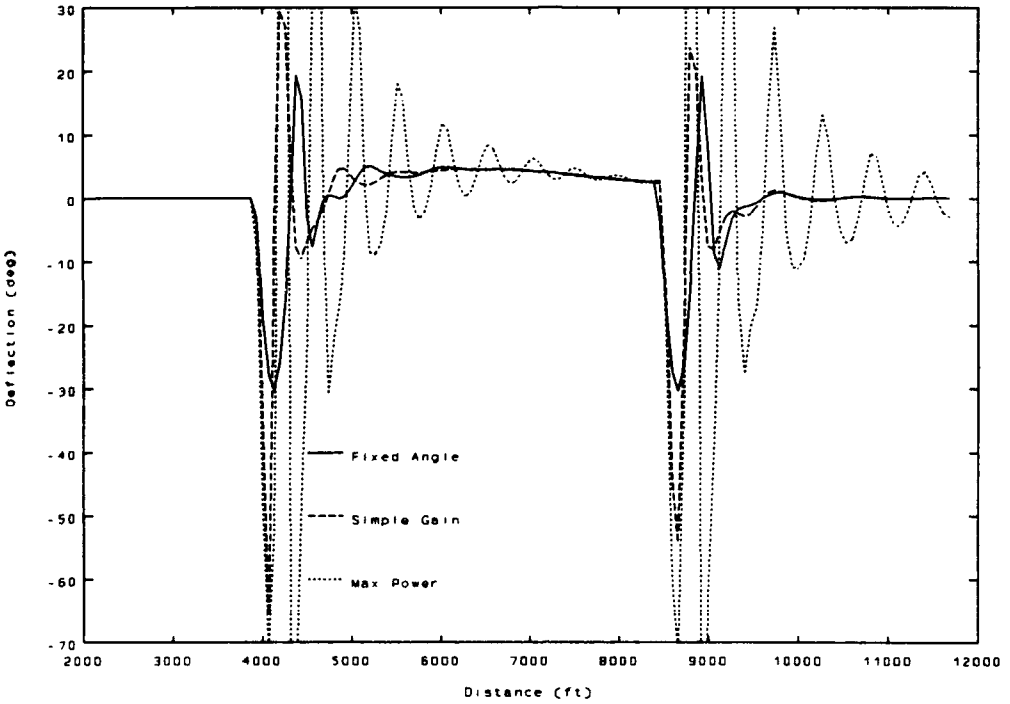

Figure 3-34: Control Power for Σ = 75 deg

the dynamic simulation requires substantially more control usage than the fixed installation to perform basically the same maneuver. Figure 3-34 is cropped to present the closest view of the dynamic methods; the max power plots are shown, but not to full deflection. In this case, as shown in Figure 3-5, the max power ranges between +175 and -90. The ability to redirect the radar shifts the timing between the two current methods, but the general shape of the curves is the same. Each have one large deflection cycle and then damp out. Unfortunately, even the fixed angle run exceeds the mechanical limits of the elevator.

Comparing the different methods at a 50 degree incidence angle presents a very similar condition. Figure 3-35 shows the position trace for

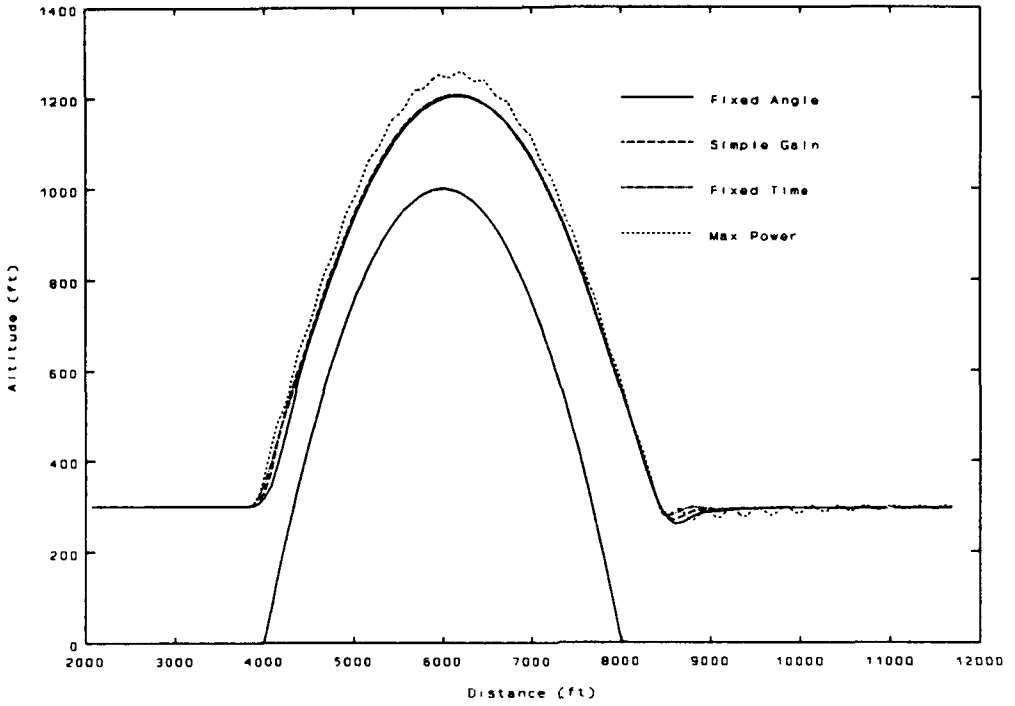

Figure 3-35: Position Trace for Σ = 50 degrees

each method. This nominal angle is the only one which successfully demonstrated all four methods and showed quantitative improvement using the dynamics over the fixed angle. Again we see that the advantage of the dynamic radar pointing is apparent only during the abrupt changes in terrain. Position during the majority of the flight is nearly identical.

The contrasts in the methods are most apparent when we examine the control power required to perform this maneuver. This control usage is shown in Figure 3-36. The control usage of the max power run is not shown.

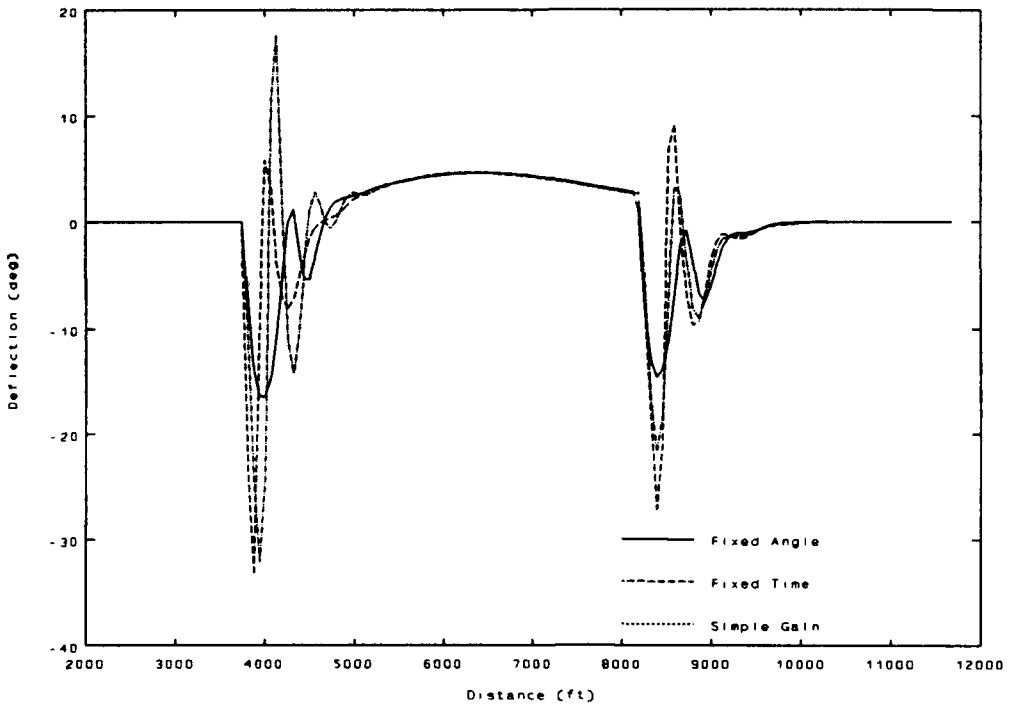

Figure 3-36: Control Power for $\Sigma = 50$ degrees

Figure 3-7 showed that plot to be high magnitude and high frequency, and therefore would only mask the real information we are trying to compare. Both methods use the same magnitude of control on the initial pullup. However, the fixed time methods seems to damp out more quickly and not use as much control on the resulting overshoots. In contrast, at the back side of the hill, the simple gain method does not require as much deflection to return the aircraft to level flight. Once again the fixed time seems to damp out more quickly and therefore both methods reach steady level flight at about the same

time. Neither dynamic method keeps the deflections within the ± 25 degree limit.

Finally, we will look at the method comparisons for a 25 degree incidence angle. The position plots at this angle, shown in Figure 3-37, do

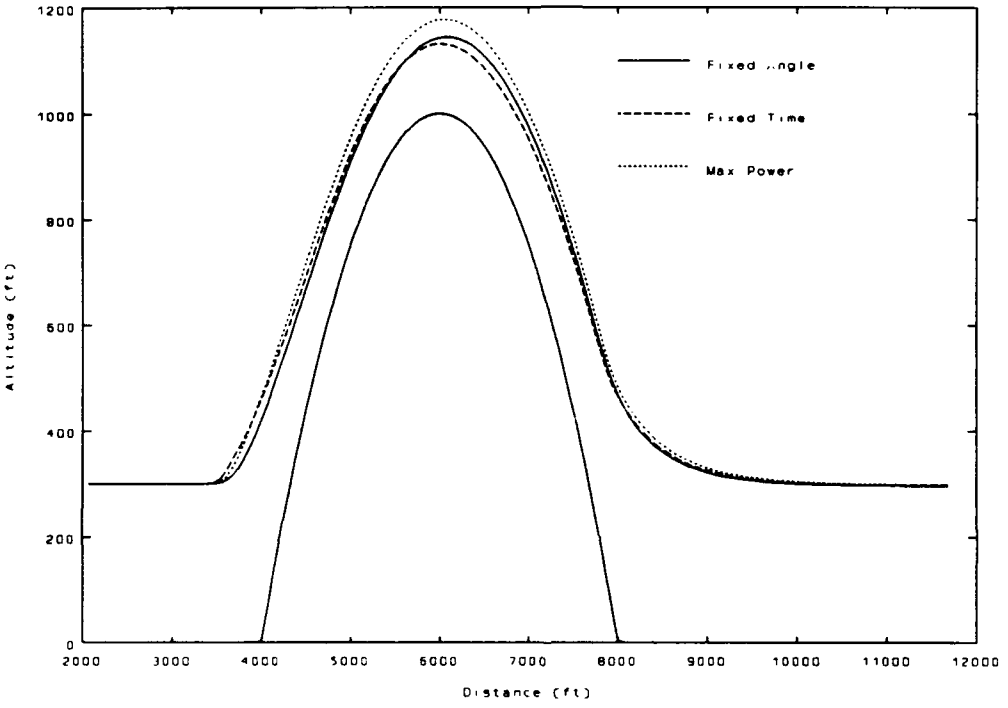

Figure 3-37: Position Trace for $\Sigma = 25$ degrees

show a difference in the flight paths each method uses. The dynamic case has a sharper pullup and maintains a higher buffer altitude throughout the ascent portion of the maneuver. Unfortunately, it also pushes over sooner and therefore does not attain the same maximum height as the fixed angle case. Neither method, nor even the max gain for that matter, even approach the 300 ft AGL desired altitude buffer on top of the hill. The control system is

looking so far ahead that it pushes over long before reaching maximum altitude in order to most closely follow the terrain on the back side. During the level-off, the dynamic run regains a slight advantage by holding a higher altitude than the fixed method.

As we have come to expect, control usage for a dynamic system is much greater than for a fixed. Figure 3-38 confirms this. The control usage

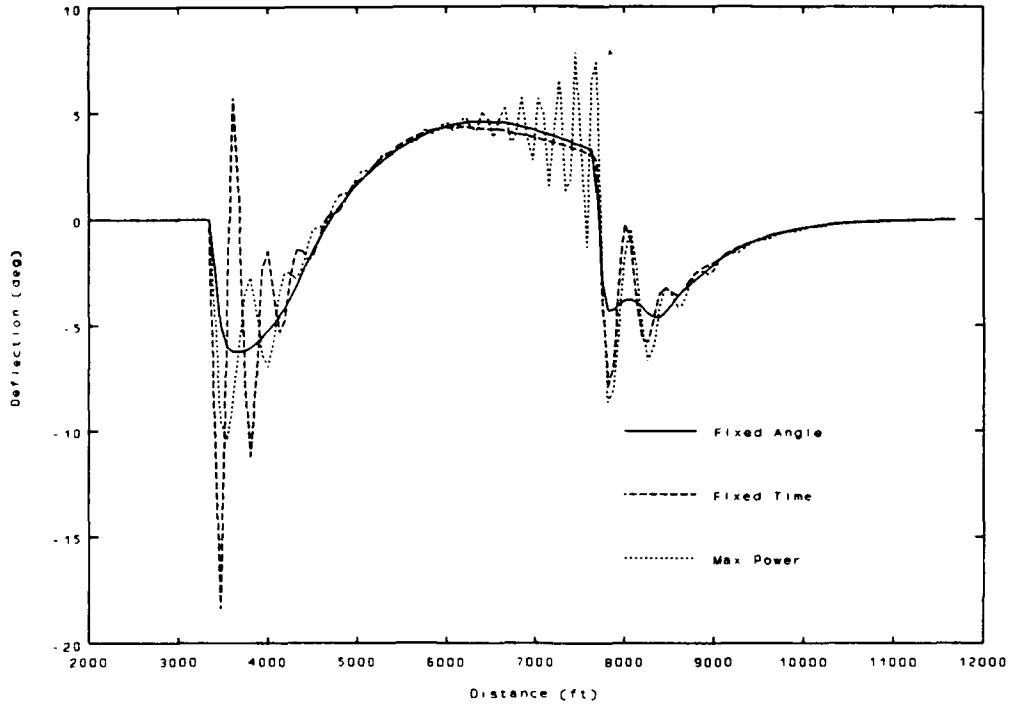

Figure 3-38: Control Power for $\Sigma = 25$ degrees

plot for a fixed angle is very smooth and of very low magnitude. In contrast, by redirecting the radar as a function of the range change, we introduce substantial oscillations into the control system. The control power required for

the dynamic method even exceeds the power required for the max gain fixed method during the initial pullup, and they are roughly equal at the level-off.

We have now examined all cases of the radar modeling methods. Although the visual comparisons show no substantial difference, we know from the quantitative score that the dynamic models do perform better at maintaining the desired altitude buffer. A nominal angle of 50 degrees is the only one which can take advantage of both dynamic methods, and also attains a much higher score than the others. Therefore, the remainder of this study will concentrate on this nominal angle and a reduced range about this nominal. We will now attempt to validate the use of this angle by showing its response to other types of terrain.

IV. Model Validation

Alternate Terrain Models

In order to validate the decision that 50 degrees is the proper choice for the radar to be projected ahead, it should be tested against other types of terrain obstacles. The obstacles this study will now investigate are a step change in terrain and two consecutive hills. The double hill should present the best challenge since the aircraft will be heading down the back side of the first hill when it encounters to ascending slope of the second. The step will show how well the system responds to a simple command. Therefore, the validation will cover both extremes, with something simple and something complex. The simulation will be run at the nominal fixed angle of 50 degrees as well as ± 20 degrees away from that nominal value. Then we will also compare the fixed 50 degree angle to runs including radar dynamics.

Step Hill Obstacle. We will first examine the model's response to flying over terrain which is mathematically equivalent to a step input. This does not test the models ability to avoid a crash so much as it allows us to observe the model's response, and the steady state error will be readily apparent. The magnitude of the step is 100 ft. This is

sufficient to cause a significant response, but does not subject the model to possible ground collision.

Fixed Angle Comparisons. The simulation was run at fixed angles of 30, 50, and 70 degrees. The position trace of the three angles shows definite differences in the response of the simulation at the different angles. Figure 4-1 graphically illustrates these

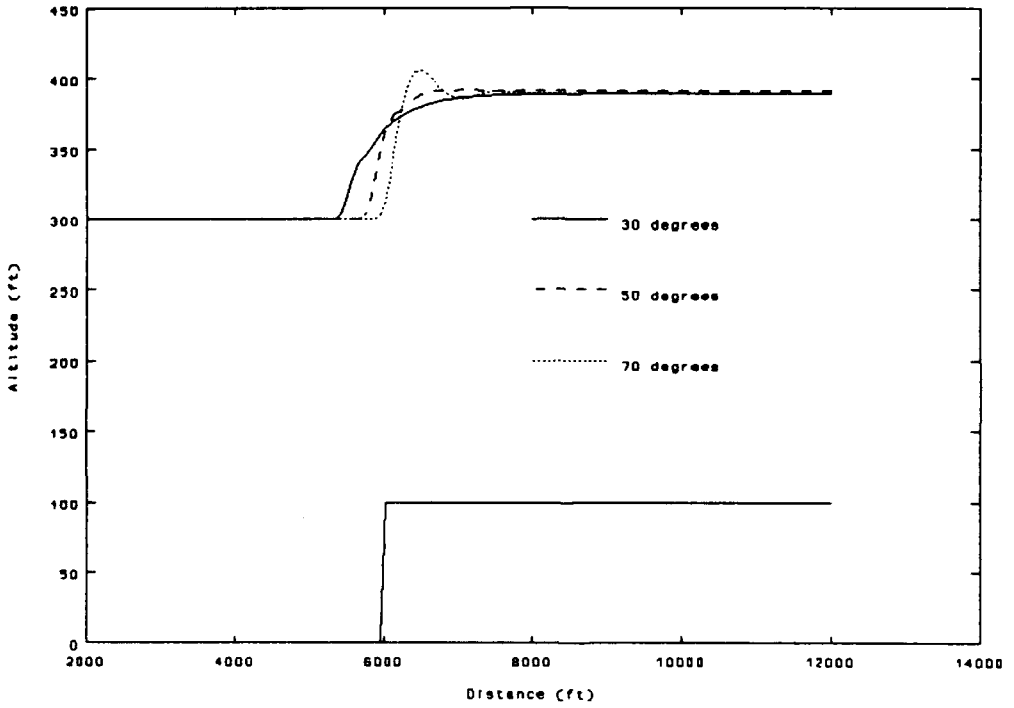

Figure 4-1: Position Response to Step Hill Input

differences. The 50 degree response shows excellent characteristics. The rise time is quick and the system does not overshoot the desired value. We do note, however, that all three systems have a steady state error of 10% in this simulation. The 30 degree angle run's response has a slower rise time, but does eventually reach the same steady state

value. The slower rise time is attributable to the lower gain which had to be used. The 50 and 70 degree runs used an elevator gain of 8. The max gain possible for a small angle model is less than 8, so a gain value of 4 was chosen for the reduced angle. Due to the lower gain, we should not expect the simulation to respond as quickly.

The elevator responses of the three systems are shown in Figure 4-2. This shows that all three systems have a quick spike of high

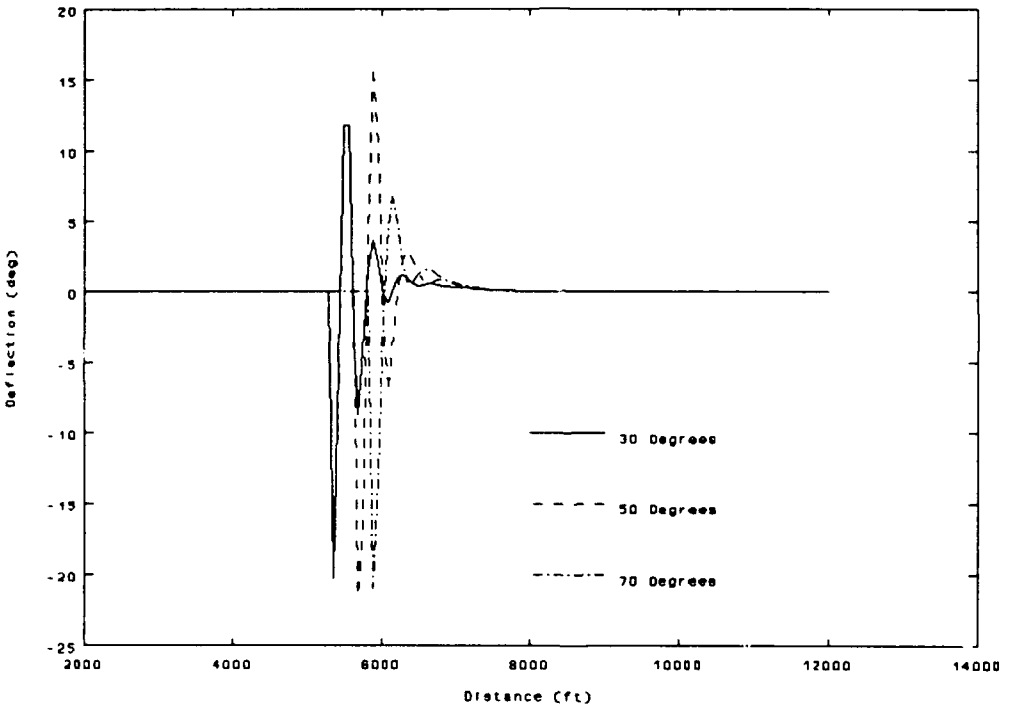

Figure 4-2: Elevator Response to Step Hill Input

magnitude which then damps out quickly. The 30 degree run is slower to damp out, but this too can be attributed to the lower gain. Surprisingly, the 50 degree run requires more control power than the 70 degree run. However, since the 50 degree run does accomplish the

maneuver without an overshoot, and both responses are within the mechanical limits of the elevator system, this is still the preferred response.

Model Comparisons. We will now look at the same obstacle using each of the models we have developed. Figure 4-3 shows the position traces for each of these simulations. Although the

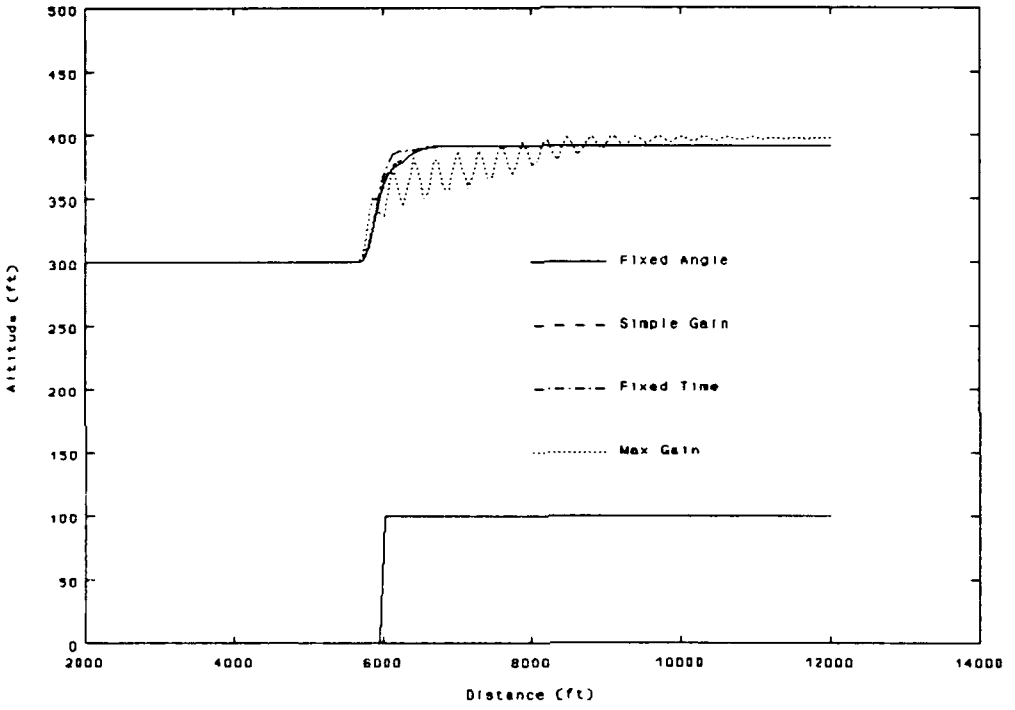

Figure 4-3: Position Response to a Step Hill Input

simple gain dynamics do very little to change the position response, the fixed time constant simulation comes much closer to approximating a true step command. The ascending portion of the response goes all the way to the steady state value without changing slope, while the fixed angle and simple gain simulations pushover to level off.

The control power required by each run to perform this maneuver is shown in Figure 4-4. This shows that the fixed time simulation does

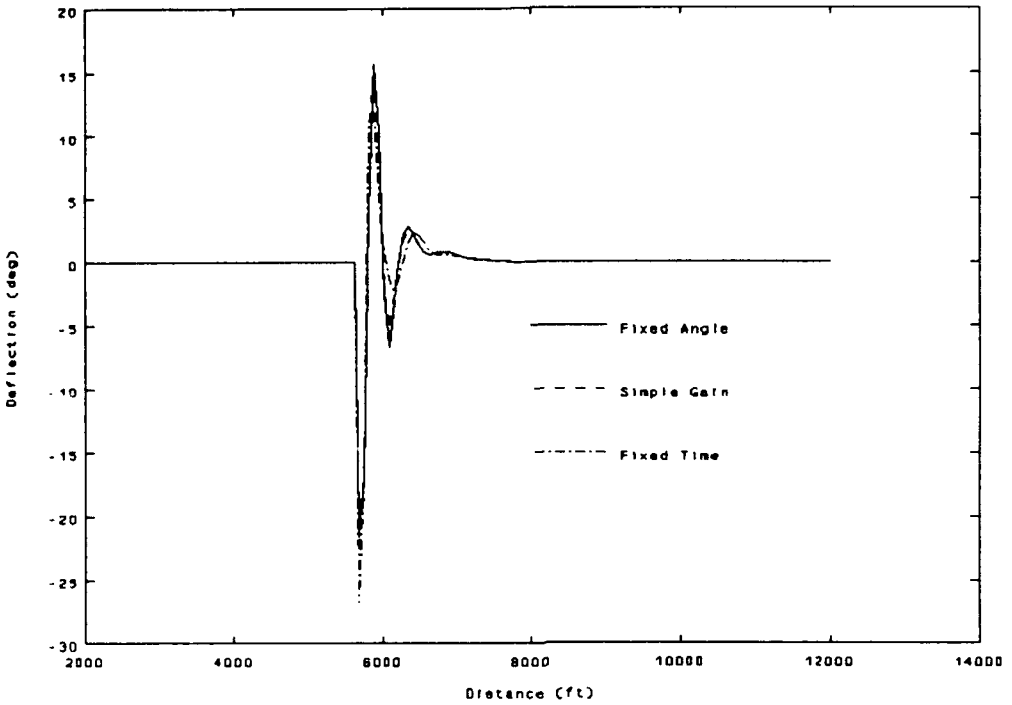

Figure 4-4: Elevator Response to a Step Input (Σ = 50)

require additional control usage to gain this better performance, while the other two cases are essentially identical. The maximum value of the constant time run does slightly exceed the 25 degree limit. Although the magnitude of the initial deflection is greater in the fixed time case, it is also less than the other runs on the remaining oscillations. All three cases damp out to the steady state value at approximately the same time.

We should now look at the differences between the positioning responses of each of the two dynamic simulations. The time history of

the radar incidence angle changes during each simulation is shown in Figure 4-5. This plot shows a drastic difference between the two

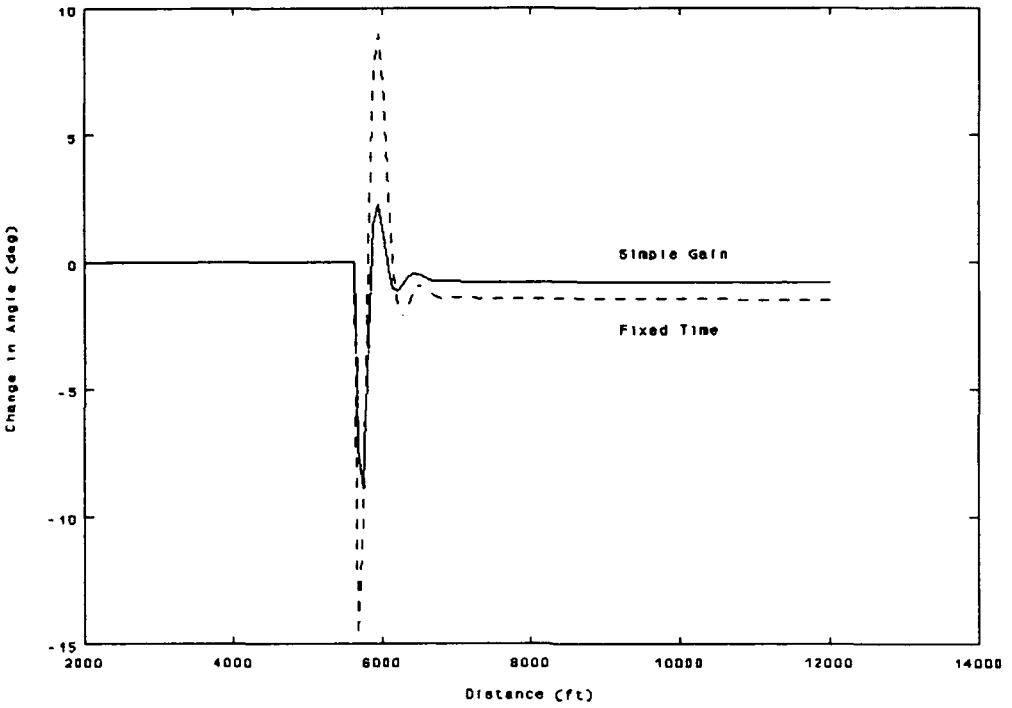

Figure 4-5: Radar Pointing Response to Step Input (Σ = 50)

dynamic methods. The magnitude of the deflections are much higher for the fixed time simulations than the simple gain, and the two cases even settle to two different non-zero steady state values.

Although the deflections are a little strong, the fixed time simulation seems to provide the best response to this simple step command. The position response more closely resembles the input and the system responds very quickly. There was very little difference in response between the fixed angle and the simple gain. The reduction in elevator response is not large enough to offset the lesser performance.

Double Hill Obstacle. The most rigorous test of the control system will be its ability to avoid a second obstacle while still recovering from the first. To test this capability, we will simulate a second hill connected to the first with a sharp valley between. As the model attempts to maintain the 300 ft AGL buffer on the first it will suddenly be confronted by the second, and will have to follow the terrain of it also. The physical shape of this double terrain obstacle is shown in Figure 4-6. The terrain is shown here in a proportionately

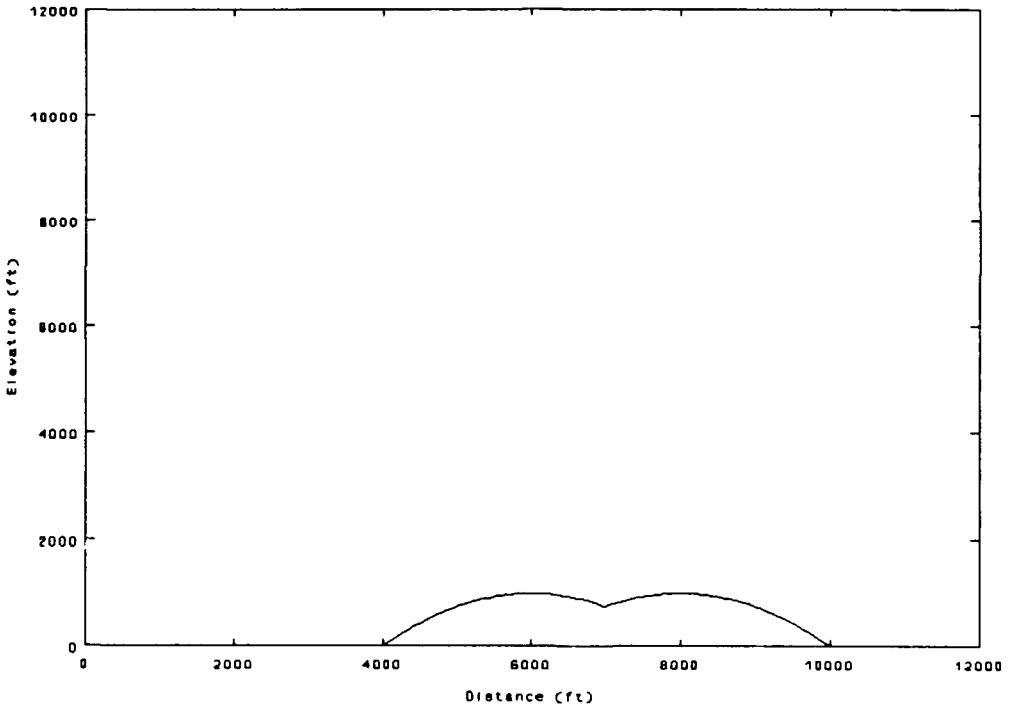

Figure 4-6: Double Hill Obstacle

square scale. All other position plots will magnify the view of the hill to allow closer inspection of the performance of the model.

Fixed Angle Comparisons. The first series of runs examined holding the radar incidence angle fixed during the flight over the obstacle. The same three angles as on the step hill (30, 50, and 70 degrees) were tested on this obstacle. The position traces for the simulation runs are shown in Figure 4-7. We see here that the 70

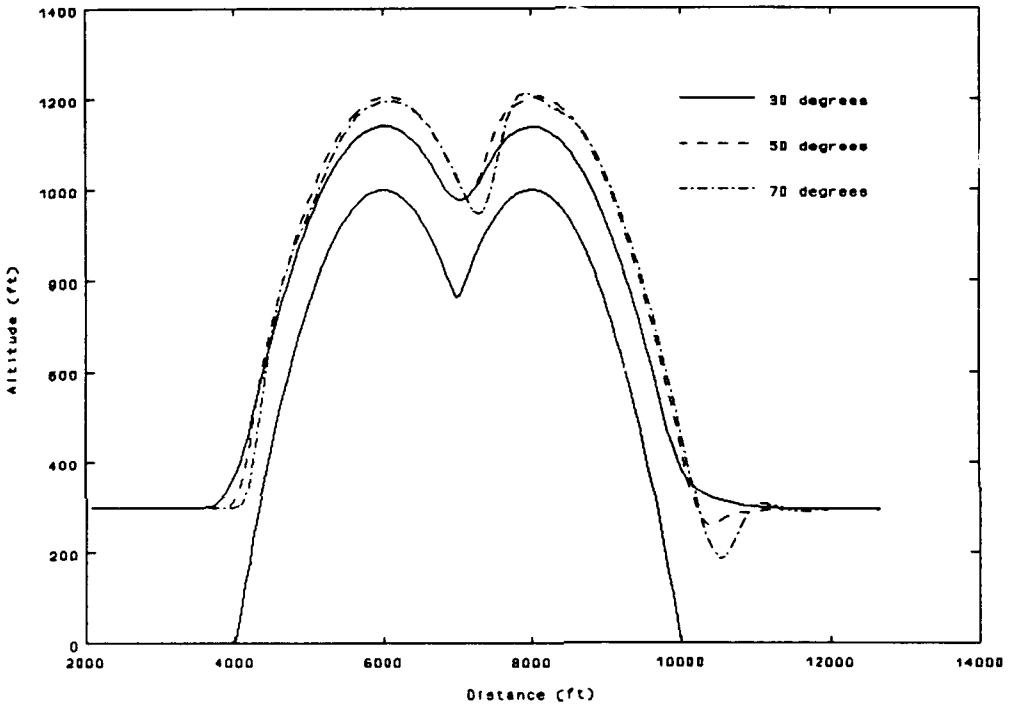

Figure 4-7: Position Trace Summary for Fixed Angles

degree simulation requires a very abrupt maneuver to avoid colliding with the second hill. However, once it does recover, it returns to the maximum height in fine shape. The 50 degree case is smooth and performs very well. It even clears the first hill with more altitude than the 75 degree run achieved. The 30 degree model is exceptionally smooth and handles the second obstacle very easily. However, it still

fails to reach the desired altitude above either obstacle. The initial pullup and the leveloff at the base of the hill show the same characteristics as they did during the single hill simulations. In general, we see that the 30 and 50 degree incidence angles performed well, while the 70 degree case looks quite abrupt.

To really determine the quality of the maneuver, we must look at the control power which was used by each simulation to complete the task. Figure 4-8 shows the elevator deflections for each run.

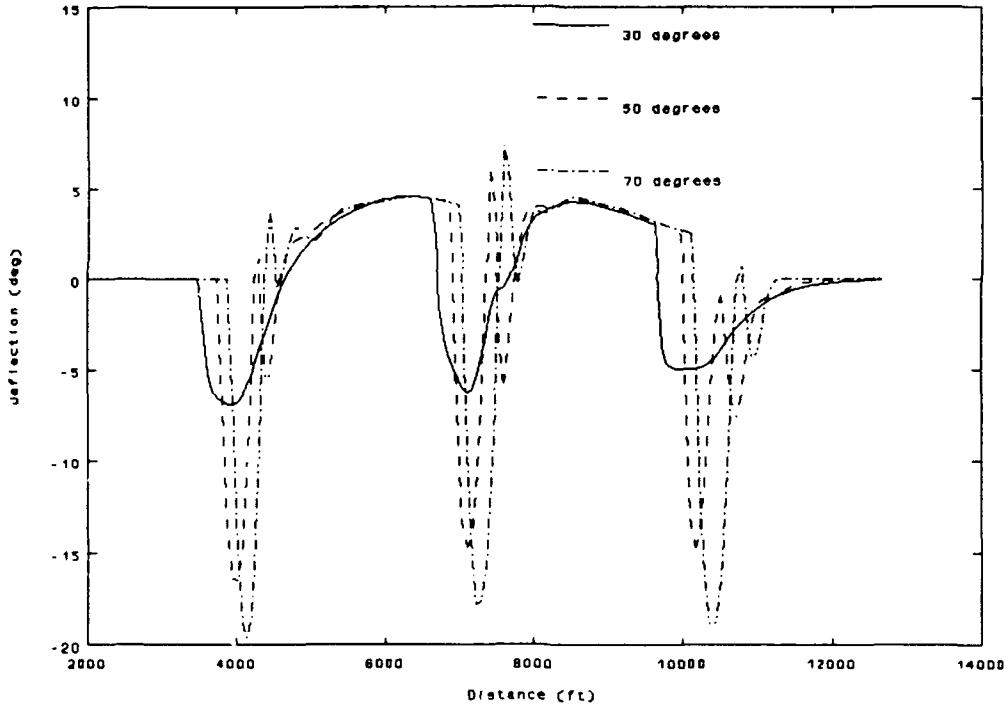

Figure 4-8: Control Power Summary for Fixed Angle

Surprisingly, none of the simulations required more than approximately 20 degrees of elevator to complete the maneuver. Even the 70 degree case, which looked like it required drastic measures to avoid a

collision, only uses 3 or 4 more degrees of elevator than the 50 degree run, which looked very smooth and controlled. There is a sharp contrast between the amount of control authority required by the small angle simulation versus the midrange case. By decreasing the incidence angle 20 degrees, we reduce the control power required 9 degrees. Conversely, if we increase the incidence angle 20 degrees, the control power changes only three degrees. Once again, the biggest factor in the difference in power required is the smaller gain which is used for the smaller angle. The two larger angles used the same gain, and therefore a direct comparison is much more valid.

In summary, by looking only at the performance measures noted here, we would be forced to conclude that the smaller incidence angle is more effective at following the terrain contours. The fact that it doesn't maintain the desired altitude buffer is a concern, but the overall performance is very good.

Comparisons of Radar Dynamics. Concentrating once again on the 50 degree nominal angle, we will now examine the advantages of adding radar dynamics to the system in order to improve the terrain following performance. It is logical to expect that, by moving the radar, we will be able to recover some of the early warning capability of the 30 degree fixed angle simulation while maintaining the high control gain which improves the clearance altitude.

The first measure to examine is the trace of the flight path for each model simulation. The position traces for each run are shown in Figure 4-9. The first notable item is that the dynamic radar enables the model to detect the second obstacle much sooner than the fixed angle model. This allows the pullup maneuver to begin sooner and makes for

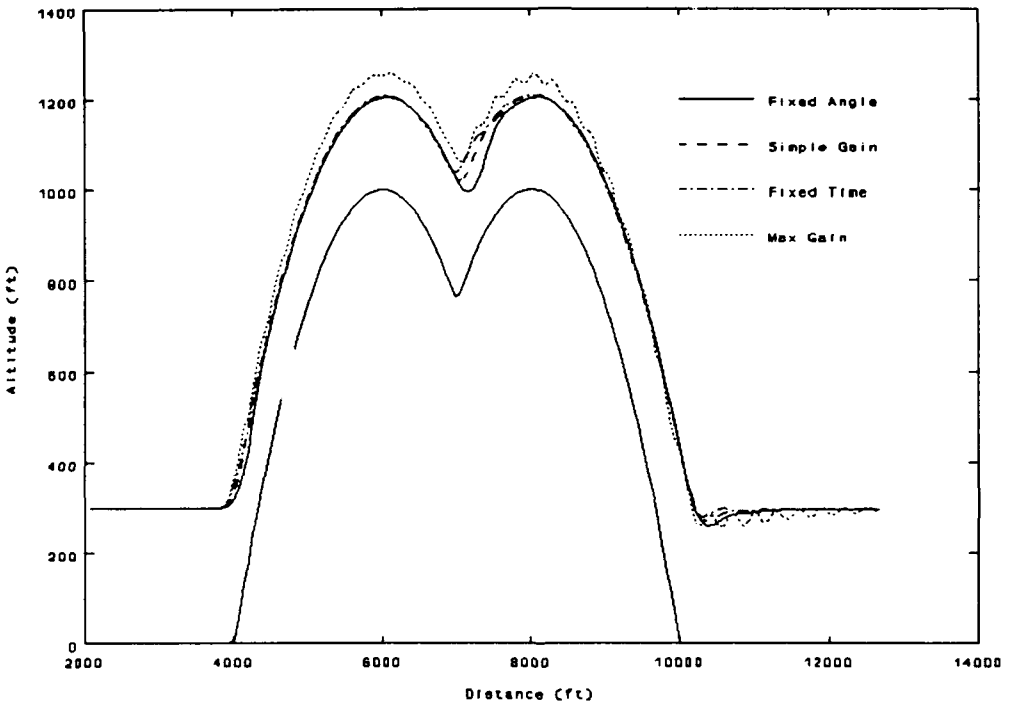

Figure 4-9: Position Trace for Σ = 50 degrees

an overall smoother ride. All of the midrange gain simulations converge on the same maximum altitude. The only major differences appear in the valley between the hills and at the beginning and end of the obstacle. This would suggest that the models all tend to agree on the best flight path during quasi-steady flight and the differences become apparent only during times of high maneuvering workload.

One significant demonstration of these differences is shown by the way in which the two dynamic models change the radar angle as the terrain is detected. Figure 4-10 shows the change in incidence angle for each simulation. We see that the two models are similar in

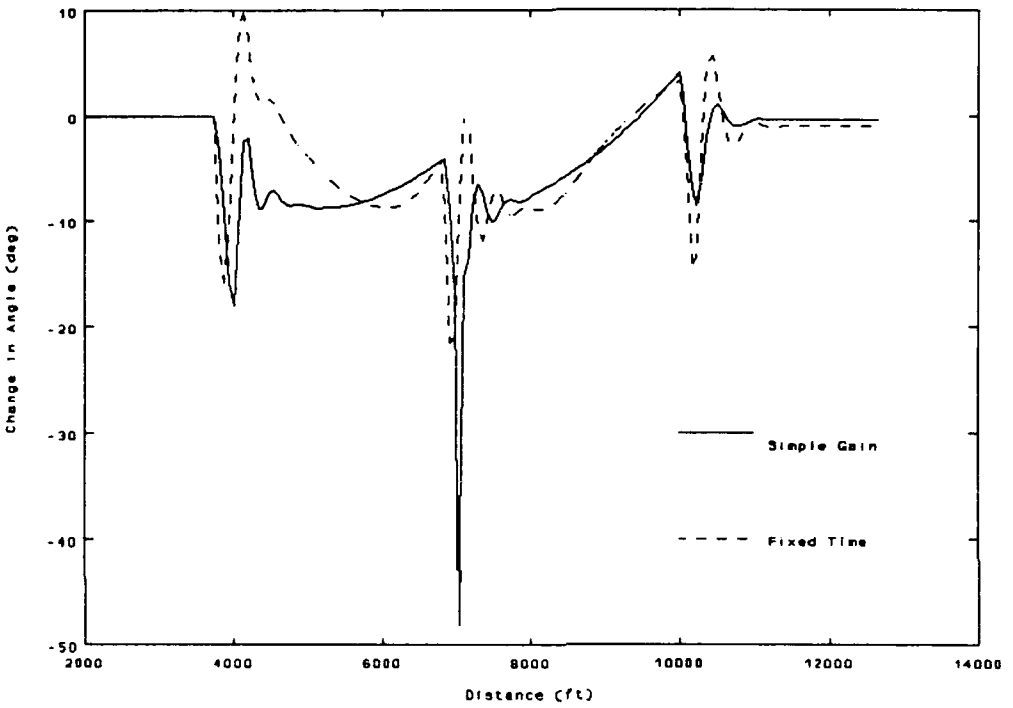

Figure 4-10: Change in Radar Angle for $\Sigma = 50$ degrees

response with the exception of the magnitude of the change commanded when the second hill is detected. The simple gain radar model responds much more strongly to the second obstacle than the fixed time constant model. This is most likely a result of the fact that the dynamics for the simple gain are tied directly to the range difference, while the fixed time constant takes into account the horizontal velocity as well.

The position of the radar directly affects the measured radar range, so we can expect a large difference between the two models in the amount of elevator deflection which is commanded. The control power used by each simulation is shown in Figure 4-11. As expected, we see a substantial spike in the simple gain model corresponding to the

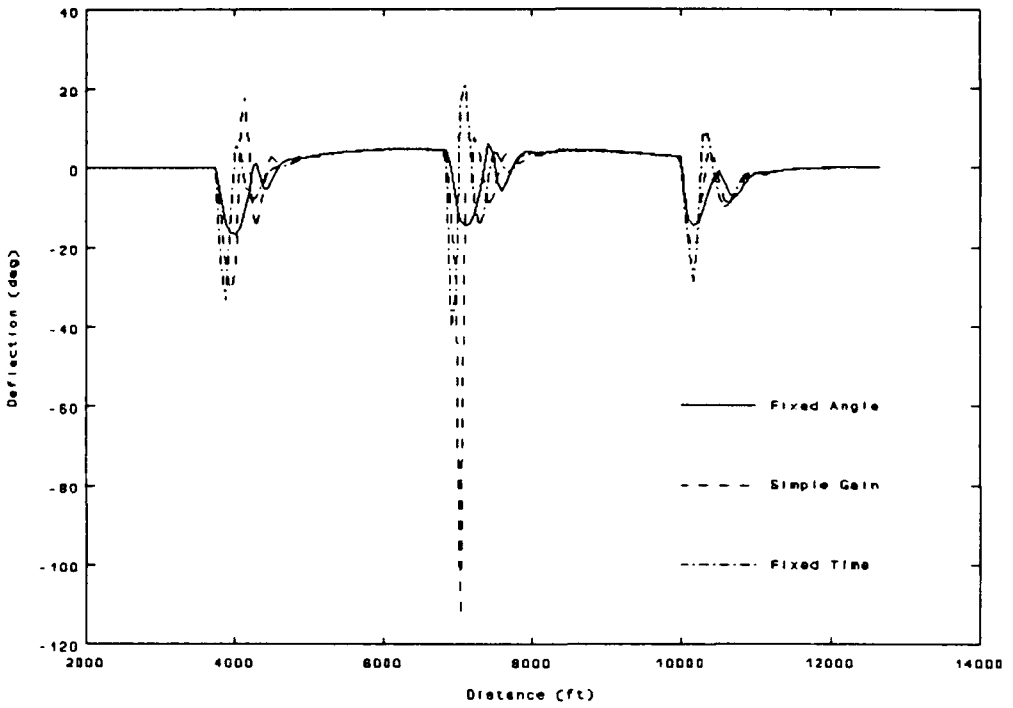

Figure 4-11: Control Power for Σ = 50 degrees

pullup to avoid the second hill. This magnitude is nearly three times that of the fixed time constant method. The general shape of the curves is the same throughout most of the rest of the maneuver. Both dynamic systems use more control power than is physically available at each of the primary maneuver points, but this could be mitigated without sacrificing a lot of performance by lowering the elevator gain.

In summary, it appears that the fixed time constant method is more reliable to use than the simple gain method and provides excellent results. The position trace shows an improvement over the fixed angle by centering the pullup more accurately over the center of the valley between the two hills. This is an improvement because it more closely follows the actual terrain.

Validation Summary

Based upon the response to the various alternate terrain models, we can confirm that 50 degrees is an adequate angle to look ahead to detect changes in the terrain the aircraft is trying to follow. The gain associated with this angle is sufficient to provide a quick response and small enough that it does not cause wild oscillations in the flight path. Reducing the incidence angle increases the sensitivity of the system and therefore decreases the allowable gain level. Lower gains reduce the responsiveness of the aircraft. Beyond simply choosing a basic incidence angle, the validation also seems to indicate that using the fixed time constant method to reposition the radar is also very effective.

V. Conclusions

Based on the results of Chapter III and the validation of Chapter IV, some conclusions can now be drawn about one method of implementing a terrain following system. Due to the technological developments which will allow directionalized ranging, it will become much more practical to implement terrain follow capability into an aircraft system which has limited computer resources or memory storage without the use of digitized maps. The secret to successfully mating this capability into the aircraft autopilot will be giving the controller enough warning of a terrain obstacle that it can initiate an evasive maneuver and still maintain a safe altitude above the terrain. The key to this early warning is the distance ahead at which the terrain data is being gathered.

This study has shown that looking too far ahead requires the system to reduce the sensitivity and responsiveness of the aircraft. Not looking far enough ahead does not provide adequate warning to the control system for maneuvering the aircraft without requiring excessively large control deflections. The best design comes from a midrange value which balances the attributes of each of the extremes. This study has shown that a nominal angle of 50 degrees is the most desirable choice of how far to aim the sensor beam. It resulted in the lowest quantitative score of any other angle tested. This indicates that

this particular simulation most closely approximated the optimal solution of maintaining a constant buffer altitude and following the terrain precisely.

In addition to having the best score by using a 50 degree angle, this study has also shown that redirecting the angle of the radar during critical phases of the flight can further improve the terrain following capability of the system. Abrupt changes in the terrain which the system is attempting to follow will call for adjustments in the direction the radar is pointing. The most critical change occurs when the measured range is significantly shorter than the expected value. The aircraft must then pitch up dramatically to avoid a ground collision. The advantage of redirecting the radar comes from knowing whether the terrain beyond the current obstacle will make matters worse or relieve some of the problem by allowing an escape route.

The results in Chapter III, which were then validated in Chapter IV, indicate that the best method to implement this dynamic motion of the radar is to attempt to keep the radar aimed at a spot on the ground which the aircraft will overfly in a preset time interval. This is accomplished by commanding the incidence angle as

$$\Sigma_{com} = \theta + \cos^{-1}\left(\frac{V_H * t_c}{R}\right)$$

In this way the controller can use the measured range, horizontal velocity, and preset time interval to determine where to direct the

radar. This technique avoids the need for gain scheduling at different flight conditions which would be required to properly implement a simple gain type of dynamic system.

The primary disadvantage to this or any dynamic system is that it requires more control power than a standard fixed angle system. However, it is likely that the advantages gained by using any type of radar dynamics will outweigh the loss of a small amount of control power due to the elevator gain being reduced. Another problem noted during the response to the step hill is that all of the simulations include a steady state error. This is clearly an area which could be pursued in greater detail. Further iterations on the controller design to include integral action would very likely eliminate the steady state error.

A second recommendation would be further trade-off studies to quantify the degradation to the system which results when the elevator gain is lowered enough to keep the control power within acceptable limits. An alternative to this would be to modify the simulation program to include magnitude and rate limiters on the allowable control power and rerunning the simulation. This comparison would definitely impact the gain values, particularly as the incidence angle increases.

A final recommendation would be to implement this procedure using the dynamics of another class of aircraft. To really utilize the approach developed in this thesis, a designer will have to know how to

scale the results to a larger and more sluggish or a smaller and more agile aircraft. Obviously the best angle at which to gather data will not be the same for all classes. In general, the more responsive the aircraft, the less warning a control system would require.

In conclusion, this thesis has demonstrated that the best terrain following control system for an A-7 aircraft at a typical sea-level cruise condition at 300 ft AGL over this class of terrain uses a dynamic radar pointing technique to gather terrain data at a time interval approximately .585 seconds ahead of the current position. This corresponds to a nominal radar incidence angle of 50 degrees. The gain value applied to the delta range measurement to control the elevator deflection was 8. Using the system developed in this thesis, the user can expect a 10% steady state error. This control system has been proven adequate in steep terrain, including multiple obstacles.

Appendix: FORTRAN Simulation Program and Input File

The following is the FORTRAN Simulation program and input file used to examine the dynamic response of the aircraft system.

The input file contains the timing parameters, state space matrices, and gains which serve as inputs to the simulation program.

```
THIS IS A TERRAIN FOLLOWING INPUT FILE
A-7 INPUT DATA WITH RADAR DYNAMICS

CONTINUATION FROM ANOTHER RUN
  N

THE TIME PARAMETERS
170000    0.00010000

THE NUMBER OF STATE VARIABLES
   17    5    5

THE A MATRIX
-1.31453D+00 1.40517D-03-2.25710D-02 9.14138D-04-3.06000D+01 0.00000D+00
 0.00000D+00 0.00000D+00 0.00000D+00 0.00000D+00 0.00000D+00 0.00000D+00
 0.00000D+00 0.00000D+00 0.00000D+00 0.00000D+00 0.00000D+00
-3.34156D+01-1.23019D-02 5.56703D-02-3.16013D+01 8.34000D+00 0.00000D+00
 0.00000D+00 0.00000D+00 0.00000D+00 0.00000D+00 0.00000D+00 0.00000D+00
 0.00000D+00 0.00000D+00 0.00000D+00 0.00000D+00 0.00000D+00
 6.72311D+02-2.51404D-03-1.91199D+00-1.61130D+00-1.65000D+02 0.00000D+00
 0.00000D+00 0.00000D+00 0.00000D+00 0.00000D+00 0.00000D+00 0.00000D+00
 0.00000D+00 0.00000D+00 0.00000D+00 0.00000D+00 0.00000D+00
 1.00000D+00 0.00000D+00 0.00000D+00 0.00000D+00 0.00000D+00 0.00000D+00
 0.00000D+00 0.00000D+00 0.00000D+00 0.00000D+00 0.00000D+00 0.00000D+00
 0.00000D+00 0.00000D+00 0.00000D+00 0.00000D+00 0.00000D+00
 1.51722D+03 1.73908D-01 4.05841D-01 1.04450D+04-1.67797D+03-1.00000D+01
 0.00000D+00 0.00000D+00 0.00000D+00 0.00000D+00 0.00000D+00 0.00000D+00
 0.00000D+00 0.00000D+00 0.00000D+00 0.00000D+00 0.00000D+00
 0.00000D+00 0.00000D+00 1.00000D+00-6.69840D+02 0.00000D+00-3.16228D+00
 0.00000D+00 0.00000D+00 0.00000D+00 0.00000D+00 0.00000D+00 0.00000D+00
-3.16228D+00 0.00000D+00 0.00000D+00 0.00000D+00 0.00000D+00
 0.00000D+00 0.00000D+00 0.00000D+00-1.24022D-10 0.00000D+00 0.00000D+00
-7.99576D+02 0.00000D+00 0.00000D+00 0.00000D+00 0.00000D+00 0.00000D+00
 0.00000D+00-7.54855D+02 0.00000D+00 0.00000D+00 0.00000D+00
 0.00000D+00 0.00000D+00 0.00000D+00 0.00000D+00 0.00000D+00 0.00000D+00
 0.00000D+00-1.31453D+00 1.40517D-03-2.25710D-02 9.14138D-04-3.06000D+01
 0.00000D+00 0.00000D+00 0.00000D+00 0.00000D+00 0.00000D+00
 0.00000D+00 0.00000D+00 0.00000D+00 0.00000D+00 0.00000D+00 0.00000D+00
 0.00000D+00-3.34156D+01-1.23019D-02 5.56703D-02-3.16013D+01 8.34000D+00
 0.00000D+00 0.00000D+00 0.00000D+00 0.00000D+00 0.00000D+00
 0.00000D+00 0.00000D+00 0.00000D+00 0.00000D+00 0.00000D+00 0.00000D+00
 0.00000D+00 6.72311D+02-2.51404D-03-1.91199D+00-1.61130D+00-1.65000D+02
 0.00000D+00 0.00000D+00 0.00000D+00 0.00000D+00 0.00000D+00
 0.00000D+00 0.00000D+00 0.00000D+00 0.00000D+00 0.00000D+00 0.00000D+00
 0.00000D+00 1.00000D+00 0.00000D+00 0.00000D+00 0.00000D+00 0.00000D+00
 0.00000D+00 0.00000D+00 0.00000D+00 0.00000D+00 0.00000D+00
-1.51722D+03-1.73908D-01-4.05841D-01-1.04450D+04 1.66797D+03 1.00000D+01
 0.00000D+00 0.00000D+00 0.00000D+00 0.00000D+00 0000000D+00-1.00000D+01
```

0.00000D+00 0.00000D+00 0.00000D+00 0.00000D+00 0.00000D+00
0.00000D+00 0.00000D+00 0.00000D+00 0.00000D+00 0.00000D+00 0.00000D+00
0.00000D+00 0.00000D+00 0.00000D+00 1.00000D+00-6.69840D+02 0.00000D+00
0.00000D+00 0.00000D+00 0.00000D+00 0.00000D+00 0.00000D+00
0.00000D+00 0.00000D+00 0.00000D+00 1.24022D-10 0.00000D+00 0.00000D+00
2.47214D+01 0.00000D+00 0.00000D+00 0.00000D+00 0.00000D+00 0.00000D+00
0.00000D+00-2.00000D+01 0.00000D+00 0.00000D+00 0.00000D+00
0.00000D+00 0.00000D+00 0.00000D+00 0.00000D+00 0.00000D+00 0.00000D+00
0.00000D+00 0.00000D+00 0.00000D+00 0.00000D+00 0.00000D+00 0.00000D+00
0.00000D+00 0.00000D+00 0.00000D+00 0.00000D+00 0.00000D+00
0.00000D+00 0.00000D+00 0.00000D+00 0.00000D+00 0.00000D+00 0.00000D+00
0.00000D+00 0.00000D+00 0.00000D+00 0.00000D+00 0.00000D+00 0.00000D+00
0.00000D+00 0.00000D+00 0.00000D+00 0.00000D+00 0.00000D+00
0.00000D+00 0.00000D+00 0.00000D+00 0.00000D+00 0.00000D+00 0.00000D+00
0.00000D+00 0.00000D+00 0.00000D+00 0.00000D+00 0.00000D+00 0.00000D+00
0.00000D+00 0.00000D+00 0.00000D+00 0.00000D+00 0.00000D+00

THE B MATRIX
0.00000D+00 0.00000D+00 0.00000D+00 0.00000D+00 0.00000D+00
0.00000D+00 0.00000D+00 0.00000D+00 0.00000D+00 0.00000D+00
0.00000D+00 0.00000D+00 0.00000D+00 0.00000D+00 0.00000D+00
0.00000D+00 0.00000D+00 0.00000D+00 0.00000D+00 0.00000D+00
0.00000D+00 0.00000D+00 0.00000D+00 0.00000D+00 0.00000D+00
0.00000D+00 0.00000D+00 0.00000D+00 3.16230D+00 0.00000D+00
0.00000D+00 0.00000D+00 0.00000D+00 0.00000D+00 7.54850D+02
0.00000D+00 0.00000D+00 0.00000D+00 0.00000D+00 0.00000D+00
0.00000D+00 0.00000D+00 0.00000D+00 0.00000D+00 0.00000D+00
0.00000D+00 0.00000D+00 0.00000D+00 0.00000D+00 0.00000D+00
0.00000D+00 0.00000D+00 0.00000D+00 0.00000D+00 0.00000D+00
0.00000D+00 0.00000D+00 0.00000D+00 0.00000D+00 0.00000D+00
0.00000D+00 0.00000D+00 0.00000D+00 0.00000D+00 0.00000D+00
0.00000D+00 0.00000D+00 0.00000D+00 0.00000D+00 0.00000D+00
0.00000D+00 0.00000D+00 0.00000D+00 0.00000D+00 0.00000D+00
0.00000D+00 0.00000D+00 0.00000D+00 0.00000D+00 0.00000D+00
0.00000D+00 0.00000D+00 0.00000D+00 0.00000D+00 0.00000D+00

THE C MATRIX
0.00000D+00 0.00000D+00 0.00000D+00 0.00000D+00 0.00000D+00 0.00000D+00
0.00000D+00 1.00000D+00 0.00000D+00 0.00000D+00 0.00000D+00 0.00000D+00
0.00000D+00 0.00000D+00 0.00000D+00 0.00000D+00 0.00000D+00
0.00000D+00 0.00000D+00 0.00000D+00 0.00000D+00 0.00000D+00 0.00000D+00
0.00000D+00 0.00000D+00 0.00000D+00 1.49289D-03 0.00000D+00 0.00000D+00
0.00000D+00 0.00000D+00 0.00000D+00 0.00000D+00 0.00000D+00
0.00000D+00 0.00000D+00 0.00000D+00 0.00000D+00 0.00000D+00 0.00000D+00
0.00000D+00 2.47072D+00-2.51404D-03-1.91199D+00-1.61130D+00-1.65000D+02
0.00000D+00 0.00000D+00 0.00000D+00 0.00000D+00 0.00000D+00
0.00000D+00 0.00000D+00 0.00000D+00 0.00000D+00 0.00000D+00 0.00000D+00
0.00000D+00 0.00000D+00 0.00000D+00 0.00000D+00 0.00000D+00 0.00000D+00
1.00000D+00 0.00000D+00 0.00000D+00 0.00000D+00 0.00000D+00
0.00000D+00 0.00000D+00 0.00000D+00 0.00000D+00 0.00000D+00 0.00000D+00
0.00000D+00 0.00000D+00 0.00000D+00 0.00000D+00 0.00000D+00 0.00000D+00
0.00000D+00 1.00000D+00 0.00000D+00 0.00000D+00 0.00000D+00

THE STATE VARIABLE INITIAL CONDITIONS
0.000000000000
0.000000000000

0.000000000000
0.000000000000
0.000000000000
0.000000000000
0.000000000000
0.000000000000
0.000000000000
0.000000000000
0.000000000000
0 000000000000
0.000000000000
0.000000000000
300.000000000000
0.000000000000
2000.000000000000

THE RADAR ANGLE
75.000000000000 8.000000000000 0.4635565000

THE ENDING TIME PARAMETERS
1000 10.010000000 0.010000000

THE STATE INFORMATION
0.000000000000 0.000000000000 0.000000000000 0.000000000000
0.000000000000 0.000000000000 0.000000000000 0.000000000000
0.000000000000 0.000000000000 0.000000000000 0.000000000000
0.000000000000 0.000000000000 0.000000000000 0.000000000000
0.000000000000 0.000000000000 0.000000000000 0.000000000000
0.000000000000 0.000000000000 0.000000000000 0.000000000000
0.000000000000 0.000000000000 0.000000000000 0.000000000000
0.000000000000 0.000000000000 0.000000000000 0.000000000000
0.000000000000 0.000000000000 0.000000000000 0.000000000000
0.000000000000 0.000000000000 0.000000000000 0.000000000000
0.000000000000 0.000000000000 0.000000000000 0.000000000000
0.000000000000 0.000000000000 0.000000000000 0.000000000000
6679.8999999998806686.5999999998796693.2999999998796699.999999999879
2000.0000000000002000.0000000000002000.0000000000002000.000000000000

THE RIGHT HAND SIDE
0.000000000000 0.000000000000 0.000000000000 0.000000000000
0.000000000000 0.000000000000 0.000000000000 0.000000000000
0.000000000000 0.000000000000 0.000000000000 0.000000000000
0.000000000000 0.000000000000 0.000000000000 0.000000000000
0.000000000000 0.000000000000 0.000000000000 0.000000000000
0.000000000000 0.000000000000 0.000000000000 0.000000000000
0.000000000000 0.000000000000 0.000000000000 0.000000000000
0.000000000000 0.000000000000 0.000000000000 0.000000000000
0.000000000000 0.000000000000 0.000000000000 0.000000000000
0.000000000000 0.000000000000 0.000000000000 0.000000000000
0.000000000000 0.000000000000 0.000000000000 0.000000000000
0.000000000000 0.000000000000 0.000000000000 0.000000000000
670.000000000000 670.000000000000 670.000000000000 670.000000000000
0.000000000000 0.000000000000 0.000000000000 0.000000000000

```
THE STATE ERROR VECTOR
 0.000000000000
 0.000000000000
 0.000000000000
 0.000000000000
 0.000000000000
 0.000000000000
 0.000000000000
 0.000000000000
 0.000000000000
 0.000000000000
 0.000000000000
 0.000000000000
 0.000000000000
 0.000000000000
 0.000000000000
0.00000D+00 0.00000D+00-0.14850D-01 0.65240D+00-0.56180D+00-0.31320D+00
0.12255D+00 0.00000D+00 0.00000D+00 0.00000D+00 0.00000D+00 0.00000D+00
0.00000D+00 0.00000D+00 0.00000D+00
```

The FORTAN simulation program begins here.

```
CCCCCCCCCCCCCCCCCCCCCCCCCCCCCCCCCCCCCCCCCCCCCCCCCCCCCCCCCCCCCCCCCCCCC
C                                                                   C
C                   ***************                                 C
C                   *   TFSOL   *                                   C
C                   ***************                                 C
C                                                                   C
C    THIS PROGRAM SOLVES THE DIFFERENTIAL EQUATIONS                 C
C    FOR TERRAIN FOLLOWING.                                         C
C                                                                   C
CCCCCCCCCCCCCCCCCCCCCCCCCCCCCCCCCCCCCCCCCCCCCCCCCCCCCCCCCCCCCCCCCCCCC
      IMPLICIT REAL*8(A-H,O-Z)
      PARAMETER (MC=5,MI=3,MS=20)
      COMMON/TIMESD/ TIME,DTIME,NMOTIO,NSTMOT,NTIME,NSTIME,PI
      COMMON/NSTATE/ ISTATE,X(MS,5),RHSMO(MS,5)
      COMMON/NCNTRL/ ICNTRL,UCOM(MC),PINPUT(MI)
      COMMON/INITIL/ XI(MS)
      COMMON/ERRORS/ ERROR(MC)
      OPEN(1,FILE='A7GINPUT.DAT')
      OPEN(8,FILE='RESTART.DAT')
      OPEN(9,FILE='OUTPUT.DAT')
C
C    SETTING THE CONSTANTS
C
      PI=4.0*DATAN(1.0D0)
C
C     READING THE INPUT DATA
C
      CALL READER
C
C    THE START OF A NEW TIME STEP
C
            TIME=TIME+DTIME
```

```
C
C     THE MASTER LOOP
C
      ICNT=0
      SCORE=0.0D0
      DO 40 I=NSTIME,NTIME
C          PRINT*,'TIME',I
           NMOTIO=I-1
      K=NMOTIO
      IF(K.LT.1)K=1
      IF(K.GT.4)K=4
C
C     SEEING IF PAST THE STARTING PROCEEDURE
C
               IF(NMOTIO.LT.3)THEN
C
C     CALLNG THE ROUTINE TO SET THE RIGHT HAND SIDE OF THE MOTION EQ
C
                    CALL RHSMOT
C
C     CALLING THE ROUTINE TO DO THE TAYLOR SERIES FOR THE STARTING
C
                    CALL TAYLOR
C
C     INCREASING THE MOTION SO FORCES WILL BE COMPUTED WITH NEW
C       ANGLES
C
                    NMOTIO=NMOTIO+1
                ELSE
C
C     THE PREDICTOR CORRECTOR PART
C
                    CALL PRAMOD
C
C     INCREASING THE MOTION SO FORCES WILL BE COMPUTED WITH NEW
C          ANGLES
C
                    NMOTIO=NMOTIO+1
C
C     CALLING THE ROUTINE TO DEFINE THE ROTATION RATES IN THE BODY
C
                      ITCN=0
   70                 CONTINUE
C
C     CALLNG THE ROUTINE TO SET THE RIGHT HAND SIDE OF THE MOTION EQ
C
                      CALL RHSMOT
C
C     CALLING THE ROUTINE TO FIND THE CORRECTOR EQUATION
C
                      CALL YFITER
C
C     DID THE SOLUTION CONVERGE
C
                         ITCN=ITCN+1
                   IF(ITCN.EQ.15)PRINT*,'HAD TROUBLE CONVERGING'
```

```
            IF(IERROR.NE.0.AND.ITCN.GT.14)GOTO 80
            IF(IERROR.NE.0)GOTO 70
 80          CONTINUE
C
C     SOLUTION HAS CONVERGED PREFORMING THE FINAL ERROR CORECTION
C
            CALL ERRCOR
         END IF
 60      CONTINUE
C
C     CALLNG THE ROUTINE TO SET THE RIGHT HAND SIDE OF THE MOTION EQ
C
         CALL RHSMOT
C
C     CALLING THE ROUTINE TO PRINT THE INTERUM RESULTS
C
            ICNT=ICNT+1
            IF(ICNT.GE.1000)THEN
            ICNT=0
         CALL IMWRIT
            END IF
C
C     THE START OF A NEW TIME STEP
C
         TIME=TIME+DTIME
C
C     CALLING THE ROUTINE THAT UPDATES THE POTENTIALS
C
         CALL UPDATE
   H=0.0D0
   H1=-(X(17,K)-6000)**2.0D0/4000.0D0+1000.0D0
   IF(H1.GE.0.0D0)H=H1
   SCORE=SCORE+(X(15,K)-H-XI(15))**2.0D0
 40 CONTINUE
   print*,' the score was ',score
C
C     WRITING THE FINAL RESULTS
C
   CALL WRITER
   STOP
   END
CCCCCCCCCCCCCCCCCCCCCCCCCCCCCCCCCCCCCCCCCCCCCCCCCCCCCCCCCCCC
C                                                          C
C              ***************                             C
C              *   READER   *                              C
C              ***************                             C
C                                                          C
C     THIS ROUTINE READS IN ALL THE APPROPRIATE DATA FROM THE  C
C     INPUT FILE.                                          C
C                                                          C
CCCCCCCCCCCCCCCCCCCCCCCCCCCCCCCCCCCCCCCCCCCCCCCCCCCCCCCCCCCC
  SUBROUTINE READER
   IMPLICIT REAL*8(A-H,O-Z)
   PARAMETER (MC=5,MI=3,MS=20)
   CHARACTER*1, YCHAR
   CHARACTER*50, DUMCH
```

```
      COMMON/TIMESD/ TIME,DTIME,NMOTIO,NSTMOT,NTIME,NSTIME,PI
      COMMON/NSTATE/ ISTATE,X(MS,5),RHSMO(MS,5)
      COMMON/NCNTRL/ ICNTRL,UCOM(MC),PINPUT(MI)
      COMMON/ERRORS/ ERROR(MC)
      COMMON/INITIL/ XI(MS)
      COMMON/MATSTA/ A(MS,MS),B(MS,MC),C(MC,MS)
      COMMON/ANGLES/ SIGMA,GAINQ,GAING
C
C       THE FORMAT STATEMENTS
C
  500 FORMAT(A50)
  510 FORMAT(3X,A1)
  520 FORMAT(I6,F15.9)
  530 FORMAT(3I6)
  540 FORMAT(1X,6D12.5)
  542 FORMAT(6(1X,E13.6))
  550 FORMAT(I6,2F15.9)
  560 FORMAT(1X,4F17.12)
  570 FORMAT(1X,F17.12)
  580 FORMAT(1X,3F17.12)
C
C       SEEING IF THIS IS A NEW RUN
C
      READ(1,500) DUMCH
      WRITE(8,500) DUMCH
      WRITE(9,500) DUMCH
      READ(1,500) DUMCH
      WRITE(8,500) DUMCH
      WRITE(9,500) DUMCH
      READ(1,500) DUMCH
      WRITE(8,500) DUMCH
      WRITE(9,500) DUMCH
      READ(1,500) DUMCH
      WRITE(8,500) DUMCH
      READ(1,510) YCHAR
      WRITE(8,510) YCHAR
C
C       READING IN THE TIME STEP AND THE NUMBER OF TIME STEPS FOR RUN
C
      READ(1,500) DUMCH
      WRITE(8,500) DUMCH
      READ(1,500) DUMCH
      WRITE(8,500) DUMCH
      READ(1,520) NTIME,DTIME
      WRITE(8,520) NTIME,DTIME
C
C       READING IN THE STATE MATRIX
C
      READ(1,500) DUMCH
      WRITE(8,500) DUMCH
      READ(1,500) DUMCH
      WRITE(8,500) DUMCH
      READ(1,530) ISTATE,ICNTRL,IOUT
      WRITE(8,530) ISTATE,ICNTRL,IOUT
      READ(1,500) DUMCH
      WRITE(8,500) DUMCH
```

```
      READ(1,500) DUMCH
      WRITE(8,500) DUMCH
      DO 10 I=1,ISTATE
      READ(1,540) (A(I,J),J=1,ISTATE)
      WRITE(8,540) (A(I,J),J=1,ISTATE)
   10 CONTINUE
      DO 17 I=1,ISTATE
      WRITE(9,542) (A(I,J),J=1,6)
   17  CONTINUE
      DO 18 I=1,ISTATE
      WRITE(9,542) (A(I,J),J=7,12)
   18  CONTINUE
      READ(1,500) DUMCH
      WRITE(8,500) DUMCH
      READ(1,500) DUMCH
      WRITE(8,500) DUMCH
      DO 20 I=1,ISTATE
      READ(1,540) (B(I,J),J=1,ICNTRL)
      WRITE(8,540) (B(I,J),J=1,ICNTRL)
   20 CONTINUE
      READ(1,500) DUMCH
      WRITE(8,500) DUMCH
      READ(1,500) DUMCH
      WRITE(8,500) DUMCH
      DO 30 I=1,IOUT
      READ(1,540) (C(I,J),J=1,ISTATE)
      WRITE(8,540) (C(I,J),J=1,ISTATE)
   30 CONTINUE
C
C       READING IN THE INITIAL STATE CONDITIONS
C
      READ(1,500) DUMCH
      WRITE(8,500) DUMCH
      READ(1,500) DUMCH
      WRITE(8,500) DUMCH
      DO 40 I=1,ISTATE
      READ(1,570) X(I,1)
      WRITE(8,570) X(I,1)
      XI(I)=X(I,1)
   40 CONTINUE
C
C       READING IN THE INITIAL RADAR ANGLE
C
      READ(1,500) DUMCH
      WRITE(8,500) DUMCH
      READ(1,500) DUMCH
      WRITE(8,500) DUMCH
      READ(1,580) SIGMA,GAINQ,GAING
      WRITE(8,580) SIGMA,GAINQ,GAING
      SIGMA=SIGMA*PI/180.0D0
C
C       SETTING THE INITIAL TIME
C
      NSTIME=1
      TIME=0.0D0
C
```

```
C      NOT READING ANY MORE DATA IF THIS IS NOT A CONTINUATION RUN
C
      IF(YCHAR.EQ.'Y')THEN
C
C      INPUTTING THE DATA FROM THE LAST RUN
C
      READ(1,500) DUMCH
      READ(1,500) DUMCH
      READ(1,550) NSTIME,TIME,DTIME
      NSTIME=NSTIME+1
      READ(1,500) DUMCH
      READ(1,500) DUMCH
      DO 50 I=1,ISTATE
         READ(1,560) X(I,1),X(I,2),X(I,3),X(I,4)
   50 CONTINUE
      READ(1,500) DUMCH
      READ(1,500) DUMCH
      DO 60 I=1,ISTATE
         READ(1,560) RHSMO(I,1),RHSMO(I,2),RHSMO(I,3),RHSMO(I,4)
   60 CONTINUE
      READ(1,500) DUMCH
      READ(1,500) DUMCH
      DO 70 I=1,ISTATE
         READ(1,570) ERROR(I)
   70 CONTINUE
      END IF
C
C     WRITING OUT THE HEADER
C
      WRITE(9,590)
  590 FORMAT(//,'  TIME    THETA    ALTITUDE    RADAR ALT',/)
      RETURN
      END
CCCCCCCCCCCCCCCCCCCCCCCCCCCCCCCCCCCCCCCCCCCCCCCCCCCCCCCCCCCCCCCCCCCC
C                                                                     C
C               ***************                                       C
C               *   IMWRIT    *                                       C
C               ***************                                       C
C                                                                     C
C      THIS ROUTINE WRITES THE INFORMATION BETWEEN TIME STEPS.        C
C                                                                     C
CCCCCCCCCCCCCCCCCCCCCCCCCCCCCCCCCCCCCCCCCCCCCCCCCCCCCCCCCCCCCCCCCCCC
   SUBROUTINE IMWRIT
      IMPLICIT REAL*8(A-H,O-Z)
      PARAMETER (MC=5,MI=3,MS=20)
      COMMON/TIMESD/ TIME,DTIME,NMOTIO,NSTMOT,NTIME,NSTIME,PI
      COMMON/NSTATE/ ISTATE,X(MS,5),RHSMO(MS,5)
      COMMON/NCNTRL/ ICNTRL,UCOM(MC),PINPUT(MI)
      COMMON/ERRORS/ ERROR(MC)
      COMMON/OUTVAR/ DX(MS),DC(MC)
      COMMON/INITIL/ XI(MS)
      I=NMOTIO+1
      IF(I.LT.1)I=1
      IF(I.GT.4)I=5
C
C      DOING THE RADIAN TO DEGREE CONVERSION
```

```
C
      DO 10 J=1,ISTATE
      DX(J)=X(J,I)
   10 CONTINUE
      DX(8)=X(8,I)*180.0D0/PI
      DO 20 J=11,12
      DX(J)=X(J,I)*180.0D0/PI
   20 CONTINUE
      DO 30 J=1,ICNTRL
      DC(J)=UCOM(J)*180.0D0/PI
   30 CONTINUE
      H=0.0D0
      H1=-(DX(17)-6000)**2.0D0/4000.0D0+1000.0D0
      IF(H1.GE.0.0D0)H=H1
C
C       WRITING OUT THIS TIME STEP
C     TIME,X-DIST,ALT,TERRAIN,RADAR DFLTA,RADAR ANGLE, ELEVATOR
C         DEFLECTION
C
      WRITE(9,515) TIME,DX(17),DX(15),H,PINPUT(1),DX(14),DX(12)
      PRINT 515, TIME,DX(17),DX(15),H,PINPUT(1),DX(14),DX(12)
  515 FORMAT(1X,7F11.4)
c     IF(DX(15).LT.H)THEN
c     write(*,*) 'you crash !!!!'
c     stop
c     end if
      print*,'theta =',x(11,I)
      RETURN
      END
CCCCCCCCCCCCCCCCCCCCCCCCCCCCCCCCCCCCCCCCCCCCCCCCCCCCCCCCCCCCCCCC
C                                                              C
C                  ***************                             C
C                  *   WRITER    *                             C
C                  ***************                             C
C                                                              C
C       THIS ROUTINE WRITES OUT THE DATA                       C
C                                                              C
CCCCCCCCCCCCCCCCCCCCCCCCCCCCCCCCCCCCCCCCCCCCCCCCCCCCCCCCCCCCCCCC
      SUBROUTINE WRITER
      IMPLICIT REAL*8(A-H,O-Z)
      PARAMETER (MC=5,MI=3,MS=20)
      CHARACTER*50, DUMCH
      COMMON/TIMESD/ TIME,DTIME,NMOTIO,NSTMOT,NTIME,NSTIME,PI
      COMMON/NSTATE/ ISTATE,X(MS,5),RHSMO(MS,5)
      COMMON/NCNTRL/ ICNTRL,UCOM(MC),PINPUT(MI)
      COMMON/ERRORS/ ERROR(MC)
C
C       THE FORMAT STATEMENTS
C
  500 FORMAT(A50)
  510 FORMAT(3X,A1)
  520 FORMAT(/,'   THE ENDING TIME PARAMETERS')
  530 FORMAT(I6)
  540 FORMAT(F15.9)
  550 FORMAT(I6,2F15.9)
  560 FORMAT(1X,4F17.12)
```

```
 570 FORMAT(1X,F17.12)
 580 FORMAT(/,'   THE STATE INFORMATION')
 590 FORMAT(/,'   THE RIGHT HAND SIDE')
 600 FORMAT(/,'   THE STATE ERROR VECTOR')
     DUMCH='  '
     I=NMOTIO+1
     IF(I.LT.1)I=1
     IF(I.GT.4)I=4
C
C      WRITING THE CURRENT TIME PARAMETERS FOR THE NEXT RUN
C
     WRITE(8,520)
     WRITE(8,550) NTIME,TIME,DTIME
     WRITE(8,580)
     DO 30 I=1,ISTATE
        WRITE(8,560) X(I,1),X(I,2),X(I,3),X(I,4)
  30 CONTINUE
     WRITE(8,590)
     DO 40 I=1,ISTATE
        WRITE(8,560) RHSMO(I,1),RHSMO(I,2),RHSMO(I,3),RHSMO(I,4)
  40 CONTINUE
     WRITE(8,600)
     DO 50 I=1,ISTATE
        WRITE(8,570) ERROR(I)
  50 CONTINUE
     RETURN
     END
CCCCCCCCCCCCCCCCCCCCCCCCCCCCCCCCCCCCCCCCCCCCCCCCCCCCCCCCCCCCCCCC
C                                                              C
C                 ***************                              C
C                 *   RINPUT    *                              C
C                 ***************                              C
C                                                              C
C      THIS ROUTINE CALCULATES THE EXTERNAL INPUTS FROM THE    C
C      CURRENT STATES AND THE GROUND INFORMATION.              C
C                                                              C
CCCCCCCCCCCCCCCCCCCCCCCCCCCCCCCCCCCCCCCCCCCCCCCCCCCCCCCCCCCCCCCC
     SUBROUTINE RINPUT
     IMPLICIT REAL*8(A-H,O-Z)
     PARAMETER (MC=5,MI=3,MS=20)
     COMMON/TIMESD/ TIME,DTIME,NMOTIO,NSTMOT,NTIME,NSTIME,PI
     COMMON/NSTATE/ ISTATE,X(MS,5),RHSMO(MS,5)
     COMMON/NCNTRL/ ICNTRL,UCOM(MC),PINPUT(MI),R
     COMMON/ERRORS/ ERROR(MC)
     COMMON/ANGLES/ SIGMA,GAINQ,GAING
     COMMON/INITIL/ XI(MS)
     I=NMOTIO+1
     IF(I.LT.1)I=1
     IF(I.GT.4)I=5
C     print*,'States 15,16,17:',X(15,I),X(16,I),X(17,I)
     IF(DABS((SIGMA+X(14,I))-X(11,I)+X(16,I)-PI/2.0D0).LT.1.0D-6)THEN
     COT=0.0D0
     XBAR=6000.0D0-X(17,I)
     XTIL=0.0D0
     ELSE
     COT=1.0D0/DTAN((SIGMA+X(14,I))-X(11,I)+X(16,I))
```

```
      XBAR=6000.0D0-X(17,I)-X(15,I)*COT
C      print*,'XBAR',XBAR
      B=DTAN((SIGMA+X(14,I))-X(11,I)+X(16,I))*4000.0D0+2*XBAR
c     print*,'B',B
      C=XBAR*XBAR-4.0D+06
c     print*,'C',C
      IF(B**2.0D0.GE.4.0D0*C)THEN
      IF(((SIGMA+X(14,I))-X(11,I)+X(16,I)-PI/2.0D0).GT.0.0D+0)THEN
      XTIL=(-B-DSQRT(B**2.0D0-4.0D0*C))/2.0D0
      ELSE
      XTIL=(-B+DSQRT(B**2.0D0-4.0D0*C))/2.0D0
      END IF
      ELSE
      XTIL=1D+10
      END IF
      END IF
      H=1000.0D0-(XBAR+XTIL)**2.0D0/4000.0D0
      IF(H.LE.0.0D0)THEN
      H=0.0D0
      XTIL=0.0D0
      END IF
C
C       FINDING THE RADAR RANGE
C
      R=DSQRT((6000.0D0-X(17,I)-XBAR-XTIL)**2.0D0
     .     +(X(15,I)-H)**2.0D0)
C
C       FINDING THE INITIAL RADAR RANGE
C
      R0=XI(15)/DSIN((SIGMA+X(14,i))-XI(11))
      PINPUT(1)=R-R0
C      print*,'RANGES',R,R0,PINPUT(1)
      IF(X(17,I).GT.2500)PINPUT(1)=-100+X(15,I)-300
      RETURN
      END
CCCCCCCCCCCCCCCCCCCCCCCCCCCCCCCCCCCCCCCCCCCCCCCCCCCCCCCCCCC
C                                                         C
C               *************                             C
C               *  RHSMOT  *                              C
C               *************                             C
C                                                         C
C     THIS SUBROUTINE CALULATES THE RIGHT HAND SIDE OF THE C
C     MOTION EQUATIONS.                                   C
C                                                         C
CCCCCCCCCCCCCCCCCCCCCCCCCCCCCCCCCCCCCCCCCCCCCCCCCCCCCCCCCCC
      SUBROUTINE RHSMOT
      IMPLICIT REAL*8(A-H,O-Z)
      PARAMETER (MC=5,MI=3,MS=20)
      COMMON/TIMESD/ TIME,DTIME,NMOTIO,NSTMOT,NTIME,NSTIME,PI
      COMMON/NSTATE/ ISTATE,X(MS,5),RHSMO(MS,5)
      COMMON/NCNTRL/ ICNTRL,UCOM(MC),PINPUT(MI),R
      COMMON/ERRORS/ ERROR(MC)
      COMMON/MATSTA/ A(MS,MS),B(MS,MC),C(MC,MS)
      COMMON/ANGLES/ SIGMA,GAINQ,GAING
C
C       CALLING THE ROUTINE TO CALCULATE THE INPUTS
```

```
C
      CALL RINPUT
      I=NMOTIO+1
      IF(I.LT.1)I=1
      IF(I.GT.4)I=5
C
C        THE CLOSE LOOP CONTROL LAW FOR PITCH
C
          UCOM(1)=0.0D0
          UCOM(2)=0.0D0
          UCOM(3)=0.0D0
          UCOM(4)=GAINQ*PINPUT(1)
C          IF(TIME.GT.1.0D0)UCOM(4)=1.0D0
C
C        THIS COMMAND INPUT IS FOR A FIXED RADAR ANGLE
          UCOM(5)=0.0D0
C
C        THIS COMMAND INPUT IS FOR A SIMPLE GAIN
C          UCOM(5)=GAING*PINPUT(1)
C
C        THIS COMMAND INPUT IS FOR A FIXED TIME CONSTANT
          VH=(670.0D0+x(9,I))*DCOS(X(11,I))
          ARG=VH*GAING/R
C          IF(ARG.GT.1.0D0)UCOM(5)=X(11,I)-DACOS(2.0D0-ARG)
C          IF(ARG.LT.1.0D0)UCOM(5)=X(11,I)+DACOS(ARG)
C
C        MAKING IT SO THAT CANNOT COMMAND MORE THAN AVAILABLE 25 DEG
C
C          IF(UCOM(4).GT.0.436332D0)UCOM(4)=0.436332D0
C          IF(UCOM(4).LT.-0.436332D0)UCOM(1)=-0.436332D0
C
C        CALCULATING THE RHS OF X DOT= A X + B U
C
      DO 10 J=1,ISTATE
          SUM=0.0D0
          DO 20 K=1,ISTATE
            SUM=SUM+A(J,K)*X(K,I)
   20     CONTINUE
          DO 30 K=1,ICNTRL
            SUM=SUM+B(J,K)*UCOM(K)
   30     CONTINUE
          RHSMO(J,I)=SUM
c        write(9,*),RHSMO(J,I),J,I
   10 CONTINUE
      RHSMO(17,I)=(670.0D0+X(9,I))*DCOS(X(11,I)-(X(10,I)/670.0D0))
     .        -X(10,I)*DSIN(X(11,I)-(X(10,I)/670.0D0))
      RHSMO(15,I)=(670.0D0+X(9,I))*DSIN(X(11,I)-(X(10,I)/670.0D0))
     .        +X(10,I)*DCOS(X(11,I)-(X(10,I)/670.0D0))
      RETURN
      END
CCCCCCCCCCCCCCCCCCCCCCCCCCCCCCCCCCCCCCCCCCCCCCCCCCCCCCCCCCCCCCCC
C                                                              C
C                   *************                              C
C                   *  TAYLOR  *                               C
C                   *************                              C
C                                                              C
```

```
C     THIS SUBROUTINE DOES THE TAYLOR SERIES EXPANSION OF THE          C
C     MOTION EQUATIONS FOR THE STARTING PROCEEDURE.                    C
C                                                                      C
CCCCCCCCCCCCCCCCCCCCCCCCCCCCCCCCCCCCCCCCCCCCCCCCCCCCCCCCCCCCCCCCCCCCCC
      SUBROUTINE TAYLOR
      IMPLICIT REAL*8(A-H,O-Z)
      PARAMETER (MC=5,MI=3,MS=20)
      COMMON/TIMESD/ TIME,DTIME,NMOTIO,NSTMOT,NTIME,NSTIME,PI
      COMMON/NSTATE/ ISTATE,X(MS,5),RHSMO(MS,5)
      COMMON/NCNTRL/ ICNTRL,UCOM(MC),PINPUT(MI)
      COMMON/ERRORS/ ERROR(MC)
      DT=DTIME
C
C       SEEING WHICH STARTING STEP THIS IS
C
      I=NMOTIO+1
      IP1=I+1
      IM1=I-1
      IM2=I-2
      IF(I.EQ.1)THEN
          DO 10 J=1,ISTATE
              X(J,IP1)=X(J,I)+DT*RHSMO(J,I)
   10     CONTINUE
      END IF
      IF(I.EQ.2)THEN
          DO 20 J=1,ISTATE
              X(J,IP1)=1.0D0/3.0D0*(4.0D0*X(J,I)-X(J,IM1))
     .        +2.0D0*DT/3.0D0*(2.0D0*RHSMO(J,I)-RHSMO(J,IM1))
   20     CONTINUE
      END IF
      IF(I.EQ.3)THEN
          DO 30 J=1,ISTATE
              X(J,IP1)=1.0D0/11.0D0*(18.0D0*X(J,I)
     .                 -9.0D0*X(J,IM1)+2.0D0*X(J,IM2))
     .        +6.0D0*DT/11.0D0*(3.0D0*RHSMO(J,I)
     .        -3.0D0*RHSMO(J,IM1)+RHSMO(J,IM2))
   30     CONTINUE
      END IF
      DO 40 J=1,ISTATE
          ERROR(J)=0.0D0
   40 CONTINUE
      RETURN
      END
CCCCCCCCCCCCCCCCCCCCCCCCCCCCCCCCCCCCCCCCCCCCCCCCCCCCCCCCCCCCCCCCCCCCCC
C                                                                      C
C                  *************                                       C
C                  *  PRAMOD  *                                       C
C                  *************                                       C
C                                                                      C
C     THIS SUBROUTINE DOES THE PREDICTOR STEP FOR THE                  C
C     DYNAMIC EQUATIONS.                                               C
C                                                                      C
CCCCCCCCCCCCCCCCCCCCCCCCCCCCCCCCCCCCCCCCCCCCCCCCCCCCCCCCCCCCCCCCCCCCCC
      SUBROUTINE PRAMOD
      IMPLICIT REAL*8(A-H,O-Z)
      PARAMETER (MC=5,MI=3,MS=20)
```

```
      COMMON/TIMESD/ TIME,DTIME,NMOTIO,NSTMOT,NTIME,NSTIME,PI
      COMMON/NSTATE/ ISTATE,X(MS,5),RHSMO(MS,5)
      COMMON/NCNTRL/ ICNTRL,UCOM(MC),PINPUT(MI)
      COMMON/ERRORS/ ERROR(MC)
      COMMON/PSTATE/ XNP(MS),XN1(MS)
      DT=DTIME
      DO 10 I=1,ISTATE
         XNP(I)=X(I,1)+4.0D0*DT/3.0D0*(2.0D0*RHSMO(I,4)
     .        -RHSMO(I,3)+2.0D0*RHSMO(I,2))
         X(I,5)=XNP(I)+112.0D0/9.0D0*ERROR(I)
   10 CONTINUE
      RETURN
      END
CCCCCCCCCCCCCCCCCCCCCCCCCCCCCCCCCCCCCCCCCCCCCCCCCCCCCCCCCCCC
C                                                          C
C                 *************                            C
C                 *  YFITER  *                             C
C                 *************                            C
C                                                          C
C    THIS SUBROUTINE DOES THE CORRECTOR STEP FOR THE       C
C    DYNAMIC EQUATIONS.                                    C
C                                                          C
CCCCCCCCCCCCCCCCCCCCCCCCCCCCCCCCCCCCCCCCCCCCCCCCCCCCCCCCCCCC
      SUBROUTINE YFITER
      IMPLICIT REAL*8(A-H,O-Z)
      PARAMETER (MC=5,MI=3,MS=20)
      COMMON/TIMESD/ TIME,DTIME,NMOTIO,NSTMOT,NTIME,NSTIME,PI
      COMMON/NSTATE/ ISTATE,X(MS,5),RHSMO(MS,5)
      COMMON/NCNTRL/ ICNTRL,UCOM(MC),PINPUT(MI)
      COMMON/ERRORS/ ERROR(MC)
      COMMON/ERROR2/ IERROR
      COMMON/PSTATE/ XNP(MS),XN1(MS)
      DT=DTIME
      IERROR=0
C
C     SETTING THE TOLERANCE
C
      TOLER=0.00001D0
      DO 10 I=1,ISTATE
         XN1(I)=1.0D0/8.0D0*(9.0D0*X(I,4)-X(I,2)
     .        +3.0D0*DT*(RHSMO(I,5)+2.0D0*RHSMO(I,4)-RHSMO(I,3)))
   10 CONTINUE
C
C     CHECKING THE TOLERANCE
C
      DO 20 I=1,ISTATE
         DIF=XN1(I)-X(I,5)
         IF(DABS(DIF).GT.TOLER)IERROR=1
   20 CONTINUE
C
C     UPDATING THE VALUES
C
      DO 30 I=1,ISTATE
         X(I,5)=XN1(I)
   30 CONTINUE
      RETURN
```

```
      END
CCCCCCCCCCCCCCCCCCCCCCCCCCCCCCCCCCCCCCCCCCCCCCCCCCCCCCCCCCC
C                                                         C
C               *************                             C
C               *  ERRCOR  *                              C
C               *************                             C
C                                                         C
C     THIS SUBROUTINE DOES THE FINAL CORRECTION WITH THE  C
C     ESTINMATE OF THE ERROR                              C
C                                                         C
CCCCCCCCCCCCCCCCCCCCCCCCCCCCCCCCCCCCCCCCCCCCCCCCCCCCCCCCCCC
      SUBROUTINE ERRCOR
      IMPLICIT REAL*8(A-H,O-Z)
      PARAMETER (MC=5,MI=3,MS=20)
      COMMON/TIMESD/ TIME,DTIME,NMOTIO,NSTMOT,NTIME,NSTIME,PI
      COMMON/NSTATE/ ISTATE,X(MS,5),RHSMO(MS,5)
      COMMON/NCNTRL/ ICNTRL,UCOM(MC),PINPUT(MI)
      COMMON/ERRORS/ ERROR(MC)
      COMMON/ERROR2/ IERROR
      COMMON/PSTATE/ XNP(MS),XN1(MS)
      DO 10 I=1,ISTATE
         ERROR(I)=9.0D0/121.0D0*(X(I,5)-XNP(I))
         X(I,5)=X(I,5)-ERROR(I)
   10 CONTINUE
      RETURN
      END
CCCCCCCCCCCCCCCCCCCCCCCCCCCCCCCCCCCCCCCCCCCCCCCCCCCCCCCCCCC
C                                                         C
C               *************                             C
C               *  UPDATE  *                              C
C               *************                             C
C                                                         C
C     THIS SUBROUTINE UPDATES THE VARIABLES.              C
C                                                         C
CCCCCCCCCCCCCCCCCCCCCCCCCCCCCCCCCCCCCCCCCCCCCCCCCCCCCCCCCCC
      SUBROUTINE UPDATE
      IMPLICIT REAL*8(A-H,O-Z)
      PARAMETER (MC=5,MI=3,MS=20)
      COMMON/TIMESD/ TIME,DTIME,NMOTIO,NSTMOT,NTIME,NSTIME,PI
      COMMON/NSTATE/ ISTATE,X(MS,5),RHSMO(MS,5)
C
C      SEEING IF THE MOTION EQUATIONS NEED UPDATING
C
      I=NMOTIO+1
      IF(I.GT.4)THEN
         DO 10 J=1,4
            JP1=J+1
            DO 20 K=1,ISTATE
               X(K,J)=X(K,JP1)
               RHSMO(K,J)=RHSMO(K,JP1)
   20       CONTINUE
   10    CONTINUE
      END IF
      RETURN
      END
```

Bibliography

1. Bice, Capt Gregory W. Development of an Automated Ground Collision Avoidance System Using a Digital Terrain Database. MS Thesis AFIT/GAE/ENY/89D-03. School of Engineering, Air Force Institute of Technology (AU), Wright-Patterson AFB OH, December 1989.

2. Maciejowski, J. M. Multivariable Feedback Design. Wokingham, England: Addison-Wesley Publishing Company, 1989.

3. Ridgeley, Capt D. Brett and Siva S. Banda. Introduction to Robust Multivariable Control. AFWAL-TR-85-3102. Wright-Patterson AFB OH: Flight Dynamics Laboratory, Air Force Wright Aeronautical Laboratories, February 1986.

4. USAF-TPS-CUR-86-02. USAF Test Pilot School, 1986.